

Charles University

Faculty of Science

Environmental Science



Marek Biskupič

Avalanche monitoring and run-out modeling using GIS

Monitorování lavinové aktivity a modelování dosahu lavin s použitím GIS

Doctoral thesis

Prague, 2017

Supervisor: Ing. Luboš Matějček, Ph.D.

I hereby declare that this Ph.D. Thesis is exclusively my own work, and that it has not been submitted (or any of its part) in order to obtain any academic degree earlier or at another institution. All publications and other sources used in the thesis have been properly quoted.

Prehlasujem, že som záverečnú prácu spracoval samostatne a že som uviedla všetky použité informačné zdroje a literatúru. Táto práca ani jej podstatná časť nebola predložená k získaniu iného alebo rovnakého akademického titulu.

V Prahe 30. 9. 2017

Marek Biskupič

Table of Contents

1	Acknowledgements.....	- 5 -
2	Abstract.....	- 6 -
3	List of included publications.....	- 7 -
4	Introduction.....	- 9 -
4.1	Snow avalanches.....	- 10 -
4.2	Snow and Avalanche research related to GIS, reemote sensing and modelling.....	- 13 -
5	Material and methods.....	- 16 -
5.1	Retrospective study on avalanche airbag use.....	- 16 -
5.2	Avalanche modelling.....	- 16 -
5.2.1	Friction parameters.....	- 17 -
5.2.2	Topographic statistical modelling of avalanche reach.....	- 19 -
5.2.3	Avalanche run-out modelling using numerical dynamic models.....	- 20 -
6	Aims of the study.....	- 24 -
7	Results.....	- 25 -
8	Conclusions.....	- 30 -
9	References.....	- 31 -
10	Publications.....	- 36 -
	Publication 1.....	- 36 -
	Publication 2.....	- 44 -
	Publication 3.....	- 51 -
	Publication 5.....	- 70 -
	Publication 6.....	- 79 -
	Publication 7.....	- 85 -
	Publication 8.....	- 103 -

1 Acknowledgements

This way I want to thank to Ing. Luboš Matějčík, Ph.D. for the consultations provided and valuable advice on the modelling of natural processes. Great thanks also to colleagues from the Avalanche prevention centre of Mountain rescue service in Slovakia namely: Jozef Richnavský, Filip Kyzek, and Ján Peťo for their valuable inputs and help with the field measurement and data analysis. Without a doubt great thank goes to Pawel Chrustek from collaborating institution of Jagelionian University in Cracow and Anna Pasek foundation.

Many of the activities would not be possible without the support of Mountain rescue service in Slovakia. The vote of thanks goes to its director Jozef Janiga for his understanding and encouragement.

Two of the studies were supported and partly funded by the Division of Scientific and Technological development of Slovak Ministry of Interior.

2 Abstract

Snow avalanches a natural phenomenon typical for snowy winter mountains consist of snow and sometimes of other material (debris, rocks, truncated trees and soil). On first sight they seem to be harmless mass of snow sliding down on a slope. But not they can be disastrous. Despite the snow avalanches event lasts for couple of seconds, they can take human lives, and destroy infrastructure. Until they occur in far and remote places they are not concern. The avalanche run-out has been always an issue. How far avalanches can travel? Is there avalanche activity out there? How large is the avalanche hazard on certain places? Will the avalanche airbag will influence the probability of not being critically buried by an avalanche. These are the question the thesis attempt to solve with the use of GIS, remote sensing and statistical analysis. The aim of the thesis was to find reasonable answers to these questions.

The effectiveness of avalanche airbags was first tested by pilot study when the artificial avalanche was triggered and motion of the dummies with different types was recorded. Additional estimation of impact forces, speed and final position of dummies was investigated and modelled (publication 6). The mechanism behind the avalanche airbags – inverse segregation was proofed to work in field test, but how is it with real avalanche incidents and the effectiveness of airbags in real life situations? To examine this question a retrospective study of avalanche airbags was done. Statistical analysis revealed that the real effectiveness of avalanche airbag is lower than previously reported (publication 1).

It was found out (publication 2 and 3) the statistical approach to avalanche modelling has its limitations and thus it is relatively easy to implement it within GIS environment, in future it will be replaced by more complex numerical simulations (publication 5, 7, 8). Simulations coupled with GIS represent very powerful tool, which should not be overestimated, still it is a simulation. Resolution of input digital elevation model and setting correct friction parameters are key factors for getting reasonable outputs.

Avalanche activity is valuable feedback for avalanche forecasting. As most of the mountain areas have very limited access, remote sensing can provide overview from above and map large areas in reasonable time and effort (publication 4).

The thesis provides further insight into avalanche monitoring using GIS, remote sensing and run-out simulation. Despite that the outputs are in experimental testing, ther is aim to make at least of them operational in avalanche forecasting and hazard zoning.

3 List of included publications

Publication 1: Haegeli, P., Falk M., Procter, E., Zweifel, B., Jarry, F., Logan, S., Kronholm K., **Biskupič, M.**, Brugger, H., 2014 The effectiveness of avalanche airbags. Resuscitation, Volume 85, Issue 9, 1197 – 1203. (IF₂₀₁₆: 5.230)

Publication 2: Biskupič, M., Barka, I., 2009, Statistical avalanche run-out modelling using GIS on selected slopes of Western Tatras National park, Slovakia., International Snow Science Workshop, Proceedings, 482-487. (Scopus)

Publication 3: Boltížiar, M., **Biskupič, M.**, Barka I., 2016, Spatial modelling of avalanches by application of GIS on selected slopes of the Western Tatra Mts. and Belianske Tatra Mts., Slovakia, Gographica Polonica, 89,79 – 90. (Scopus)

Publication 4: Frauenfelder, R., Lato, M. J., Biskupič, **M.**, 2015, Using eCognition to automatically detect and map avalanche deposits from the spring 2009 avalanche cycle in the Tatra mts., Slovakia, Int. Arch. Photogramm. Remote Sens. Spatial Inf. Sci., XL-7/W3, 791-795. (Scopus)

Publication 5: Richnavský, J., **Biskupič, M.**, Mudroň, I., Devečka, B., Unucka, J., Chrustek, P., Lizuch, M., Kyzek, F., Matějček, L., 2011, Using Modern GIS Tools to reconstruct the avalanche: A case study of Magurka 1970. GIS Ostrava 2011 Proceedings 175- 185. (per reviewed)

Publication 6: Biskupič, M., Richnavský J., Lizuch M., Kyzek, K., Žiak I., Chrustek, P., Procter, E., 2012, Three different shapes of avalanche balloons a pilot study, International Snow Science Workshop, Proceedings, 482-487.

Publication 7: Chrustek P., Wężyk P., Kolecka N., **Biskupič M.**, Bühler Y., Christen M., 2012 Using high resolution LiDAR data for snow avalanche hazard mapping in Kozak, J., Ostapowicz, K., Anna (Eds.) Integrating Nature and Society towards Sustainability, Springer, 290 p. (book chapter)

Publication 8: Liščák, P., **Biskupič, M.**, Richnavský, J., Bednařík, P., Geological hazards, in Dalezios, N., R., (Eds.) Environmental Hazards Methodologies for Risk Assessment and Management, IWA Publishing, London, (book chapter)

Author's contributions

Publication 1: Marek Biskupič collected the data of avalanche incidents in Italy and Slovakia, co-write the manuscript.

Publication 2: Marek Biskupič performed all the field work as well as the statistical analyses and led writing of the manuscript.

Publication 3: Marek Biskupič performed the GIS analysis GPS field work and post processing a

Publication 4: Marek Biskupič obtained the VHR satellite data, analyzed the avalanche cycle and co co-writes the manuscript.

Publication 5: Marek Biskupič collected and processed the GPS data performed the field work, prepare the data for simulation and analyzed the outputs together with co-writing of the manuscript.

Publication 6: Marek Biskupič managed the pilot study, process the data and led writing of the manuscript.

Publication 7: Marek Biskupič analyzed the data, co-write the manuscript.

Publication 8: Marek Biskupič wrote the chapters dealing with snow avalanches.

The supervisor of the doctoral thesis Luboš Matějček, fully acknowledges the contribution of Marek Biskupič as stated above.

Ing. Luboš Matějček, Ph.D.

4 Introduction

Snow is a natural phenomenon in the mountain alpine environment. Fluffy nicely shaped snowflakes seem to be harmless and peaceful. That is true until they form large masses of snow on steep slopes and creates a snow avalanche. The snow avalanche is gravitational, sudden, downslope movement of snow mass on a mountain slope. Unless they do not occur in settlements and threaten infrastructure and human lives they are not a concern. When avalanches occur in remote locations they are fascinating natural hazard with enormous energy.

The attempt to understand all the processes associated with the instability of the snow cover and consequent avalanche and minimize their negative impact has led the humans to explore study and research the avalanches. They have been subject of scientific research for long time. Monitoring of avalanche hazard and their frequency is crucial for planning and realization of effective prevention measures. Especially important is the ability to predict the avalanche risk and the conditions that lead to its increase. The use of various remote sensing techniques and technology to monitor avalanches and GIS to map and model the avalanche spatial distribution has recently recorded relatively great progress. The use of numerical avalanche models in practice is a common part of the avalanche forecast, especially in the Alpine countries, Canada, the USA and also in Japan. However, the systematic use of modern GIS in avalanche prevention in Slovak and Czech mountain regions is still absent. One of the main goals of this work is to assess the possibilities of using innovative methods in standard practice in avalanche prevention. The publications included in the thesis deal with two types avalanches. First of all it deals with human triggered avalanches and the impact of avalanche balloon on the survival of users wearing the avalanche balloon backpack. In the next step the field testing of avalanche balloon was performed to examine the performance of airbags in real avalanche conditions.

The numerical avalanche dynamic model was used to estimate the impact forces and speed of an experimental avalanche and its influence on dummies wearing avalanche balloon. The other part of the work is devoted to run-out modelling based on statistical methods and implementation of the model into GIS environment. Avalanche modelling and estimating run-outs based on numerical avalanche dynamics model is current state of art trend in avalanche run-out simulations. By modelling of avalanche dynamics, we are able to estimate the devastating potential of the avalanche. Determination of the possible path and defining the potential zones of the avalanche reach is an important basis for designing and dimensioning avalanche defence structures. Snow is one of the most complex natural materials for mathematical description. The dynamics of the avalanche movement is therefore extremely variable within the individual avalanches. Current knowledge and experience, proves that avalanche modelling and mapping methods can greatly help to understand the avalanche behaviour and hence reduce avalanche risk in mountainous terrain. Complementary to avalanche modelling avalanche monitoring and mapping is crucial for the proper estimation of avalanche danger level, calibration of numerical

models and it is used as valuable feedback for avalanche forecasters. The final publication is a book chapter, which summarizes all the modelling aspects of avalanches as a part of bigger group of geological hazards.

4.1 Snow avalanches

Avalanches are a characteristic phenomenon of every snowy mountain. It is a natural phenomenon that greatly affects the mountain environment and human activities as well. At the same time, it represents one of the greatest hazards for skiers, tourists and climbers moving in the winter mountainous terrain. The term avalanche is most commonly understood as the sudden movement of snow and its gravitational displacement along the mountain slope.

The avalanche triggers in release zone (Figure 1), gain speed in transportation zone and decelerate and stops in run-out zone (Figure 2). The initiation of naturally triggered avalanche depends on the development of two factors: a) the weather which influences the snow cover properties, and b) the morphological properties of the terrain (Milan, 1981). Snow is the material

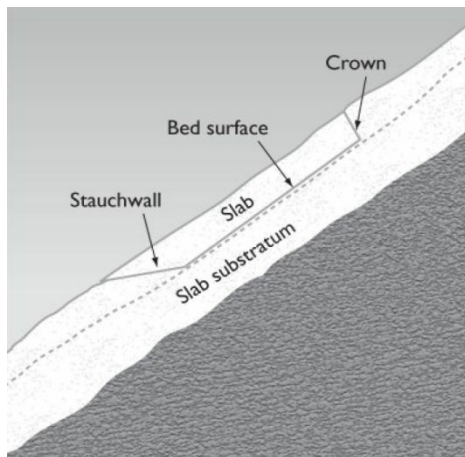


Figure 1 Anatomy of avalanche release zone.
(source: McLung)

of every avalanche meanwhile the wind is the architect of unstable snow slabs and pillows. There is a great deal relationship among these factors, and it is relatively difficult to judge it individually. The fall of the avalanche is always the result of the complex action of all three of the mentioned groups of factors. Topographic features such as slope, exposure, altitude, horizontal and vertical topography, vegetation cover, and size of the release zone predominantly determine the friction effect, dynamics, behaviour avalanche size its shape, and finally avalanche effects on nature.

Of the meteorological elements, the temperature, wind and overall duration and intensity of snowfall have the important influence on the characteristics and the formation of avalanches. They also determine the avalanche's size - especially their volume and weight. The specific physical and mechanical characteristics of the snow cover are also shaped by the specific effects of topographic and meteorological elements. Of these, moisture, hardness, specific gravity, breathability, porosity, cohesion, adhesion, and the size of snow crystals and grains have the greatest influence on avalanche formation. A more detailed description of the influence of individual factors on the avalanche is not the aim of this work and is described in more detail in many other works e. g. Kňazovický, McLung, Tremper. Avalanche release occurs when the tension in the snow cover is at a certain point larger than its strength and when the friction resistance of the snow layer over its base is exceeded. The immediate cause of the avalanche can be considered to be a disturbance of the stress balance in the snow cover on the inclined slope (Midriak, 1977). The existence of internal tensions in the snow cover is caused

mainly by the actual weight of snow, increasing after each snowfall and changes in its structural structure (Kňazovický, 1967) or by human additional load. The increase of the tension in snow cover is initialized mainly by the addition of new snow, internal changes in snow cover, or with any additional load caused by human and animals.

However, the complex structure of tension within the snow cover also causes by large variation in the mechanical and physical properties of its individual layers. The snow crystals in the snow cover are subject to a continuous process of constructive and destructive metamorphosis. The difference in course, intensity and duration of these processes ultimately results in the different mechanical and physical properties of each layer of the snow cover. The stress concentration increases especially in those layers exhibiting the smallest plasticity (Kňazovický, 1967).

In addition to its layering the terrain topography also influences the size and occurrence of stresses in the snow cover. Terrain morphology impacts the properties of the snow cover not only directly, but also indirectly by affecting uneven snow deposition. Snow cover and its height in the mountains have great variability influenced by many factors. The tension ratios are greatly influenced by the strong variation in the height of the snow cover (Kňazovický, 1967).

Increase, resp. the decrease of the height of the snow cover in the direction of the slope greatly affects the tensile, pressure loads of snow layers. Due to this tension stress and disorders within the snowpack the slide of avalanche is initialized. If the tension in the snow cover exceeds the adhesive forces (adhesion of two neighbouring snow layers or snow cover and subsoil), the snow pack structure breaks down, and the static friction between the different snow crystals is replaced by a much smaller kinetic friction (Midriak, 1977). The conditions of avalanche formation and their subsequent movement and character are therefore highly variable. Under a certain combination of conditions, avalanches show to some extent similar characters, which led to their classification.

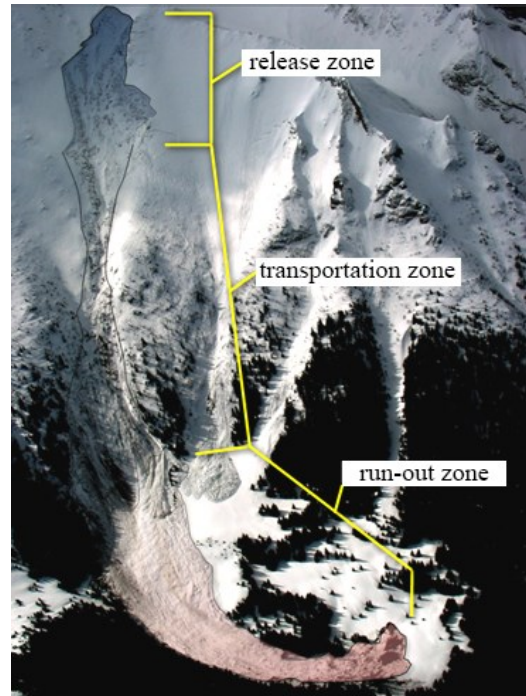


Figure 2 Avalanche track one of the avalanches in large avalanche cycle in Tatra mtns. in 2009. (source: Richnavský, 2012; archive of Avalanche prevention centre)

However, not every type of avalanche is suitable and can be modelled using dynamic models. Each type of avalanche has its a characteristic behaviour and the physical-mathematical representation of their movement varies considerably. The best described are so called slab avalanches. Based on the type of snow entrained the in slab we do distinguish soft slabs (Figure 3 and hard slabs (Figure 4).



Figure 3. Soft slab avalanches: (a) in the Western Tatra in April 2008, (b) avalanche from the Prislop in Žiarska dolina in the West Tatra in February 2006 (c) the avalanche in the Kartárik in the High Tatra. (source: Richnavský, 2012; Avalanche prevention centre)



Figure 4. Hard slabs avalanches: (a) avalanche from the Latiborská hola in the Low Tatras in April 2008 (b) Ďurková in the Low Tatra in January 2010) (c) Zelená dolina in the Western Tatra in December 2007. (source: Richnavský, 2012; Avalanche prevention centre)

The simulation of avalanche motion using dynamic numerical models is currently focused mainly on slab avalanches from both dry and wet snow. These are the greatest hazards in most mountain areas. For modelling, it is also very important to know certain properties of the snow cover. The physical properties of snow have the greatest importance for the dynamic numerical modeling of the avalanche range, namely the height of the tear and the specific snow weight ($\text{kg}\cdot\text{m}^{-3}$). This is why efforts are being made to obtain these data from most registered avalanches in Slovak mountainous areas as well.

4.2 Snow and Avalanche research related to GIS, reemote sensing and modelling

Research in the field of snow and avalanches has a relatively rich tradition mainly in the Alpine countries. There are several research topics and directions such as: snow meteorology, metamorphosis and snow physics, meteorological and topographic patterns, avalanche terrain morphology and others. This was mainly due that settlements, transport facilities and other infrastructure were threaten by avalanches. One of the oldest works which describes the influence of avalanches and attempts to investigate the causes of the avalanche is the work of Coaz: *Die Lawinen der Schweizeralpen* (Coaz, 1888).

In 1965 B. Cottman analysed the impact of the morphological conditions on avalanche release. Among others, K. Chomicz's publications (1965) are also valuable because they focused on the Polish side of Tatra Mountains. Extensive knowledge about processes of avalanches and their consequences is presented in Salm (1982) and Munter (1992).

Publication *The Avalanche Handbook* (McLung, Shaer, 2006) offers one of the most comprehensive information on the avalanches issued in English. The publication is based on the long-term experience of North-western avalanche authors and can serve as a basic textbook for avalanche experts. The exploitation of GIS in the research of the avalanche issue began to appear in the works of foreign authors at the end of the 1990s. The first countries in which avalanche-oriented GIS applications are emerging are Switzerland, Norway, France and the USA. First use of GIS for mapping avalanche hazard in Iceland is well described in the work of L. Tracy (Tracy, 2001), which has a practical implications of building proper and efficient avalanche defence structures. However the Swiss Avalanche and Snow Research Centre (SLF) have a long term tradition with intensive implementation of GIS in avalanche research. Gruber, in 2001, (Gruber, 2001) uses the GIS for avalanche hazard mapping in Switzerland to describe how to use GIS to determine individual zones of avalanche threat. Gruber and Maggioni used GIS to analyse historically documented avalanches and the influence of topographic factors on the avalanche release dimension and frequency. Their publication describes the topographical parameters that contribute most to the release of an avalanche (Gruber, Maggioni, 2006). Delparte, in her publication *Statistical runout modelling of snow avalanches using GIS in Glacier National Park, Canada* (Delparte, 2008) claims that models from these well-documented avalanche tracks can then be transferred to places where this documentation was missing. GISs are also useful in calculating avalanche run-out using statistical models.

The most pronoun issue of avalanches is when they do interfere with settlement and infrastructure. So in early stages of avalanche run-out modelling a simple statistical-topographic model were developed mainly in Norway. The model based on topography obtained by field surveys and regression relations between the topographical parameters (Lied, Bakkehoi, 1983). Nowadays many topographical patterns and properties can be obtained by spatial calculations

using digital terrain models in GIS. In Colorado Bovis and Mears addressed the issue of the statistical prediction of snow avalanche run-out from terrain variables (Bovis, Mears 1976). The Canadian McLung coped well with extreme avalanche run-out and their modelling with statistical alpha - beta model (McLung, 2000).

The other research direction of modelling avalanches is numerical simulation of their behaviour based on treating/approximating avalanches as granular flows. There are several ongoing studies, works and large scale testing sites to calibrate the mathematically complex models. Their development and use is a relatively young field of research, but in the background of most of these tools there are more or less the mathematical relations for mass movement over the surface defined by Voellmy (Voellmy, 1955). Voellmy's equations was partly adapted by Salm (Salm, 1966, 1968) and valuable historical source on avalanche dynamics is provided in the work of Mears (Mears, 1989). The modelling part of the thesis is based on the numerical model RAMMS developed in Switzerland at the department of avalanche dynamics at SLF. The problems of avalanche modelling using dynamic numerical models are addressed by various publications (Christen et al., 2002; Bartelt et al., 1999; Gruber and Bartelt, 2007; Bühler et al., 2011;). Nowadays the shift from one dimensional model (Gruber, Bartelt 2002) to two-dimensional (P. Bartelt et al., 2008) is obvious.

The background of numerical model-RAMMS is well described by Christen (Christen et al., 2008; Christen et al., 2010). Sensitivity of snow avalanche simulations to digital elevation model quality and resolution has an influence on final simulation results, but generally DEM with very high resolution have negligible asset (Borstad, McLung 2009). The most complex work on avalanche dynamics has been done by Pudasaini and Hutter (Pudasaini, Hutter, 2006). During the last two decades various models have been developed also outside SLF. A team of authors around at the Department of Avalanche and Torrent Research in Innsbruck are involved in the development and testing of the SAMOS and ELBA numerical model used to model avalanche dynamics (Sailer, 2008).

In the context of avalanche modelling, the work of Mergili from the Institute of Geography at the University of Innsbruck in Austria must be mentioned. The author devolved a model integrated in open source GRASS GIS to model granular flow of avalanche directly in GIS environment. This promising approach shows reasonable results but has to be further investigated (Mergili, 2007).

Despite that in the Carpathian Mountain area avalanches is far not a concern than it the Alps, there's long term tradition in snow an avalanche research. This research is concentrate at the Avalanche prevention centre of Mountain Rescue service and other collaborating institutions. First attempts to model avalanche release zones were done in Tatra Mountains by (Hreško, 1998) and Belianske Tatra mountains (Hreško, 1999). Hreško developed a simple and efficient model capable to estimate avalanche release zones based on topographical parameter. His work was followed by Barka and Rybár (Barka, Rybár, 2003) and they focused on the area of Mala Fatra. In their work they use statistical alpha beta model to estimate the run-outs. The model is

integrated in GIS environment and thus can be used on larger are in automated manner (Bárka, 2003). Avalanche are not subject of research only in Slovakia but also on Polish side of Tatra Mountains there is extensive research on application of GIS in avalanche mapping and modelling.

A great and valuable work has been done at the Institute of Geography of Jagiellonian University in Krakow by P. Chrustek of. In his work, he explores the use of GIS in the research of the alpine landscape and also application of numerical model (RAMMS) to local geomorphology of polish Tatra Mountains (Chrustek et al., 2009, 2010).

Today, remote sensing is key for the identification, quantification and monitoring of natural hazards. Recent developments in data collection techniques are producing imagery at previously unprecedented and unimaginable spatial, spectral, radiometric and temporal resolution. The advantages of using remotely sensed data vary by topic, but generally include safer evaluation of unstable and/or inaccessible regions, high spatial resolution, spatially continuous and multi-temporal mapping capabilities (change detection) and automated processing possibilities. Of course, as with every method, there are also disadvantages involved with the use of remotely sensed data. These are generally in relation to the lack of ground truth data available during an analysis and to data acquisition costs. Publications on the use of optical remote sensing for hazard applications include: landslide and rockfall evaluation (e.g., Mantovani et al., 1996; Roessner et al., 2005; Miller et al., 2012;), flood mapping and modelling (e.g., Townsend and Walsh, 1998; Sanyal and Lu, 2004), glacier- and permafrost related hazard assessments (e.g., Kääb et al., 2005) and avalanche detection (Bühler et al., 2009; Lato et al., 2012). A list of various satellite and airborne sensors with sufficient resolution for such analyses is given in, for example, Lato et al. (2012). Automatic avalanche mapping in very high resolution optical imagery is seen as most sensible to update avalanche cadastres after, e.g., large avalanche cycles. For more near real-time and operationally oriented applications (such as avalanche danger forecasting), the use of SAR data is seen as most feasible, due to the independency of clear sky.

5 Material and methods

5.1 Retrospective study on avalanche airbag use

For the publication 1 it was necessary to collect all relevant records of documented avalanche incidents involving at least one avalanche airbag user. The data were collected from national registries of avalanche incidents from Canada, France, Slovakia, Norway, Switzerland and the United States. Incident reports were examined in detail a consistent dataset was produced. The avalanche airbags are designed to reduce the probability of critical burial, the analysis focused on avalanche involvements with potential of critical burial. Accident records were therefore only included if the size of the avalanche was ≥ 2.0 according to the Canadian avalanche size classification, because the sizes < 2.0 are too small to bury or harm a person. Only seriously involved users and non-users of airbags were included in the dataset. Finally only the accidents with multiple involvements and different users of avalanche airbags (non-users, users with non-inflated airbags, and users with inflated airbags) were included in the analysis. This extraction eliminated the likely reporting bias.

The univariate analysis was based on Fisher's exact tests for count data and Wilcoxon rank-sum tests for ordinal or non-normal numeric parameters. Two-sided $P < 0.05$ was considered statistically significant and $0.05 \leq P < 0.10$ marginally significant. Effectiveness of avalanche airbags was expressed as absolute risk reductions for critical burial and mortality. For the multivariate analyses used stepwise binomial logistic regression were models starting with all available factors influencing grade of burial and mortality. $P > 0.10$ was used as the exclusion criteria for factors to prevent overfitting of the models.

5.2 Avalanche modelling

Avalanche dynamics modelling is closely related to hydrological modelling, which deals with the formation and properties of the snow cover. At the input and output level, these two modelling domains can be linked through different GIS (Figure 5.) Snow precipitation determines the distribution and properties of the snow cover. Together with terrain morphology they do determine the location of potential avalanche release zones. However, snow avalanches can significantly influence the hydrological proportions of the area.

The modelling of avalanche hazard consists of four main steps (Anecy, 2008):

- Specification of snow precipitation distribution, and crown height.
- Estimating and assessing the potential release area
- Avalanche simulation
- Estimating the potential run-out

The relationship between known inputs and unknown values of the output quantity is solved at a given time and space. It is essential that the model responds to the physical laws that work in the real world. With the increasing development of computer technology and its capability to handle large scale data, the models are getting more complex. Thus the modelling results can be very effectively applied in operative practice in avalanche prevention.

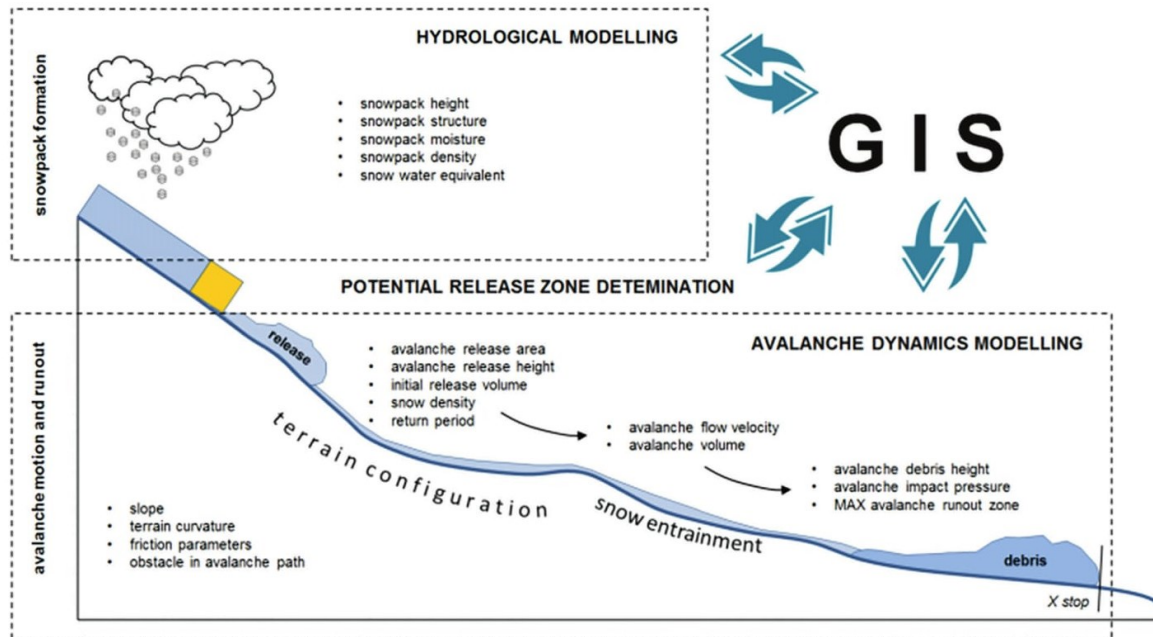


Figure 5 Avalanche process and application GIS in modelling (source: Richnavský, 2012)

5.2.1 Friction parameters

The friction is the main reason for most of peculiarities and differences in avalanche dynamics. Friction develops among moving masses of snow and ground within the internal structure of avalanche. Its size is proportional to the area of the layers sliding alongside, as well as the difference in velocity and the coefficient of snow viscosity (Kňazovický, 1967). The friction in the avalanche core is conditioned by the interference of the snow particles and their contact with the sliding surface. As a result of this friction, heat is generated to form a small amount of water on the surface of the snow particles. After the avalanche stops, the water freezes on the surfaces of these sticks to create a very tough avalanche coating. This is why the extraction of human body from avalanche deposits is very difficult, time consuming and demanding. Generally, friction causes a reduction in flow velocity. Individual types of avalanches are characterized by a characteristic movement. This knowledge is a basic prerequisite for solving feasible dynamic numerical models. In the flowing avalanche two opposing sets of forces are controlling the avalanche dynamics: driving force and friction force. Driving force is the result of a tension

parallel to the incline of the slope. Resistance force principally inhibits avalanche movement and consists of several components (Mears, 1976):

- the shear friction between the avalanche and the underlying layer of snow, or a soil, rock, or vegetation cover (R_1)
- internal dynamic shear resistance caused by collisions and a change in momentum between snow particles and snow pieces (R_2),
- internal friction inside the snow-air suspension (R_3),
- shear friction between avalanche and ambient air (R_4),
- Hydrodynamic resistance at the head of avalanche (R_5).

The final force available for acceleration ($F_{acceler}$) of the avalanche is thus the resultant of all the forces involved:

$$F_{acceler} = F - (R_1 + R_2 + R_3 + R_4 + R_5)$$

While F is a tensile force component parallel to the slope surface [N].

Estimation of maximum avalanche reach is one of the most important aspects of avalanche hazard zoning. This is one of the main objectives of in avalanche dynamics. However at the same time, it is also one of the most complex and controversial problems in a avalanche research (Bakkehøi and Lied, 1983). The avalanche distance depends on a complex of factors that are spatially and temporally variable. The characteristics of the segregation zone, the diversity of the terrain and the snow conditions are ultimately reflected in the large variability of the avalanches in the avalanche path. At present, there are several approaches and methods for analysing avalanche hazard by estimating maximum avalanche impacts and run-outs.

In particular, the implementation of GIS has greatly expanded of the methods of determining potential avalanche impacts and the shape of the avalanche track. Generally, there are 3 approaches:

- Classical, traditional methods - manual avalanche terrain mapping and field investigation based on the experience and observation of avalanche expert.
- Topographic - statistical methods - use of statistical topographic models - alpha-beta regression model publication 2, 3.
- Dynamic numerical modelling - use of 1D dynamic models (AVAL-1D) and 2D dynamic models (RAMMS, SAMOS) publication 4, 7.

All three approaches are interconnected and, in some aspects they do supplement each other. The classic and statistical approaches allow an estimate of the maximum avalanche reach but they are

not capable to determine the speeds and pressures. These two important variables can be simulated only by dynamic models. However, the theoretical basis of multiple numerical models is based on long-term statistical analysis of observed and well-documented avalanche events.

5.2.2 Topographic statistical modelling of avalanche reach

The statistical $\alpha - \beta$ model requires the morphometric analyses of terrain and calibration of the model based in of well know avalanches. This model was used in publication 2 and 3. $\alpha - \beta$ model

The model was developed at the Norwegian Geotechnical Institute (NGI) in Oslo in 1980. Lied and Bakkehoi analysed 206 avalanche tracks and based on regression analysis, they selected 4 morphometric parameters that best correlate with the length of the avalanche. This selection was later narrowed to two parameters, between which a very tight correlation was demonstrated (Publication 2). The model thus predicts the maximum length of the avalanche path based on the morphometric parameters of the relief of the given path. Morphometric parameters include a reference point (so called the β point) with β angle defined as the average gradient of the avalanche path profile from the position where the slope decreases to 10° to the trigger zone (Figure 6.) The α is the angle sighting from the extreme run out position to the trigger zone. Least square regression analysis showed correlation between α and β angle have form of equation (Lied and Bakkehøi, 1983).

$$\alpha = C_0 + C_1\beta$$

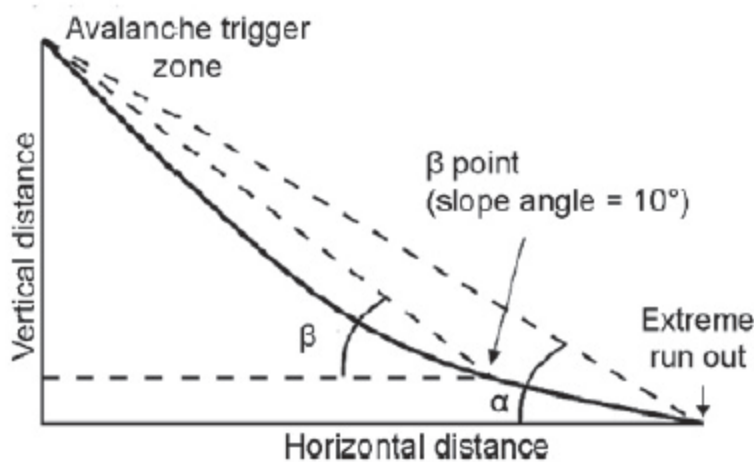


Figure 6. $\alpha - \beta$ model also known as topographical or statistical run-out model (source: Lied, Bakkehoi 1983)

To determine the position of points α and β , it is appropriate to use at least 30 detailed avalanche paths (McLung, 2000) in the evaluated area. The location of the point was determined based using GPS by field measurement. The position of the β points is determined on the basis of the slope analysis in the GIS environment. If the positions of these points are determined, their horizontal and vertical distance from the release zone is calculated. Angle α and β

values are then determined on the basis of known relationships in the triangle (Figure 6). After the relationship between these angles is calculated by regression analysis, the coefficients C_0 and C_1 are determined. The model can then be used to calculate potential avalanche run-outs. Such a statistical approach has been used in several countries, and it has been found that each mountain

range differs with its morphometric avalanche parameters and therefore it is not possible to use the equally calibrated model for different areas. The model was used in Canada (McLung and Mears, 1991), in the US (Mears, 1989).

5.2.3 Avalanche run-out modelling using numerical dynamic models

In many cases the limitations of classic avalanche mapping methods and the limitation of statistical models have led to the development of multiple numerical simulation tools that make it possible to model the motion of snow avalanche. A dynamical approach to numerical modelling of avalanche behaviour is currently state of art in avalanche research. Such models are capable to simulate a variety of situations, from simple to complex. This development has been particularly concentrated in countries where the avalanche mapping has the greatest long-term tradition (Switzerland, Austria and Canada). The use of the dynamic models has many advantages and especially it is suitable also for very complex terrain where statistical avalanche run-out modelling reveals unfeasible results. On the hand numerical models are more mathematically complex and requires rather large computational capacity and input data accuracy.

In general input data into numerical models are divided into three categories (Haeberli et al., 2004):

- Release zone parameters – crown height, snow density,
- Flow parameters - friction parameters, snow-pack parameters,
- Specific simulation parameters - spatial resolution, time step, simulation length.

The first attempts to map the avalanche danger using avalanche dynamics go back to 1955. Voellmy described the first model of the avalanche flow. The model is based on basic hydraulic theories with two resistance forces (Voellmy, 1955). However, not all avalanches move similarly to liquid and cannot be adequately modelled using fluid mechanics relations. However, such approximation is more appropriate than purely subjective models. Voellmy describes avalanche movement as the flow of matter, principally affected by two friction parameters:

- Static (independent of flow rate), shear friction (friction coefficient μ), proportional to normal pressure based on the avalanche current. At low speeds the shear friction dependency can be neglected - we are talking about dry, Coulomb friction
- Speed-dependent, viscous (turbulent) friction (friction coefficient ξ), proportional to the square of avalanche velocity. This parameter also includes aerodynamic resistance and friction resistance (Jamieson et al., 2008).

Voellmy model is based on the assumption that a frictional resistance is generated on the slope with the vertical height h , which is proportional to the area of the snow cover. While in the turbulent motion the frictional resistance is e proportional to average speed and density of the snow ρ .

The Voellmy equation for the maximum velocity v_{max}^2 which the avalanche reaches on a uniform path under angle α is given by relation (Voellmy, 1955):

$$v_{max}^2 = \xi h (\sin \alpha - \mu \cos \alpha)$$

where

h is the height of the avalanche current [m]

ξ is the coefficient of turbulent friction [m / s²]

μ is the coefficient of shear friction

α is slope angle [°]

The equation provides results, particularly valid for dry avalanches from dry snow on open slopes. The result of this equation largely depends on the values of coefficients ξ and μ and the height of snow in avalanche (h). However, there are only approximate guidelines based on experimentally measured data to determine the correct values of these coefficients. The values of the turbulent friction coefficient (ξ) change with respect to surface roughness.

When using this model, it is necessary to specify the reference point in which the avalanche begins to slow down. The path (S) that the avalanche passes in its braking phase in the impact zone inclined at the angle β is given by:

$$S = \frac{v^2}{2g(\mu \cos \beta - \tan \beta + 0.5 v^2 \xi h)}$$

where

h is the height of the avalanche flow [m]

g is the gravitational acceleration [m / s²]

ξ is the coefficient of turbulent friction [m / s²]

μ is the coefficient of shear friction

The equation is very sensitive to the values of the coefficients ξ and μ and to the values of the height of the avalanche flow and its velocity. In practice determination of reasonable values of these coefficients represents a relative issue.

Most of the other attempts to describe avalanche dynamics primarily originate from Voellmy model. The most significant modifications of this model were made by Salm. By including the impact of the counter pressure (due to stopping the simulated avalanche flow in the reach zone) and the flow width, the model was adapted to so called, known as the Voellmy-Salm model (Salm 1966). After many years of validation and calibration, this model was also embedded in the Swiss Guideline for Avalanche Runout Calculation (Salm et al., 1990).

So far the mentioned models operated in one dimension. With onset larger computation capacity and better understanding of avalanche behaviour the transition from one dimensional to two dimensional modelling is apparent. RAMMS (RAPid Mass Mass MovementS) is a modern numerical simulation tool used to model the movement of geophysical mass movements from trigger to run-out within a three-dimensional terrain (Christen et al., 2010). The RAMMS model was developed by Avalanche, Debris Flow and Rock-fall, group, working at the WSL Institute for Snow and Avalanche Research. The RAMMS model is capable to simulate and predict not only the avalanche reach the but also the speed, impact pressure and mass entertained in avalanche motion.

Avalanche flow is characterized as uneven motion with varying height of drifting snow and speed. For each simulation in the RAMMS model, the differential equations are solved for the snow height $H(x, y, t)$, the mean avalanche velocity $U(x, y, t) = (U_x(x, y, t), U_y(x, y, t))^T$ and the kinetic energy associated with the random movement of the snow grains $R(x, y, t)$. The equations are solved at time t where the topography $Z(X, Y)$ is given in the Cartesian system. X and Y represent horizontal coordinates. The surface shape is generated by the local coordinate system x, y, z . It is discretized so that its projection in the $X - Y$ plane leads to a structured grid. Based on the first principle of conserving matter and momentum, the basic equilibrium rules are derived (Christen et al., 2010):

$$\begin{aligned} \partial_t H + \partial_x(HU_x) + \partial_y(HU_y) &= Q_{(x,y,t)} \\ \partial_t(HU_x) + \partial_x\left(HU_x^2 + g_z k_{a/p} \frac{H^2}{2}\right) + \partial_y(HU_x U_y) &= S_{gx} - S_{fx} \\ \partial_t(HU_y) + \partial_x(HU_x U_y) + \partial_y\left(HU_y^2 + g_z k_{a/p} \frac{H^2}{2}\right) &= S_{gy} - S_{fy} \\ \partial_t(HR) + \partial_x(HRU_x) + \partial_y(HRU_y) &= \alpha S_f \|U\| - \beta R \end{aligned}$$

Avalanche motion is described as a moving block of snow that is slowed down by force, directly proportional to the square of the speed of that flow. The friction resistance S in [Pa] is then defined as follows (Christen et al., 2010):

$$S = \mu\rho Hg \cos\phi + \frac{\rho g U^2}{\xi}$$

where

ρ is the flow density,

g is gravitational acceleration,

ϕ is the slope angle of the slope,

H is the height of the flow

U is the flow rate

This model divides the friction resistance of the surface into two components. Dry type of friction (coefficient μ) in the RAMMS model referred to as μ . The second coefficient ξ , in the RAMMS model called ξ , is the coefficient of resistance in which is in relation to the square of velocity given in [m / s²].

This equation has found application in many applications for mass movement, especially snow. The Voellmy model has been used for a long time in Switzerland. The μ and ξ coefficients, also referred to collectively as $\mu\xi$, also depend on the global simulation parameters in RAMMS (return period and volume of snow in avalanche). These two coefficients can be calibrated in three altitude zones for different terrain types (open slope, gully, flat surface, forest). However the Voellmy equation, insufficiently describes the flow at the avalanche forehead and the avalanche's tail.

The measurements indicate a significant increase in friction and thus a decrease in flow velocity. This causes the RAMMS model to be somewhat limited in the prediction behaviour of the avalanche decelerating and depositing snow. Modelling of the avalanche process is still under development, and each new addition and enhancement of the RAMMS model is continuously released.

6 Aims of the study

The focus of the dissertation work and of the whole research is based on close cooperation with the Avalanche Prevention Centre for of Mountain Rescue Service in Slovakia and was design to produce relevant outputs applicable in operational mode in avalanche forecasting, designing avalanche defence structures, delineating avalanche hazards zones and reviewing the safety equipment and its influence on survival of avalanche victims.

The aims of the work are as follows:

- To review of avalanche safety – avalanche balloons equipment on survival of avalanche victims and test the various avalanche balloon packs in real avalanche and estimate the impact forces using numerical modelling and GIS (Publication 1 & 6)
- Statically model avalanche run-outs in Western Tatra and implement the run-out model into GIS environment(Publication 2)
- Compare the statistical run-out modelling and release zones estimation using GIS within two various geographical locations (Publication 3)
- Develop and algorithm capable of automated detection of avalanche deposits from very high resolution satellite imagery (Publication 4)
- To determine appropriate parameterization and calibration of used numerical models and establish a procedure for obtaining sufficiently precise data needed to model avalanche impacts (Publication 5)
- To investigate use of high resolution LIDAR for avalanche hazard mapping (Publication 7)
- To summarize the main findings from modelling and research on snow avalanches and delineate a future perspective of avalanche hazard zoning using results from numerical simulations. (Publication 8)

The long-term goal pursued by this work is to support the effort of integrating modern GIS technologies and numerical computational modelling tools into the standard practice of avalanche prevention implemented by the Avalanche Prevention Centre in Slovakia.

7 Results

The results of the thesis are summarized in eight publications from which two are book chapters. All of them (except publication 6) are reviewed and published in international journals or proceedings. Publication 1 was published in international journal with impact factor.

Publication 1: Haegeli, P., Falk M., Procter, E., Zweifel, B., Jarry, F., Logan, S., Kronholm K., **Biskupič, M.**, Brugger H., 2014 The effectiveness of avalanche airbags. Resuscitation, Volume 85, Issue 9, 1197 – 1203.

Publication 1 retrospectively studied the use avalanche airbags and investigated its effectiveness on avalanche survival and mortality. Binomial linear regression models showed main effects for airbag use, avalanche size and injuries on critical burial, and for grade of burial, injuries and avalanche size on mortality. The adjusted risk of critical burial is 47% with non-inflated airbags and 20% with inflated airbags. The adjusted mortality is 44% for critically buried victims and 3% for non-critically buried victims. The adjusted absolute mortality reduction for inflated airbags is –11 percentage points (22% to 11%; 95% confidence interval: –4 to –18 percentage points) and adjusted risk ratio is 0.51 (95% confidence interval: 0.29 to 0.72). Overall non-inflation rate is 20%, 60% of which is attributed to deployment failure by the user. Conclusion: Although the impact on survival is smaller than previously reported, these results confirm the effectiveness of airbags. Non-deployment remains the most considerable limitation to effectiveness. Development of standardized data collection protocols is encouraged to facilitate further research.

Publication 2: **Biskupič, M.**, Barka, I., 2009, Statistical avalanche run-out modelling using GIS on selected slopes of Western Tatras National park, Slovakia. International Snow Science Workshop, Proceedings, 482-487.

Results from the model estimating probable avalanche paths correlates well with avalanche cadaster map figure 7. It was expected that trigger zones estimated by the model will occur in upper parts of historical avalanche paths. Some historical path and modeled trigger zones show some inconsistency. Field investigation and aerial imagery inspection indicated large forest succession in these places for last 25 years. Due to this succession avalanche activity was reduced to minima. Using up to date land cover maps and ortho imagery as an input for the model resulted in the proper estimation of potential avalanche trigger hazard. Model revealed that 67,45% of the study area falls into the zone with small avalanche trigger potential 21,56% with medium 10,4% with high and 0,59% as very high avalanche trigger potential. See figure 5. Due to the implementing the curvature factor, estimated release zones reflects the nature of avalanche triggering. It can be seen from figure 6. Ridges were properly classified as places with minimal avalanche trigger potential. On the other hand GIS with the help of script language (Avenue)

allowed implementing statistical run out modeling in automated way. This was done on selected slopes. The final regression equation for the Western Tatras is $\alpha = 0,91\beta - 0,04^\circ$. Correlation coefficient for this regression is 0,95 coefficient of determination is 0,9 and standard error of predicted α angle is 1,1. Figure 7 shows final run outs on the two of the selected avalanche paths. It can be said that in this case model outputs are in well correlation with historical avalanche cadastre map. In some other cases model failed to represent run outs naturally e. g run ups, channeled curvy run outs. Because the avalanche movement was approximated as water flow, circumstances occurred in narrow channels where all the flowlines gathered together and from certain point they flowed together. This was partially solved by channel module in SAGA. Anyway some in some extremely narrow channels satisfying results were not obtained and different methods should be used for determining avalanche width.

Publication 3: Boltížiar, M., Biskupič, M., Barka I., 2016, Spatial modelling of avalanches by application of GIS on selected slopes of the Western Tatra Mts. and Belianske Tatra Mts., Slovakia, *Gographica Polonica*, 89,79 – 90.

The model revealed that in the Žiarska valley, 68% of the area studied falls into a zone with small avalanche trigger potential; 21% with medium; 10% with high and 1% with very high avalanche trigger potential and in the Predné Med'odoly valley: 62% of the area studied falls into the zone with small avalanche trigger potential; 14% with medium; 14% with high and 10% with very high avalanche trigger potential (Fig. 4). High or very high risk potential was given to the steep gullies and vast steep slopes covered with grass. This is one of the reasons why the Predné Med'odoly valley has more 'very high' avalanche release potential areas.

Publication 4: Frauenfelder, R., Lato, M. J., Biskupič, M., 2015, Using eCognition to automatically detect and map avalanche deposits from the spring 2009 avalanche cycle in the Tatra mts., Slovakia, *Int. Arch. Photogramm. Remote Sens. Spatial Inf. Sci.*, XL-7/W3, 791-795.

Even though the results of the first training runs looked seemingly satisfactory when just analyzing a small portion of the imagery, the algorithm did not perform satisfactory on larger subsets of the data. On the one hand side the mapped avalanche debris was punctuated by small holes (i.e., errors of omission); at the same time many areas, especially wind-blown areas and rock outcrops, were falsely classified as avalanche debris (i.e., errors of commission). Analyzing the Slovakian imagery more closely, we observed a distinct "rake" pattern in many lower-lying areas of the imagery. We found that the rake pattern is more pronounced at lower altitudes, with the 1700 m a.s.l. contour line approximately delineating the height below which the problem starts occurring. The features showed to be the result of melting processes, caused either by a rain-on-snow event or even just by increasing air temperatures. Therefore we had to adapt the algorithm in order to eliminate these features prior to the actual avalanche debris mapping. The quantitative comparison of the algorithm performance with respect to the expert mapping shows a good overall performance with comparable rates of errors of omission and errors of commission

if one takes the expert mapping as the "true" situation. A qualitative comparison between expert mapping and automatic classification by the algorithm indicate that the algorithm struggles in areas with strong pixel saturation. However, oversaturation seems to be more of an issue in WorldView-1/2 imagery than in previously explored data sets such as QuickBird imagery and airborne push broom scanner data.

Publication 5: Richnavský, J., **Biskupič, M.**, Mudroň, I., Devečka, B., Unucka, J., Chrustek, P., Lizuch, M., Kyzek, F., Matějček, L., 2011, Using Modern GIS Tools to reconstruct the avalanche: A case study of Magurka 1970. GIS Ostrava 2011 Proceedings 175- 185.

Friction coefficients (μ , ξ) are necessary inputs for adjusting the proper simulation using RAMMS model. Coefficients, which were determined and used in one valley, can also be used in avalanche simulations in the adjacent valleys. These friction coefficients determine the surface friction in different heights. Coefficients, which were determined and used in one valley, can also be used in avalanche simulations in the adjacent valleys. There is a big probability that surface resistance to the avalanche flow will be similar in adjacent valleys as well. This experience was used for modelling potential avalanche events in the valley of Viedenka, which is situated to the west of Ďurková valley. In contrast with the reconstructed avalanche in the Ďurková valley, similarly great avalanche in the valley of Viedenka will affect significantly the urban space of Magurka settlement. Many cottages in this settlement will be damaged or ruined as a consequence of destructive power of a similar avalanche. In this locality, some experimental simulations were calculated with different heights of potential release zones. Fig. 8. shows results of particular cases of these simulations. It is obvious that a fracture height more than 2 m causes a significant spreading of the runout and more cottages are endangered.

Publication 6: **Biskupič, M.**, Richnavský J., Lizuch M., Kyzek, K., Žiak I., Chrustek, P., Procter, E., 2012, Three different shapes of avalanche balloons a pilot study, International Snow Science Workshop, Proceedings, 482-487.

The dummy with the Snowpulse/Mammut Lifebag was dragged by the avalanche for 132 m in 20 s. The average speed was 6.6 ms⁻¹ (23.76 kmh⁻¹) while it reached a maximum speed of 17.8ms⁻¹ (64.08 kmh⁻¹). Acceleration occurred over 89 m with an average velocity of 3.56 ms⁻². When the avalanche stopped moving, this dummy was buried from the hips down (Figure 2). The lower part of the body was anchored in the snow deposit and the whole body was partially buried in a tilted position. This was a partial-not critical burial, the airways were not obstructed and the head was not impaired by the snow. The balloon was clearly visible on the avalanche surface. The dummy equipped with ABS Vario system was carried over 123 m in 18 s. The maximum velocity reached by this dummy was 18.6 ms⁻¹ (66.96 kmh⁻¹) while the average speed was 6.9 ms⁻¹(24.84 kmh⁻¹).The avalanche reached the highest speed at 9 s. At 9 s the dummy had been carried 93 meters from its starting point, reaching an acceleration of 3.36 ms⁻². The dummy was

deposited in a horizontal face-up position lying on its back with the head pointing down the slope. There was a block of snow (approximate diameter 70 cm) lying on its abdomen and additional snow laterally. The grade of burial was between partially buried and not buried. It is questionable if a human being would be capable of freeing himself in this position without additional help from companions. Important is that the airways were not obstructed and the head was not impaired with snow. One leg was visible and the balloons were clearly visible as well. The dummy wearing the BCA Float balloon was carried along the shortest distance of 114 m with an average velocity of 8.1 ms⁻¹ (29.16 kmh⁻¹). The dummy reached a maximum speed of 16.8 ms⁻¹ (60.48 kmh⁻¹) with an acceleration of 3.72 ms⁻² after 84 m. From this moment the dummy started to decelerate until the point of stopping in a supine position (Figure 4). The head and the airways were free of snow except and only a few small snow chunks were deposited on the trunk. Probably a human could free himself with no additional help. Based on this the burial was classified as no burial. The surrounding chunks of snow left the airways unobstructed and the head was not impaired by the snow. Both legs and one arm were sticking out from the deposited snow. The balloon was clearly visible on the snow surface. The grade of burial was different for each dummy. The dummy which travelled furthest was the most seriously buried and the one with the shortest path had the least serious grade of burial. This was due to the fact that the dummy with the Snowpulse/Mammut Lifebag was transported closer to the main flow and therefore closer to the front of deposition zone than the others. The dummies stopped within 88 m to 116 m of the deposition front (BCA Float 116 m, ABS Vario 96 m and Snowpulse/Mammut Lifebag 88 m). The extremities of the dummies were twisted and positioned in unnatural positions. In the case of real human beings, they would probably have suffered injuries. On the other hand, no dummy accurately represents a real human example in an avalanche and humans may, for example, try to actively escape from the main flow.

Publication 7: Chrustek P., Wężyk P., Kolecka N., Marek **Biskupiĉ** M., Bühler Y., Christen M., 2012 Using high resolution LiDAR data for snow avalanche hazard mapping in Kozak, J., Ostapowicz, K., Anna (Eds.) Integrating Nature and Society towards Sustainability, Springer, 290 p.. (book chapter)

DEM with various resolutions was used to simulate: maximum velocity, flow height and pressure of simulated avalanche at Goryczkowy test site. The quantitative differences between output parameters calculated for different DEMs with different resolution do not seem to be significant but more discrepancies were noticed when analyzing their spatial variations (Fig. 5). Analyzed examples showed that ALS models allow to predict avalanche flow process more precisely (even after reducing the model resolution) than Topo models, including also such terrain as the surrounding of the Goryczkowy test site where topographic surface is not very complex. The influence of various DEM types and different resolutions on the maximum distance was also investigated. When comparing 1 m ALS and 1 m Topo data differences between calculated distances were about 25 m (distance for Topo dataset was greater, Fig. 5a, b). The same

comparison for 25 m resolution datasets showed that the difference was much bigger – about 40 m (distance for ALS dataset was greater, Fig. 5b, c). The biggest difference was obtained after changing resolution in ALS dataset. Difference between maximum flow distance for 1 and 25 m was about 50 m (distance for ALS 25 m was greater, Fig. 5a, c). The same comparison for Topo dataset showed difference that was about 30 m (distance for Topo 1 m was greater, Fig. 5b, d). Based on the results presented in Table 2 it can be stated that parameter differences between calculated PRAs are noticeable during dynamics calculation as well. This test showed that differences were bigger when spatial resolution was changed for ALS data. These discrepancies for Topo data were less noticeable. However, direct relation between estimated volume and maximum distance calculated by the model was not investigated (when comparing results from different resolutions). Interesting results were obtained when analyzing ALS data. Despite of much lower estimated volume (by 5.4%, 2,358.3 t less), calculated distance for 25 m dataset was 40 m longer than for 1 m dataset. It means that smoothing the topography while decreasing the spatial resolution, strongly influences calculation results. This influence is more significant when analyzing LiDAR data.

Publication 8: Liščák, P., Biskupič, M., Richnavský, J., Bednařík, P., Geological hazards, in Dalezios, N., R., (Eds.) Environmental Hazards Methodologies for Risk Assessment and Management, IWA Publishing, London. (book chapter)

Publication is book chapter dealing with avalanches and it's modelling as larger group of geological hazards. It summarizes the progress in modelling which has been done for last years in Slovakian mountains. Most of the work has been done as a part of this PhD thesis. Nowadays, the physically based numerical tools are the most widespread group of tools and they represent the most complex tool for quantitative analysis of a studied system. They are much less encumbered with the simplifying assumptions used in analytical tools. Therefore, they are more appropriate for solving more complicated problems in more difficult conditions (Unucka, 2001). The main aim of avalanche dynamics studies is the answer to the question: in what way, how fast and how far does an avalanche move and what destructive potential is this movement connected with. The potential of dynamic numerical models is significant especially for the identification of potential avalanche runout distances. This identification is crucial for the evaluation of an avalanche danger. Furthermore, the avalanche impact pressure can be estimated by avalanche dynamics modelling (Figure 10.19) that brings a completely new dimension to the evaluation of an avalanche danger. The biggest danger of modelling is the possibility to easily generate the outputs that have little in common with reality. However, every model works on a certain level of reliability and it is necessary to verify and test the acquired prognosis. In the case of avalanche dynamics modelling, a calibration refers especially to the adjustment of terrain friction coefficients. According to these coefficients, an avalanche flow accelerates or decelerates. However, the avalanches in individual mountain areas have a very specific progress, due to a different combination of local, meteorological, geomorphological and climatic conditions.

8 Conclusions

The retrospective study on avalanche incidents revealed that effectiveness of avalanche airbags is lower than previously reported, but still the airbags are the only active equipment capable to reduce the likelihood of critical burial and save human lives. It was assumed that the non-inflation rate decreased compared to the early stages of airbags, but surprisingly the rate remains high (20%). This shows that the airbag should be treated carefully and it has to be periodically tested and checked not just for technical failures but also for the practising of the deployment. It is advisable that the airbags use is not overestimated and should not give the false feeling of security as the airbags do not work in every scenario (large avalanches, terrain trap, cliffs). Airbags do not guarantee the survival under all circumstances.

Model for detecting the avalanche release zones have been tested and implemented into GIS environment. The raster algebra model is suitable for implementation in GIS. This enable to automatically process large areas and whole workflow can be automated. Still the results require verification and field inspection. The remaining issue is to properly detect the lower part of release area called stauchwall. The results from statistical modelling point out that the model cannot be applied to all avalanche paths in the area. In particular, the model fails to simulate the behaviour of shorter avalanches which did not reach the retardation beta point or the cases when the avalanche hit the encounter slope. Insufficiency was also demonstrated in the case of slopes with considerable turgidity of the avalanche. The model is only suitable for straight slopes with a slightly inclined run-out zone.

The automated detection and mapping of snow avalanche debris using was investigated with an algorithm implemented in eCognition. The described method and is flexible and easily adaptable to data from different very-high to high resolution optical sensors but needs further improvement before applicable in any operational setting. A large drawback of optical methods is their dependency of clear sky conditions and good illumination. In order to be able detect avalanches also during bad weather conditions the radar satellite data should be tested.

Numerical models (like RAMMS), coupled with field observations and historical records are especially helpful in understanding avalanche flow in complex terrain (Christen et al., 2008). Back calculations or outlining future scenarios of avalanche hazard is particularly important and applicable in the avalanche protection and prevention. It is obvious that modeled result differs from the event mapped in 1970. We have to bear in mind that it still a model and has limitations. The process of snow entertaining in the avalanche flow has not yet been precisely mathematically described. It greatly affects the amount of snow in the avalanche and thus its dynamics, speed, impact pressure, run-outs and volumes. Another influencing factor is the quality of input parameters particularly the DEM. The accuracy and spatial resolution influences the precision of the release area estimation, calculated topography parameters, calculated release volume, location of avalanche track and another parameters calculated by dynamic models.

9 References

- Ancey, C., Extreme, Avalanches. In Davos Meeting 2008 [online]. Davos : [s.n.], 2008 [cit. 2011-08-11]. [www: http://www.coes.ethz.ch/projects/hazi/EXTREMES/talks/anceyDavosJan08.pdf](http://www.coes.ethz.ch/projects/hazi/EXTREMES/talks/anceyDavosJan08.pdf)
- Bakkehoi, S., Domaas, U. and Lied, K., 1983. Calculation of snow avalanche runout distance. *Annals of Glaciology*, 4: 24-29.
- Barbolini, M. and Keylock, C.J., 2002. A new method for avalanche hazard mapping using a combination of statistical and deterministic models. *Natural Hazards and Earth Systems Sciences*, 2: 239-245.
- Bartelt, P., Salm, B. and Gruber, U., 1999. Calculating dense-snow avalanche runout using a Voellmy-fluid model with active/passive longitudinal straining. *Journal of Glaciology*, 45(150): 242-254.
- Bartelt, P.,; Busler, O., Frictional relaxation in avalanches. *Annals of Glaciology*. 2010, volume 51, issue 54, s. 98-104.
- Bartelt, P., Salm, B., Gruber, U., 1999 Calculating dense-snow avalanche runout using a Voellmy-fluid model with active/passive longitudinal straining. In *Journal of Glaciology* : vol. 45, no.150 . International Glaciological Society
- Bárka, I. - Rybár, R. 2003. Bitter, L.:2003. *Geodézia*. Alfa Bratislava, 3. vyd., 2008, 440.
- Barka, I., Rybár, R.,. Identification of snow avalanche trigger areas using GIS. In *Ekológia* : vol. 22, Supplement 2/2003. Bratislava : SAV, 2003. p. 182-194.
- Biskupič, M., Modelovanie dosahu lavín s použitím GIS, 2008. 87 s. Diplomová práca. UK Praha, Přírodovědecká fakulta.
- Borstad, Ch., McClung, D., M., Sensitivity analyses in snow avalanche dynamics modeling and implications when modeling extreme events. *Canadian Geotechnical Journal*. September 2009, vol. 46, no. 9, s. 1024-1033.
- Boltížiar, M. 2003. Mapovanie a analýza vzťahu krajínnej štruktúry a reliéfu vysokohorskej krajiny Tatier s využitím výsledkov DPZ a GIS. In: *Kartografické listy*. Kartografická spoločnosť SR a Geografický ústav SAV, Bratislava. Vol. 11, 5-15.
- Bovis, M.J. and Mears, A.I., 1976. Statistical prediction of snow avalanche runout from terrain variables in Colorado. *Arctic and Alpine Research*, 8(1): 115-120.
- Bovis, M., Mears, A.,. Statistical prediction of snow avalanche run-out from terrain variables in Colorado. In *Arctic and Alpine Research* : vol. 8, no. 1
- Brabec, B., Meister, R., Stöckli, U., Stoffel, A. and Stucki, T., 2001. RAIFoS: Regional Avalanche Information and Forecasting System. *Cold Regions Science and Technology*, 33(2-3): 303-311.
- Bühler, Y., Hüni, A., Christen, M., Meister, R., Kellenberger, T. 2009. Automated detection and mapping of avalanche deposits using airborne optical remote sensing data. *Cold Reg. Sci. Technol.*, 57, 99–106.
- Christen, M., Bartelt, P. and Gruber, U., 2002. AVAL-1D: An avalanche dynamics program for the practice, International Congress Interpraevent 2002 in the Pacific Rim, Matsumoto, Japan, 715-725.
- Christen, M., et al., 2010, RAMMS: Numerical simulation of dense snow avalanches in three-dimensional terrain. In *Cold Regions Science and Technology* : vol. 63/ 1 –
- Christen, M., et al., 2010 Back calculation of the In den Arelen avalanche with RAMMS : interpretation of model results. In . *Annals of Glaciology* : vol. 52, issue 54 [online].
- Christen, M., et al., 2008 Calculation of dense snow avalanches in three-dimensional terrain with the numerical simulation programm RAMMS. In *International Snow Science Workshop 2008, Proceedings* : September 21-27 [online]. Whistler, BC, CAN,
- Christen, M., et al., 2007. Modelling Avalanches. In *GEOconnexion International* .

- Christen, M., et al., 2005, Numerical calculation of snow avalanche runout distances. In . Computing in Civil Engineering : Proceedings of the 2005 International Conference, Cancun, Mexico,
- Chrustek, P., et al.. 2010, Comparison of different methods for obtaining snow avalanche data. Poster. In: Forum Carpathicum 2010. Krakow,.
- Chrustek, P., et al.. 2010, Using high resolution LiDAR data for snow avalanche hazard mapping. Poster. In: Forum Carpathicum 2010. Krakow,.
- Chrustek, P., et al.. 2009, Using high resolution LiDAR data to estimate potential avalanche release areas on the example of Polish mountains regions. In International Snow Science Workshop : Proceedings. Davos : Swiss Federal Institute for Forest, Snow and Landscape Research WSL
- Delparte, D., Jmieseon, B., Waters, N., 2004. Statistical runout modeling of snow avalanches using GIS in Glacier National Park, Canada. In Cold regions science and technology : vol. 54, issue 3.
- Engler, M. 2001. Die Weise Gefahr : Schnee und Lawinen – Erfahrungen Mechanismen, Risikomanagement,. Salzberg, 2001, 301.
- Buhler, Y., et al. Sensitivity of snow avalanche simulations to digital elevation model quality and resolution. Annals of Glaciology. 2011, 72, vol. 52, no. 58, p. 72-80.
- Fischer, J. T., et al. Dynamic Avalanche Modeling in Natural Terrain. In International Snow Science Workshop : Proceedings. Davos : Swiss Federal Institute for Forest, Snow and Landscape Research WSL, 2009. p. 448 - 453.
- Furdada, G. and Vilaplana, J.M., 1998. Statistical predication of maximum avalanche run-out distances from topographic data in the western Catalan Pyrenees(northeast Spain). Annals of Glaciology, 26: 285-288.
- Fredston, J., Fesler, D., Snow Sense : A Guide to Evaluating Snow Avalanche Hazard. 2nd Revised edition. Alaska Mountain Safety Centre, 2000. 120 p.
- Gauer, P., et al. α - β model : Can we learn more from the statistical avalanche model with respect to the dynamical behavior of avalanches. In International Snow Science Workshop : Proceedings. Davos : Swiss Federal Institute for Forest, Snow and Landscape Research WSL, 2009. p. 405 - 408.
- Gruber, U., 2001. Using GIS for avalanche hazard mapping in Switzerland, Proceedings of the 2001 ESRI International User Conference, San Diego.
- Gruber, U. and Bartelt, P., 2007. Snow avalanche hazard modelling of large areas using shallow water numerical methods and GIS. Environmental Modelling & Software, 22: 1472- 1481.
- Gruber, U. and Margreth, S., 2001. Winter 1999: a valuable test of the avalanche-hazard mapping procedure in Switzerland. Annals of Glaciology, 32: 328-332.
- Gruber, U. and Sardemann, S., 2002. High frequency avalanches: Release areacharacteristics and runout distances. In: J.R. Stevens (Editor), International Snow Science Workshop (ISSW), Penticton, BC, Canada, 84-89.
- Haberli, W., et al., 2004, GIS applications for snow and ice in high-mountain areas : Examples from Swiss Alps. In BISHOP, Michael P.; SHROEDER JR, John F. Geographic Information Science and Mountain eomorphology. Chichester, UK : Springer, p. 381-402.
- Holý, D. 1980. Meteorologické a topografické podmienky a faktory vzniku lavín v Západných Karpatoch , (kandidátska dizertačná práca) , Jasná, 1980.
- Holý, D., 1990 Meteorologické podmienky vzniku lavín v Západných Karpatoch. Geografický časopis. 42, 1, p. 38-56.
- Hreško, J., 1998: Lavínová ohrozenosť vysokohorskej krajiny v oblasti Tatier, Acta Facultatis Stud. Hum. et Naturae Univ. Prešovensis, Folia geographica 2, roč.XXIX, s. 326-328.
- Hreško, J. - Bugár, G., 1999: Lavínová ohrozenosť JV časti Belianskych Tatier. In: Krajinnoeologické plánovanie na prahu 3. tisícročia. Hrnčiarová, T., Izakovičová, Z. (Eds.). Bratislava: Ústav krajinej ekológie SAV, 1999. 268-269.

- Holko, L., Kostka, Z., Parajka, J. 2001. Snehová pokrývka. In: Životné prostredie, číslo 3. Bratislava, 2001. 138-141.
- Hutter, K., Wang, Y., Pudasaini, S., 2005, The Savage–Hutter avalanche model : how far can it be pushed?. In *Philosophical Transactions of The Royal Society. A* 2005 363. 28. Keylock, C.J., McClung, D. and Magnusson, M.M., 1999. Avalanche risk mapping by simulation. *Journal of Glaciology*, 45(150): 303-314.
- Jamieseno et al., 2008 , Application and Limitations of Dynamic Models For Snow Avalanche Hazard Mapping. In *International Snow Science Workshop : Proceedings . Whistler : Montana State University*,
- Kääb, A., Huggel, C., Fischer, L., Guex, S., Paul, F., Roer, I., Salzmann, N., Schläefli, S., Schmutz, K., Schneider, D., Strozzi, T., Weidmann, Y. 2005. Remote sensing of glacier- and permafrost-related hazards in high mountains: an overview. *Nat. Hazards Earth Syst. Sci.*, 5, p.527–554.
- Klimánek, M., et al. 2011 Using GPS for snow depth and volume measurement of centennial avalanche field in High Tatras. In *Cold Regions Science and Technology* , 65, 3, . p. 392 – 400.
- Kohút, F. 2005. Prírodné procesy ohrozujúce vysokohorskú krajinu – Jalovecká dolina Rigózna práca. Nitra : Univerzita Konštantína Filozofa, 2005. 110.
- Kňazovický, L. 1967. Lavíny. Bratislava : SAV, 1967. 149.
- Kňazovický, L. 1970. Západné Tatry. Bratislava : SAV, 1970.209.
- Lato, M., Frauenfelder, R., Bühler, Y. 2012. Automated detection of snow avalanche deposits: segmentation and classification of optical remote sensing imagery. *Nat. Haz. And Earth. Syst. Sci.*, 12, 2893–2906.
- Lato, M., Frauenfelder, R., Bühler, Y. 2012. The eye in the sky’’: Detecting and monitoring geohazards from space. A case study on avalanche detection.. Available from:
https://www.researchgate.net/publication/303844588_The_eye_in_the_sky_Detecting_and_monitoring_geohazards_from_space_A_case_study_on_avalanche_detection [accessed Sep 22, 2017].
- Lied, K. and Bakkehoi, S., 1980. Empirical calculation of snow-avalanche run-out distance based on topographic parameters. *Journal of Glaciology*, 26(94): 165-177.
- Lied, K., Weiler, S., Bakkehoi, S. and Hopf, J., 1995. Calculation methods for avalanche run-out distance for the Austrian Alps. The contribution of scientific research to safety with snow, ice and avalanche., ANENA, Grenoble, France, 63-68.
- Longley, P.A., M.F. Goodchild, P.A. Maguire and D.W. Rhind. 2001. *Geographic Information Systems and Science*. New York: John Wiley and Sons, Inc: 485
- Maggioni, M. and Gruber, U., 2003. The influence of topographic parameters on avalanche release dimension and frequency. *Cold Regions Science and Technology*, 37: 407-419.
- Mantovani, R., Soeters, R., van Western, C. J. 1996. Remote sensing techniques for landslide studies and hazard zonation in Europe. *Geomorphology*, 15, 213–225.
- Maggioni, M., Gruber, U. and Stoffel, A., 2001. Definition and characterisation of potential avalanche release areas, *Proceedings of the 2001 ESRI International User Conference*, San Diego.
- Maggiioni, M., Gruber, U., 2003 The influence of topographic parameters on avalanche release dimension and frequency. In *Cold Regions Science and Technology* : vol. 37, issue 3[
- Mears, A.I., 1988. Comparisons of Colorado, Eastern Sierra, coastal Alaska, and Western Norway runout data, *International Snow Science Workshop (ISSW)*, Wistler, BC, 232-238.
- Mears, A.I., 1989. Regional comparisons of avalanche-profile and runout data. *Arctic and Alpine Research*, 21(3): 283-287.
- Mears, A.I., 1989, *Avalanche Runout Distances and Dynamics : Current Methods and Limitations*. In *The Avalanche Review*: vol. 7, No. 4. Pagosa Springs: Colorado: American Avalanche Association.,
- Mears, A.I., 1976, *Avalanche Dynamics*. In *Avalanche Zoning & Dynamics* [online]. Colorado : WestWide Avalanche Network.

- Mergili, M., et al., 2008, An Open Source model for the simulation of granular flows : First results with GRASS GIS and needs for further investigations. In Academic Proceedings of the 2008 Free and Open Source Software for Geospatial (FOSS4G) Conference : Sept. 29 – Oct. 3 Cape Town, South Africa.
- McClung, D., 2001. Characteristics of terrain, snow supply and forest cover for avalanche initiation caused by logging. *Annals of Glaciology*, 32: 223-229.
- McClung, D. and Lied, K., 1987. Statistical and geometric definition of snow avalanche runout. *Cold Regions Science and Technology*, 13: 107-119.
- McClung, D., Mears, A.I., 1991. Extreme value prediction of snow avalanche runout. *Cold Regions Science and Technology*, 19(163-175). 166
- McClung, D., Schaerer, P., 2003. *The Avalanche Handbook*. The Mountaineers, Seattle, WA, 271.
- McClung, D., Schweizer, J., 1999. Skier-triggering, snow temperatures and the stability index for dry-slab avalanche formation. *Journal of Glaciology*, 45(150):190-200.
- McKittrick, L.R. and Brown, R.L. 1993: A statistical model for maximum avalanche run-out distances in southwest Montana. *Annals of Glaciology* 18, 295-99.
- Midriak, R. 1999. Geomorfologické procesy a krajinné formy na rozličných povrchoch v kryoniválnom morfo genetickom systéme západných karpát. In: *Acta Facultatis Ecologiae (Zvolen)*, VI. Zvolen, 1999. 9–21
- Milan, L. – Šmárka, Š. 1988. *Nebezpečenstvo Lavín*. Bratislava : Šport, 1988. 151.
- Milan, L. 2001. Lavíny na želanie. In: *Tatry, číslo 2.Slza, Tatranská Lomnica*, 2001, 14-15.
- Perla, R., et al., 1980, A two-parameter model of snow-avalanche motion. In *Journal of Glaciology*: vol.26, issue 94. International Glaciological Society, p 197 - 207.
- Peťo, J., *Praktické metódy na približné určenie dosahu lavín*. Praha : Výbor Horskej služby ÚV ČSTV, 1989. 17 p.
- Pudasaini, S.,P., Hutter, K., 2006, *Avalanche Dynamics : Dynamics of Rapid Flows of Dense Granular Avalanches*. 1 edition. Springer, 626 p.
- Richnavský, J., 2012, *Stanovenie lavínových dosahov s využitím dynamického numerického modelovania a GIT*, Dizertačná práca, Vysoká škola banská – Technická univerzita Ostrava.
- Sailer, R., et al., 2008, Snow avalanche mass-balance calculation and simulation-model verification. In *Annals of Glaciology* : vol. 48., International Glaciological Society,
- Sailer, R., et al., Case studies with SAMOS - comparison with observed avalanches. In *AVL International User Meeting* : 14-15. Oct. 2003 [online]. Graz : AVL - Advanced Simulation Technologies,
- Salm, B., Burkard, A., and Gubler, H. (1990). "Berechnung von Fließlawinen: eine Anleitung für Praktiker mit Beispielen." *Mitteilung 47*, Eidg. Institut für Schnee- und Lawinenforschung SLF Davos. STREDISKO LAVÍNOVEJ PREVENČIE. *Sneh a Lavíny : Ročenka 2008/2009*. Jasná : Horská záchranná služba, 2009. 77 s. Dostupné z WWW: <http://www.laviny.sk/data/Rocenska_08_09.pdf>.
- Salm, B. (1966) *Contribution to avalanche dynamics*.
- Schweizer, J. and Jamieson, B., 2000. Field observations of skier-triggered avalanches, *International Snow Science Workshop (ISSW)*. American Avalanche Association, Big Sky, Montana, USA, 192-199.
- Schweizer, J. and Jamieson, B., 2001. Snow cover properties for skier triggering of avalanches. *Cold Regions Science and Technology*, 33: 207-221.
- Schweizer, J., Jamieson, B. and Schneebeli, M., 2003. Snow avalanche formation. *Reviews of Geophysics*, 41(4): 2.1 - 2.25. 169
- Schweizer, J., Kronholm, K., Jamieson, B. and Birkeland, K., 2006b. Spatial variability - so what?, *International Snow Science Workshop (ISSW)*, Telluride, Colorado, 365-376.
- Smith, M.J. and McClung, D., 1997. Avalanche frequency and terrain characteristics at Roger's Pass, British Columbia, Canada. *Journal of Glaciology*, 43(143): 165-171.

Stoffel, A., Brabec, B. and Stoeckli, U., 2001. GIS Applications at the Swiss Federal Institute for Snow and Avalanche Research, Proceedings of the 2001 ESRI International User Conference, San Diego.

Stoffel, A., Meister, R. and Schweizer, J., 1998. Spatial characteristics of avalanche activity in an alpine valley--a GIS approach. *Annals of Glaciology*, 26: 329-336/105.

Townsend, P.A., Walsh, S.J. 1998. Modeling floodplaininundation using an integrated GIS with radar and optical remote sensing. *Geomorphology*, 21(3-4), pp. 295-312.

Tracy, L., 2001. Using GIS in Avalanche Hazard Management, Proceedings of the 2001 ESRI International User Conference, San Diego.

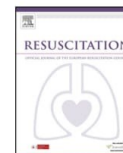
Voellmy, A., 1955 Uber die Zerstiirungskraft von Lawinen. *Schweizerische Bauzeitung* 73, 159-162, 212-217, 246-249, 280-285

Vojtek, M. 2002. Meteorologické podmienky vzniku lavín vo Vysokých Tatrách a ich modelovanie : Diplomová práca. Bratislava : Univerzita Komenského.

10 Publications

Publication 1

Publication 1: Haegeli, P., Falk M., Procter, E., Zweifel, B., Jarry, F., Logan, S., Kronholm K., **Biskupič, M.**, Brugger, H., 2014 The effectiveness of avalanche airbags. Resuscitation, Volume 85, Issue 9, 1197 – 1203. (IF₂₀₁₆: 5.230)



Clinical Paper

The effectiveness of avalanche airbags[☆]

Pascal Haegeli^{a,b,*}, Markus Falk^c, Emily Procter^d, Benjamin Zweifel^e, Frédéric Jarry^f, Spencer Logan^g, Kalle Kronholm^h, Marek Biskupič^{i,j}, Hermann Brugger^d

^a Avisaualanche Consulting, 2-250 E 15th Avenue, Vancouver, BC, V5T 2P9, Canada

^b School for Resource and Environmental Management, Simon Fraser University, 8888 University Drive, Burnaby, BC, V5A 1S6, Canada

^c Inova Q Inc., Tinkhauserstrasse 5b, 39031 Bruneck/Brunico, Italy

^d EURAC Institute of Mountain Emergency Medicine, Drususallee 1, 39100 Bozen/Bolzano, Italy

^e WSL Institute for Snow and Avalanche Research SLF, Flüelistrasse 11, 7260 Davos, Switzerland

^f National Association for Snow and Avalanche Studies (ANENA), 15 rue Ernest Calvat, 38000 Grenoble, France

^g Colorado Avalanche Information Center, 325 Broadway WS1, Boulder, CO 80305, USA

^h Norwegian Geotechnical Institute (NGI), Sognsveien 72, N-0855 Oslo, Norway

ⁱ Avalanche Prevention Center, Jasná, 032 51 Demänovská Dolina, Slovakia

^j Institute for Environmental Studies, Charles University, Ovocný trh 3-5, 116 36 Praha 1, Czech Republic

ARTICLE INFO

Article history:

Received 13 March 2014

Received in revised form 15 May 2014

Accepted 21 May 2014

Keywords:

Avalanche accidents

Mortality

Safety equipment

Burial prevention

ABSTRACT

Aim: Asphyxia is the primary cause of death among avalanche victims. Avalanche airbags can lower mortality by directly reducing grade of burial, the single most important factor for survival. This study aims to provide an updated perspective on the effectiveness of this safety device.

Methods: A retrospective analysis of avalanche accidents involving at least one airbag user between 1994 and 2012 in Austria, Canada, France, Norway, Slovakia, Switzerland and the United States. A multivariate analysis was used to calculate adjusted absolute risk reduction and estimate the effectiveness of airbags on grade of burial and mortality. A univariate analysis was used to examine causes of non-deployment.

Results: Binomial linear regression models showed main effects for airbag use, avalanche size and injuries on critical burial, and for grade of burial, injuries and avalanche size on mortality. The adjusted risk of critical burial is 47% with non-inflated airbags and 20% with inflated airbags. The adjusted mortality is 44% for critically buried victims and 3% for non-critically buried victims. The adjusted absolute mortality reduction for inflated airbags is –11 percentage points (22% to 11%; 95% confidence interval: –4 to –18 percentage points) and adjusted risk ratio is 0.51 (95% confidence interval: 0.29 to 0.72). Overall non-inflation rate is 20%, 60% of which is attributed to deployment failure by the user.

Conclusion: Although the impact on survival is smaller than previously reported, these results confirm the effectiveness of airbags. Non-deployment remains the most considerable limitation to effectiveness. Development of standardized data collection protocols is encouraged to facilitate further research.

© 2014 Elsevier Ireland Ltd. All rights reserved.

1. Introduction

Between 2004 and 2010, an average of 160 recreationists died per winter in avalanches in Europe and North America.¹ The majority of victims are young, healthy individuals recreating in avalanche terrain on skis, snowboards or snowmobiles.² If caught in an avalanche, grade of burial (defined as either

critically buried, i.e., head under the snow and breathing impaired, or *non-critically buried*, i.e., unobstructed airways) is the strongest single factor for survival³ and asphyxia is the primary cause of death among critically buried avalanche victims.^{4–6} An analysis of Swiss avalanche accidents showed that while the mortality of critically buried individuals was 52% (385/735), the mortality of non-critically buried individuals was only 4% (48/1151).⁷ Furthermore, survival analyses have shown that survival of critically buried victims is strongly correlated to duration of burial.^{6–8} While survival rates are high in the first few minutes of critical burial, they drop precipitously after 10–18 min, leaving only a very short time window for successful extrication. Consequently, the prevention of critical burial is fundamental for increasing avalanche survival.

[☆] A Spanish translated version of the abstract of this article appears as Appendix in the final online version at <http://dx.doi.org/10.1016/j.resuscitation.2014.05.025>.

* Corresponding author at: Avisaualanche Consulting, 2-250 E 15th Avenue, Vancouver BC, V5T 2P9, Canada.

E-mail address: pascal@avisualanche.ca (P. Haegeli).

<http://dx.doi.org/10.1016/j.resuscitation.2014.05.025>

0300-9572/© 2014 Elsevier Ireland Ltd. All rights reserved.

Avalanche airbags are a relatively new avalanche safety device that consists of a backpack or vest with one or two inflatable balloons. When caught in an avalanche, users manually deploy the device by pulling an activation handle, which instantly inflates the stowed balloon(s) to a total volume of approximately 150 l. As long as the user is flowing freely within the avalanche, airbags function through a physical process called *inverse segregation* where larger particles are sorted toward the surface, thus reducing the user's chance of becoming critically buried.⁹ In comparison to the currently recommended standard avalanche safety equipment (avalanche transceiver, shovel and avalanche probe)¹⁰ that can reduce the duration of burial, avalanche airbags are the only avalanche safety device that can directly prevent critical burial.¹¹

Robust statistical evaluations of airbag use in avalanche involvements are scarce; though the effectiveness of airbags has been supported,¹¹ such statistical analyses have important limitations and results should be interpreted accordingly. First, analyses focus exclusively on avalanche involvements with airbags from Switzerland and may not be applicable to other geographic regions. Second, sample sizes are too small to precisely isolate the effect of avalanche airbags. Third, the criteria used to include accident records are not adequately reported (i.e., was there potential for mortality). Fourth, comparing survival rates for avalanche airbag users with survival rates of non-users extracted from other existing avalanche accident databases is questionable because of probable differences in reporting biases and other unknown confounding factors. The interest of the community in the new device and encouragements from manufacturers to submit incident reports likely resulted in a higher reporting rate of accidents without injuries or fatalities among airbag users than non-users, which inadvertently leads to an overestimation of the effectiveness of airbags.

The aim of this study is to provide an updated and more thorough perspective on the effectiveness of avalanche airbags by evaluating (i) their influence on the grade of burial and mortality in individuals involved in avalanches with the potential of mortality using a multivariate approach with an unbiased control group and (ii) the frequency and reasons for deployment failures.

2. Materials and methods

2.1. Data sources

Existing records of well-documented avalanche accidents involving at least one avalanche airbag user were collected from data sources in Canada (Canadian Avalanche Association), France (National Association for Snow and Avalanche Studies), Slovakia (Avalanche Prevention Center), Norway (Norwegian Geotechnical Institute, Norwegian Red Cross), Switzerland (WSL Institute for Snow and Avalanche Research SLF) and the United States (Colorado Avalanche Information Center). Available accident reports were examined in detail and newly coded to produce a consistent dataset. Collected data included background information on accidents and victims (country, date, activity, avalanche professional) and parameters known to affect burial depth (e.g., presence of terrain traps), mortality (e.g., grade of burial, traumatic injuries, use of avalanche transceiver) or suspected impact on inverse segregation (e.g., relative location when avalanche was triggered—victims located in the runout zone when the avalanche is triggered will likely not be effectively sorted toward the surface of the avalanche) (Table 1).

Since avalanche airbags are designed to reduce the likelihood of critical burial, the analysis focused exclusively on avalanche involvements with potential for critical burial. Accident records were therefore only included if the destructive size of the avalanche

Table 1
Parameters included in dataset.

Parameter	Levels
Accident information	
Country of accident location	See Table 3
Date	1994–2012
Activity	Backcountry skiing Mechanized skiing Out-of-bounds/off-piste skiing (incl. snowboarding) Ski patrolling Snowmobile riding
Avalanche characteristics	
Avalanche size	Numeric sizes ranging from 2.0 to 4.0 (incl. half sizes; Table 2) according to Canadian avalanche size classification ¹²
Characteristics of runout zone	Smooth runout Terrain trap
Victim information	
Avalanche professional	Yes (e.g., mountain guide, ski patroller) No
Use of avalanche transceiver	Yes No
Use of avalanche airbag	No Yes—non-inflated (also includes partially inflated) Yes—inflated
Reason for non-inflation	Destroyed in accident Technical device failure Deployment failure by user Maintenance error Unknown reason
Relative location when triggered	Starting zone Track or runout
Grade of burial	Non-critical (no impairment of airways) Critical (impairment of airways)
Traumatic injuries	None or minor (not requiring hospitalization) Major (requiring hospitalization)
Fatality	Yes No

was ≥ 2.0 according to the Canadian avalanche size classification (Table 2),¹² since sizes < 2.0 are too small to bury a person by definition. Furthermore, only seriously involved users and non-users of airbags were included, which means severely involved in the flow of the avalanche or hit by the avalanche from above and non-critically or critically buried as a result. Marginally involved individuals (e.g., only slightly moved at the edge of the avalanche, remained standing during entire involvement or managed to ride out of avalanche) were excluded as airbags are unable to affect the outcomes of these types of involvements (Supplemental Table 1).

Supplementary table can be found, in the online version, at <http://dx.doi.org/10.1016/j.resuscitation.2014.05.025>.

2.2. Data analysis

2.2.1. Effectiveness of avalanche airbag on grade of burial and mortality

The dataset for this analysis included only accidents with multiple involvements and different users of avalanche airbags (non-users, users with non-inflated airbags, users with inflated airbags) (Fig. 1). This allowed extraction of both the treatment and control groups from the same set of accidents, which eliminates the likely reporting bias and potential influence of additional unknown confounding factors. The effectiveness of avalanche airbags was examined from two perspectives: (i) effectiveness of only inflated airbags (users with inflated airbags versus non-users and users with non-inflated airbags) and (ii) effectiveness when non-inflations are taken into account (non-users versus users with non-inflated

Table 2
Canadian avalanche size classification.¹²

Size & data code ^a	Avalanche destructive potential	Typical mass	Typical path length
1	Relatively harmless to people	<10 t	10 m
2	Could bury, injure, or kill a person	10 ² t	100 m
3	Could bury and destroy a car, damage a truck, destroy a wood frame house, or break a few trees	10 ³ t	1000 m
4	Could destroy a railway car, large truck, several buildings, or a forest area up to 4 hectares (~10 acres)	10 ⁴ t	2000 m
5	Largest snow avalanche known; could destroy a village or a forest of 40 hectares (~100 acres)	10 ⁵ t	3000 m

^a Half-sizes may be used for avalanches that are between two size classes.

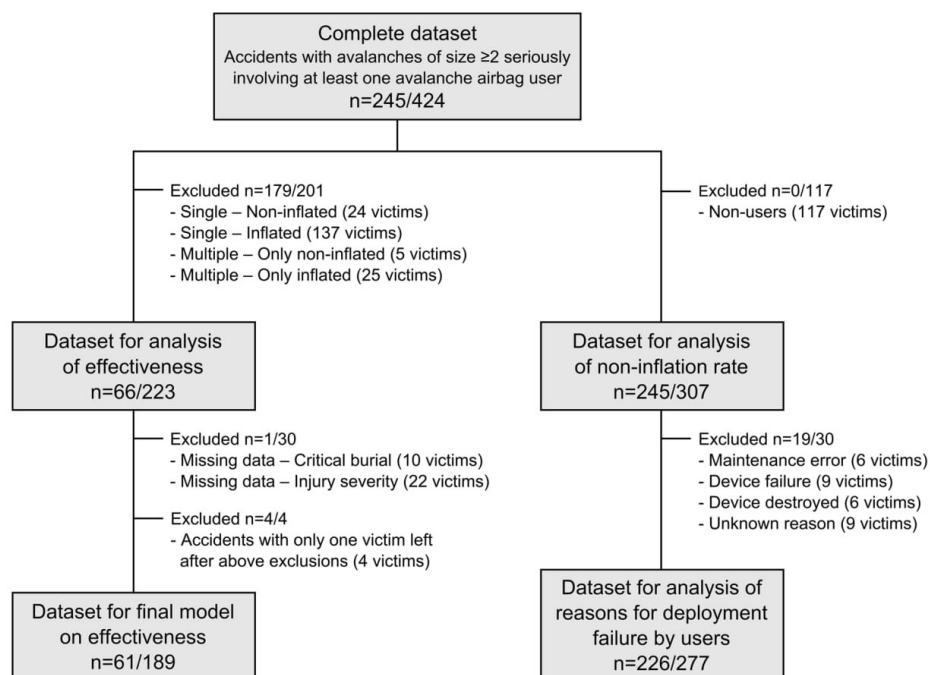


Fig. 1. Data included in the analysis on effectiveness and non-inflations (reported as number of accidents/number of victims).

airbags and users with inflated airbags). While the first perspective offers insights on the performance of the device in its intended use alone, the second assessment is more comprehensive as it examines the combined performance of the device and its user, who has to actively deploy the device.

For the univariate analyses we used Fisher's exact tests for count data and Wilcoxon rank-sum tests for ordinal or non-normal numeric parameters. Two-sided $P < 0.05$ was considered statistically significant and $0.05 \leq P < 0.10$ marginally significant. Effectiveness of avalanche airbags was expressed as absolute risk reductions for critical burial and mortality.

For the multivariate analyses we used stepwise binomial logistic regression models starting with all available factors influencing grade of burial and mortality. $P > 0.10$ was used as the exclusion criteria for factors to prevent overfitting of the models. To make the results more interpretable, the parameter estimates were converted to adjusted absolute risk reduction and adjusted risk ratios for critical burial and mortality using the method of Kleinman and Horton.¹³ A Monte Carlo simulation with 10,000 random samples from the analysis dataset was used to estimate the overall effect of avalanche airbags on mortality by combining their effect on grade

of burial with the mortality model and to calculate associated confidence intervals.

2.2.2. Non-inflation rates and underlying causes

The dataset for this analysis included all accidents with avalanche airbag users (inflated and non-inflated) (Fig. 1). Information on the causes of non-inflations was taken from accident reports. The influence of external factors on deployment failure during involvements was analyzed using a univariate approach.

3. Results

3.1. Overview of dataset

The complete dataset consists of 245 avalanche accidents with information on 424 seriously involved individuals (Table 3). Eighty-three percent (204/245) of accidents records were from Europe and 15% (38/245) were from North America. Accidents occurred between the winters of 1994 and 2012 and 75% (183/245) occurred between 2007 and 2012. Out-of-bounds/off-piste skiing (including snowboarding) and backcountry skiing were the most prominent

Table 3
Number of accidents and seriously involved victims by country (percentages in brackets).

Country	Number of accidents	Number of seriously involved victims				Fatalities
		Total	Non-users	Non-inflated	Inflated	
Austria	63 (26)	110 (26)	30 (27)	14 (13)	66 (60)	13 (12)
Canada	28 (11)	62 (15)	25 (40)	15 (24)	22 (35)	19 (31)
France	74 (30)	95 (22)	7 (7)	10 (11)	78 (82)	13 (14)
Italy	12 (5)	23 (5)	9 (39)	2 (9)	12 (52)	6 (26)
Norway	4 (2)	15 (4)	9 (60)	0 (0)	6 (40)	8 (53)
Switzerland	49 (20)	93 (22)	28 (30)	17 (18)	48 (52)	15 (16)
USA	10 (4)	16 (4)	6 (38)	2 (13)	8 (50)	4 (25)
Others ^a	5 (2)	10 (2)	3 (30)	1 (10)	6 (60)	2 (20)
Total	245 (100)	424 (100)	117 (28)	61 (14)	246 (58)	80 (19)

^a Denmark – Greenland (1 accident/1 victim), India (1/3), Russia (1/4), Slovakia (1/1) and Turkey (1/1).

activities, comprising 43% (102/245) and 35% (84/245) of accidents, respectively. All other activity types accounted for <10% each.

Overall mortality in the dataset was 19% (80/424) (Table 3). In total 58% (246/424) of victims had inflated airbags, 14% (61/424) had non-inflated airbags and 28% (117/424) did not have airbags. Ninety-nine percent (362/365) of victims carried avalanche transceivers.

3.2. Effectiveness of airbags on grade of burial and mortality

The reduced dataset for this analysis included 66 accidents with at least one user and one non-user leading to a total of 223 seriously involved individuals (Fig. 1; Supplemental Table 2). Compared to the excluded cases, the sample was older ($P=0.033$) and included a higher proportion of backcountry skiing accidents (47% versus 31%; $P=0.002$). While the avalanches included in this sample were larger (median size 2.5 versus 2.0; $P<0.001$), no difference was found in the character of the runout zone. Furthermore, the percentage of avalanche professionals (e.g., mountain guides, ski patrollers) was lower (9% versus 29%; $P<0.001$) and a higher percentage of victims was located in the track or runout zone when the avalanche was triggered (56% versus 24%; $P<0.001$). Whereas no difference was observed in the severity of traumatic injuries, the mortality was higher in the analysis sample (26% versus 11%; $P<0.001$). No difference was observed in the mortality of airbag users between the two samples ($P=0.318$), but the rate of non-inflation in the sample dataset was higher (30% versus 14%; $P=0.001$).

The univariate analysis showed an association between avalanche size and both grade of burial and mortality, where larger avalanches were associated with higher percentages of critical burials and fatalities (both $P<0.001$). Location of the victim when the avalanche was triggered and grade of burial exhibited a marginally significant association, where a higher percentage of victims were critically buried when caught in the track or runout zone compared to the starting zone (55% versus 40%; $P=0.059$). There was an association with severity of traumatic injuries, where major injuries were associated with higher percentages of critical burials (54% versus 34%; $P=0.033$) and fatalities (46% versus 15%; $P<0.001$). Critical burials were associated with a higher percentage of fatalities (61% versus 2%; $P<0.001$). All non-critically buried fatalities were due to trauma. Finally, the univariate analysis showed an association between use of airbags and both critical burial and mortality (both $P<0.001$) (Table 4). The absolute risk reduction for critical burial was –35 percentage points for users with inflated airbags and –29 percentage points when non-inflations were taken into account. The absolute mortality reduction was –23 percentage points for users with inflated airbags and –17 percentage points when non-inflations were taken into account (Table 4).

The multivariate analysis for critical burial and mortality included 61 accidents with 189 seriously involved individuals (Fig. 1, Supplemental Table 1). The non-inflation rate in this dataset

was 28% (27/95). The regression model for critical burial showed main effects for airbag use, avalanche size and injuries (Table 5) without any interaction effects. Since initial models with airbag use as a three-level variable (not used, non-inflated and inflated) showed that non-inflated airbags did not have an impact on grade of burial, this variable was reduced to two levels (not used/non-inflated and inflated) for the regression analysis. Whereas the use of airbags reduced the odds of critical burial (Table 5), only grade of burial, injuries and avalanche size were significant in the regression model for mortality, highlighting that avalanche airbags only affect mortality indirectly by reducing the risk of critical burial.

Based on the method of Kleinman and Horton¹³ the adjusted risk of critical burial was 47% for non-users and users with non-inflated airbags and 20% for users with inflated airbags. Similarly, the adjusted mortality was 44% for critically buried victims and 3% for non-critically buried victims. The overall effect of avalanche airbags on mortality was calculated by combining the results of the two models (Fig. 2). The overall adjusted mortality was 11% (95% confidence interval: 6 to 16%) for victims with inflated airbags and 22% (95% confidence interval: 15 to 29%) for victims with no or non-inflated airbags. The resulting adjusted absolute mortality reduction with inflated airbags was –11 percentage points (95% confidence interval: –4 to –18 percentage points), i.e., mortality was cut in half with inflated airbags (adjusted risk ratio: 0.51; 95% confidence interval: 0.29 to 0.72). Using the same two-step calculation but taking non-inflated airbags into account (not shown in Fig. 2), the adjusted absolute mortality reduction is –8 percentage points (from 22 to 14%; 95% confidence interval: –2 to –14 percentage points) and the adjusted risk ratio is 0.65 (95% confidence interval: 0.44 to 0.86).

3.3. Non-inflation rates and underlying causes

The overall non-inflation rate in the sample of airbag users was 20% (61/307). Information on suspected causes of non-inflations was available for 52 cases: 60% (31/52) were attributed to deployment failure by users, 12% (6/52) to maintenance errors (e.g., canister not attached properly), 17% (9/52) to device failures (i.e., performance issues that resulted in design and/or production revisions) and 12% (6/52) to destruction of the airbag during involvements. Relative to the total number of users, the rate of airbags destroyed in involvements was 2% (6/307) and the rate of device failures was 3% (9/307).

Of the users with inflated or non-inflated airbags due to deployment failure by the user, the non-deployment rate was 11% (30/277). Based on univariate comparisons the absolute risk of non-deployment for avalanche professionals was 5% (3/67) compared to 14% (28/196) for non-avalanche professionals ($P=0.030$), resulting in an absolute risk difference of +10 percentage points. No association was observed between deployment and avalanche

Table 4
Univariate absolute risk reduction in critical burials and absolute mortality reduction with (a) inflated airbags and (b) non-inflated or inflated airbags (pp: percentage points).

a) Airbag use	Critical burial		Risk of critical burial	Fatality		Mortality
	No	Yes		No	Yes	
No	49	62	} 54%	77	40	} 34%
Yes – non-inflated	15	13		22	10	
Yes – inflated	60	14		19%	66	
Absolute risk reduction			-35pp	Absolute mortality reduction		-23pp

b) Airbag use	Critical burial		Risk of critical burial	Fatality		Mortality
	No	Yes		No	Yes	
No	49	62	} 56%	77	40	} 34%
Yes – non-inflated	15	13		22	10	
Yes – inflated	60	14		27%	66	
Absolute risk reduction			-29pp	Absolute mortality reduction		-17pp

Table 5
Regression models for critical burial and mortality.

Parameter	Level	Estimate	P-value	OR (95% conf. interval)
(a) Model for critical burial with inflated airbag				
Intercept		-3.753	<0.001	0.023 (0.005–0.109)
Airbag use	No or Yes–non-inflated	0.000		
	Yes–inflated	-1.504	<0.001	0.222 (0.098–0.472)
Traumatic injuries	None or minor	0.000		
	Major	0.799	0.072	2.223 (0.935–5.375)
Avalanche size		1.377	<0.001	3.965 (2.258–7.278)
(b) Model for critical burial with non-inflated and inflated airbags combined				
Intercept		-3.715	<0.001	0.024 (0.005–0.114)
Airbag use	No	0.000		
	Yes–non-inflated or inflated	-1.029	<0.001	0.357 (0.181–0.693)
Traumatic injuries	None or minor	0.000		
	Major	0.831	0.055	2.295 (0.983–5.431)
Avalanche size		1.370	<0.001	3.936 (2.257–7.158)
(c) Model for mortality				
Intercept		-6.970	<0.001	0.001 (0.000–0.011)
Burial	Non-critical	0.000		
	Critical	3.983	<0.001	53.653 (14.026 – 364.873)
Traumatic injuries	None or minor	0.000		
	Major	2.032	0.002	7.630 (2.289–31.177)
Avalanche size		0.951	0.020	2.589 (1.190–6.019)

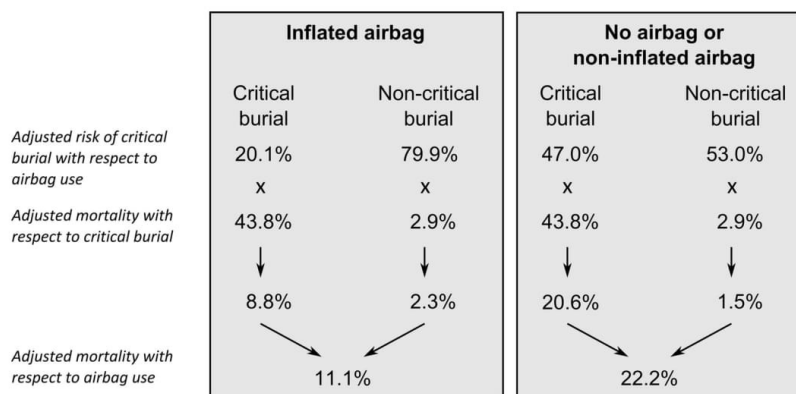


Fig. 2. Calculation of adjusted mortality with respect to avalanche airbag use.

size. Univariate analyses for other causes of non-inflation were not possible due to small sample sizes.

4. Discussion

This study evaluated the effectiveness of avalanche airbags for the first time in a process-oriented fashion that explicitly acknowledges that airbags affect mortality indirectly by reducing the risk of critical burial. In comparison to a previous statistical evaluation,¹¹ these results were derived using a multivariate approach with a larger and geographically more diverse dataset, focused on serious involvements only and with an unbiased control group.

Whereas these results support findings that airbags reduce mortality in serious avalanche involvements, the effect is lower than the previously reported absolute mortality reduction of –16 percentage points (19% mortality in non-users versus 3% mortality in users of inflated and non-inflated airbags).¹² While the absolute mortality reduction in our dataset is similar using an equivalent univariate analysis (–17 percentage points), the adjusted absolute mortality reduction using a multivariate perspective is lower (–8 percentage points; 95% confidence interval: –2 to –14 percentage points). The difference in the two estimates highlights the importance of both controlling for other factors that affect mortality (i.e., avalanche size and traumatic injuries) and properly representing the effect of airbags via critical burials. The lower mortality reduction in this particular comparison is partially caused by the considerably higher non-inflation rate in the present dataset (28% versus 20%¹¹). However, the adjusted absolute mortality reduction of –11 percentage points (95% confidence interval: –4 to –18 percentage points) revealed by the comparison of users of inflated airbags versus non-users and users with non-inflated airbags—the upper limit of the effectiveness of airbags under the conditions of the analysis dataset—is still lower than previous estimates.

The observed overall non-inflation rate of 20% (61/307) clearly highlights that non-inflations still pose a considerable threat to the performance of avalanche airbags. Deployment failure by the user was identified as the main cause of non-inflations. Whereas the independence of deployment rate and avalanche size indicates that non-deployments are not the result of more violent avalanche involvements, the lower failure rate among avalanche professionals suggests that familiarity with avalanche airbags and their deployment may improve the use of these devices. By extension, familiarity with deployment procedures and proper maintenance are paramount for ensuring that airbags work properly.

Furthermore, absolute mortality for airbag users was higher (11%) than in a previous study (3%).¹¹ While this difference is partially a result of the cases included in this analysis (i.e., larger avalanche accidents with multiple involvements), it also highlights that avalanche airbags do not guarantee survival under all circumstances. Even if every victim in the present dataset had been equipped with inflated airbags, one of every nine victims would have died.

While there is no empirical evidence to date on risk compensation behavior with avalanche airbag use, it is a common concern when weighing their potential benefits. Interestingly, the parameter estimates from the binomial regression model on critical burial indicate that the effect of using an airbag on critical burial is roughly the same size as the effect of avalanche size. Thus, the risk reduction gained from the use of an airbag is equivalent to the risk increase from being involved in an avalanche of one size class larger. Even though risk compensation was not explicitly analyzed in this study, these results show that personal safety benefits from airbags are quickly nullified if used to justify increased exposure to avalanche hazard.

4.1. Limitations

In order to extract an appropriate control group, the sample used for the analyses was substantially smaller than the complete dataset—65% (201/307) of all records with avalanche airbag users were accidents with single users—and included larger avalanches with multiple involvements. The analysis dataset also had a lower percentage of avalanche professionals and a higher percentage of victims located in the track or runout when the avalanche was triggered. While absolute mortality in the complete dataset (i.e., with single involvements and smaller avalanches) was lower than in the analysis dataset, it is unclear how the effectiveness of airbags shown in the present analysis transfers and contributes in relation to the reduced mortality from the smaller avalanche sizes and other differences.

5. Conclusions

Avalanche airbags are a valuable avalanche safety device, but the impact on mortality is lower than previously reported and they do not guarantee survival. Non-deployment remains the most considerable limitation to effectiveness. While our results show that avalanche airbags can reduce mortality in serious avalanche involvements, a larger dataset of accidents with airbag users would allow the integration of interaction effects to better define situations where this device does or does not provide benefit. However, collecting reliable avalanche accident data is challenging and records are often incomplete. We encourage national avalanche safety agencies, international bodies and airbag manufacturers to develop standardized data collection protocols and reporting guidelines to increase the comparability of data and avoid misleading statements on the impact of these devices.

Conflict of interest statement

This study was not supported financially or materially by any manufacturers of avalanche airbags. None of the authors are involved financially in the production or sale of avalanche airbag nor have they received any related grants or patents.

Acknowledgements

We thank the many individuals who contributed to the collection of avalanche accident information and made this research possible.

References

1. International Commission for Alpine Rescue (ICAR) [accessed 10.03.14] <http://www.ikar-cisa.org/eXtraEngine3/WebObjects/eXtraEngine3.woa/wa/menu?id=298&lang=en>
2. Boyd J, Haegeli P, Abu-Laban RB, Shuster M, Butt JC. Patterns of death among avalanche fatalities: a 21 year review. *CMAJ* 2009;180:507–11.
3. Brugger H, Durrer B, Elsensohn F, Paal P, Strapazzon G, Winterberger E, et al. Resuscitation of avalanche victims: Evidence-based guidelines of the international commission for mountain emergency medicine (ICAR MEDCOM): intended for physicians and other advanced life support personnel. *Resuscitation* 2013;84:539–46.
4. Hohlieder M, Brugger H, Schubert HM, Palvic M, Ellerton J, Mair P. Pattern and severity of injury in avalanche victims. *High Alt Med Biol* 2007;8:56–61.
5. McIntosh SE, Grissom CK, Olivares CR, Kim HS, Tremper B. Cause of death in avalanche fatalities. *Wilderness Environ Med* 2007;18:293–7.
6. Haegeli P, Falk M, Brugger H, Etter HJ, Boyd J. Comparison of avalanche survival patterns in Canada and Switzerland. *CMAJ* 2011;183:789–95.
7. Brugger H, Durrer B, Adler-Kastner L, Falk M, Tschirky F. Field management of avalanche victims. *Resuscitation* 2001;51:7–15.

8. Falk M, Brugger H, Adler-Kastner L. Avalanche survival chances. *Nature* 1994;368:21.
9. Kern M. PhD thesis Inverse grading in granular flow. Lausanne, Switzerland: École Polytechnique Fédérale de Lausanne; 2000 <http://biblion.epfl.ch/EPFL/theses/2000/2287/EPFL.TH2287.pdf> [accessed 10.03.14].
10. Tremper B. Staying alive in avalanche terrain. 2nd ed. Seattle, WA: The Mountaineers; 2008.
11. Brugger H, Etter HJ, Zweifel B, Mair P, Hohlrieder M, Ellerton J, et al. The impact of avalanche rescue devices on survival. *Resuscitation* 2007;75:476–83.
12. Canadian Avalanche Association (CAA). Observation guidelines and recording standards for weather, snowpack, and avalanches. Revelstoke, Canada: Canadian Avalanche Association; 2007.
13. Kleinman LC, Norton EC. What's the Risk? A simple approach for estimating adjusted risk measures from nonlinear models including logistic regression. *Health Serv Res* 2009;44:288–302.

Publication 2

Biskupič, M., Barka, I., 2009, Statistical avalanche run-out modelling using GIS on selected slopes of Western Tatras National park, Slovakia. International Snow Science Workshop, Proceedings, 482-487. (Scopus)

Statistical avalanche run-out modelling using GIS on selected slopes of Western Tatras National park, Slovakia

Marek Biskupic^{1,2,*} and Ivan Barka³

¹ Faculty of Science, Charles University in Prague, Czech Republic

² Mountain Rescue Service, Jasná Low Tatras, Slovakia

³ National Forest Centre, Zvolen, Slovakia

ABSTRACT: Without doubt avalanche run-out distances play a key role in land use planning within avalanche prone areas. The Žiarska valley in Western Tatras is considered as one of the most avalanche prone valleys in the whole area of Carpathian Mountains. This environment represents a perfect opportunity for studying and modelling extreme avalanche run-outs. The valley is frequently visited by backcountry skiers as well as roads and several cabins are located there. Therefore a careful land use planning with respect to extreme avalanche run-out is crucial. First of all avalanche release zones were estimated by using an existing model proposed by Hrečko. This model was changed and calibrated using avalanche data extracted from a database which is maintained by Slovak Centre for Avalanche Mitigation. The alpha-beta regression model developed in Norway has been used for estimating avalanche run-outs. This model is calibrated for use in Western Tatras. Topographical parameters from well known extreme avalanche paths have been collected using GPS. Data processing and model calibration have been elaborated in GIS environment. Avenue script for ArcView was written to perform automated run-out estimation based on alpha-beta regression model. Model managed fairly well to estimate runouts on some slopes while it failed to model runups. Finally the results were visualized by creating the fly-through simulations and 3D views. Winter season 08/09 with catastrophic avalanches showed the importance of avalanche run-out modelling. Many installations have been damaged due to improper land use planning without respect to extreme avalanches. Comparison between model calculation and avalanche cadastre showed correlation.

KEYWORDS: Snow avalanches, GIS, run-out modelling, Western Tatras.

1 INTRODUCTION

For several decades estimation of avalanche run-out based on topographical parameters has been carried out in some countries within Europe and North America. Early attempts were done in USA (Bovis and Mears, 1976) and Norway (Lied and Bakkehøi, 1980). Since then in many countries and mountain ranges along the world (Fujisawa et al., 1993; Furdada and Vilaplana, 1998; Johannesson, 1998; Barka Jones and Jamieson, 2004; Lied et al., 1995; Delparte, 2008) the so called alpha-beta regression model (Lied and Bakkehøi, 1980) has been introduced. Later on with advance of computers and geoinformatics and their application within natural hazards zoning, GIS has been widely adopted. Terrain models (Toppe, 1986) and GIS has been used either to estimate the probable avalanche release zones

(Hrečko, 1998; M. Maggioni and Gruber, 2003), model avalanche run-outs (Barka; Delparte 2008;) or assess the protective function of forest against avalanches (Sitko, 2008; Bebi, 2009).

Four thousand avalanche paths are registered within five Slovak mountain ranges. Several hundreds of the avalanche tracks intersect with the roads, hiking trails and places often frequented by winter travellers and backcountry skiers. Avalanches have been observed for last 50 years and these observations have been documented either in written form or drawn into avalanche cadastre maintained by Slovak Centre of Avalanche Prevention SCAP. Several catastrophic avalanches with extreme run-outs occurred for last decade, shown that avalanche cadastre suffers from spatial accuracy and it is not up to date. Therefore its use for land use planning is in questionable.

So far there have been several works dealing with estimation of probable avalanche trigger zones using GIS in Slovak mountain ranges (Hrečko, Barka, Barka and Rybar, Kohut, Sitko). Most of them were carried as part of research at home universities. The aim of this work is to show how GIS might be used to estimate probable avalanche trigger zone and model runouts on selected slopes. Simple equation model (Hrečko, 1998) for release zones is implemented and used to automate the mapping of

Corresponding author address:

Marek Biskupic, Institute of Environmental studies, Charles University in Prague
mabis@seznam.cz, tel 00421903026168

release zones in GIS. The model calibration has been based on data from Avalanche database maintained by SCAP. Avalanche path model uses statistical regression model described by Lied and Bakkehøi (Lied and Bakkehøi, 1980). The model is implemented into GIS by script written in Avenue programming language. Despite that the model failed to accurately represent runups and curvy channeled paths, it has worked well with linear straight down sloping paths.

2 METHODS

2.1 Statistical analyses of Avalanche database SLPDB

Avalanche database contains information about avalanches that has occurred within the area of Slovakia. The database consists of information on release zones (elevation, exposition, aspect, type of snow etc.), transport zones (shape, topographic parameters), deposition zones (shape, height, type, etc.), casualties and damages number of people involved, injured, deceased, forest damages). First record is dated to 1937. For the purpose of release zones identification, relevant information (aspect and elevation of release zones) from database has been extracted. Based on these parameters avalanche trigger zones model has been calibrated.

2.2 Data sources and preprocessing

The accuracy of the model results goes hand in hand with accuracy of data inputs. Therefore there is requirement for relative high accuracy of data inputs. Both models are based on topographical factors what claim on accurate digital elevation model (DEM). 5 m interval contours were used as a base for creating DEM. They were scanned from "The base map of Slovak republic" at scale 1:10 000. Consequently they were vectorized and DEM was computed using spline function with tension (Mitáňová and Hofierka 1993). Because of the presence of artificial undulations in the DEM (profile curvatures varied from concave to convex around contours), DEM pre-processing was performed. Random points with elevation attribute were extracted from the DEM. Points from valley bot-

Equation (1) result Av	Avalanche trigger hazard
0 – 15	Low
15 – 22,5	Medium
22,5 – 30	High
30 – 36	Very high

Table 2. Final reclassification table.

tom contours (in strips 20 m wide on each side of thalwegs) were added to random points. As a result new elevation data points were created. This way of DEM creation prevented generation of depressions in the valleys. It might be argued that there are more accurate ways of digital elevation model creation e.g. digital photogrammetry, aerial or terrestrial laser scanning or geodetic survey, but these methods are way more costly and time consuming.

Landcover layer obtained by analyzing the large scale vegetation maps and aerial imagery was important data input for estimating terrain roughness.

2.3 Probable Avalanche release zones model

Avalanche trigger or release zone can be described as places with certain topographical natures which allow deposition of snow masses. These snow masses might be until certain conditions released as snow avalanche. Hreňko proposed simple equation model for avalanche release zones estimation. The equation and model factors were changed according to the results of statistical analysis of Avalanche database. This step was done to link the real avalanche situations with the proposed model.

$$Av = (Al + Ex + Fx + Fy) * S * Rg \quad (1)$$

Where **Av** is value estimating potential avalanche trigger zones, **Al** is elevation factor, **Ex** is aspect factor, **Fx** is profile curvature factor, **Fy** is plan curvature factor, **S** is slope inclination factor and **Rg** is roughness factor.

Landcover layer and DEM are two main data inputs for model calculation. Each of the factors (Al, Ex, Fx, Fy, S, Rg) were classified according to table 1 and using map algebra the final grid

Elevation (m a. s. l.)	Elevation Factor(Al)	Plan Curvature	Curvature Factor(Fy)	Profile Curvature	Curvature Factor(Fx)
1200 - 1450	0,1	-4 – -0,2	1	4 – 0,2	1
1450 - 1700	1	-0,2 – 0,2	1	0,2 – -0,2	1
1700 - 1950	2	0,2 – 0,5	1	-0,2 – -0,5	1
1950 - 2200	0,5	0,5 – 4	0,5	-0,5 – -4	0,5
Cover type					Roughness Factor (Rg)
forest (coniferous, deciduous, mixed)					0,5
open forest with dwarf-pine, rough stony debris and slope covered by lesser blocks					1,2
deciduous shrub wood					1,4
open forest					1,5
dwarf-pine and slope with juts of parent rock under 50 cm					2,5
grass, with sporadic dwarf-pine, and small size slope debris					2,8
compact grass areas and rock plates					3
Slope (°)	Slope Factor (S)	Aspect	Aspect Factor (Ex)		
0° - 10°; 70° - 90°	0	N	0,5		
10° - 19°; 60° - 70°	0,4	NE	0,5		
19° - 25°; 55° - 60°	0,8	E	0,7		
25° - 30°; 50° - 55°	1,2	SE	1,5		
30° - 35°; 45° - 50°	1,6	S	2		
35° - 45°	2	SW	1		
		W	1,7		
		NW	0,4		

Table 1. Factors used to estimate probable avalanche trigger zones.

layer (Av) was calculated. Avalanche prone areas are reaching higher values of Av.

Consequent reclassification according to the table 2 resulted into final grid layer represents avalanche prone areas.

ArcGIS was used to fully automate probable trigger zones estimation by using model builder module figure 1. For later avalanche run out modelling the zones reaching the Av value at least 22,5 or more were selected. The final output was compared with avalanche cadastre map, visually assed and imported into ArcScene to create 3D bird's eye views.

from SCAP maximum run outs were measured in terrain using GPS. Survey of aerial imagery accompanied the fieldwork to increase the accuracy of measurements. Topographical parameters of each path were extracted in ArcGIS and regression analysis performed using statistical package NCSS. Acquired regression coefficients together with avalanche trigger zones (with $Av \geq 22,5$) served as the input parameters for script written in Avenue for ArcView3.x. This script models avalanche movement as flowing water. It creates flowlines from the certain points

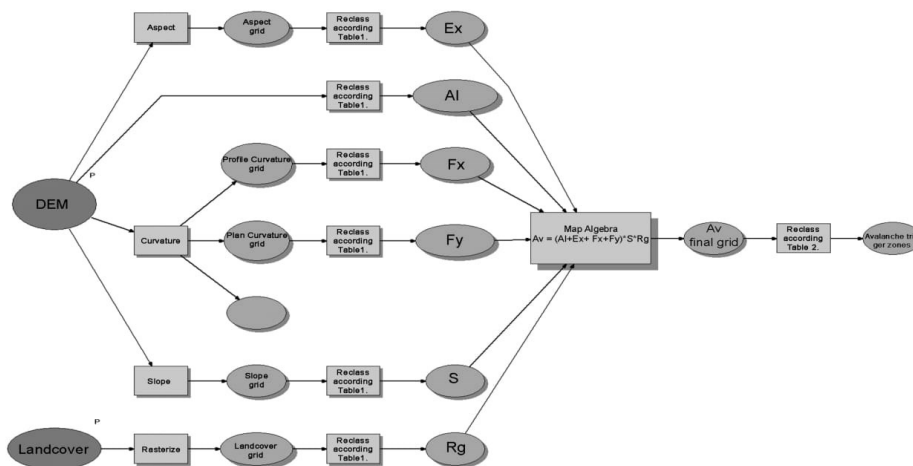


Figure 1. Workflow of the model.

2.4 Avalanche run out modelling

For the purpose of this work model developed in Norway by Lied and Bakkehøi was implemented into GIS. Model predicts maximal avalanche run out, using terrain parameters of the avalanche chute. Avalanche dynamics is not taken into account. The authors based the model on analyses of hundreds of well known avalanche chutes. They chose a reference point (so called the β point) with β angle defined as

the average gradient of the avalanche path profile from the position where the slope decrease to 10° to the trigger zone (Figure 2.)

The α is the angle sighting from the extreme run out position to the trigger zone. Least square regression analysis showed correlation between α and β angle have form of equation (Lied and Bakkehøi, 1980).

$$\alpha = C_0 + C_1\beta \quad (2)$$

Model was calibrated on dataset of 30 avalanche paths with well know run outs. With the help of avalanche expert knowledge of J. Pet'o

(avalanche trigger zones) than it finds β points calculates the β angle and based on the equation 2 it estimates α angle. Consequently it esti-

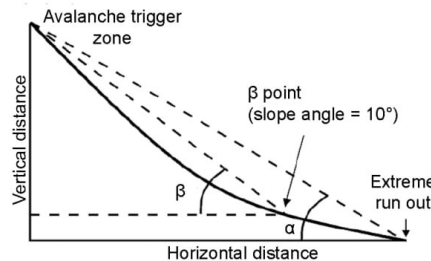


Figure 2. Topographical run-out model.

mates α point and cuts flowline in this place. Script runs automatically and beside the input points it needs DEM in form of TIN. Because the avalanche movement is modeled as water some problems raised. In one point all the flowlines connected and continued as one flowline which is natural behavior of the water but not common to avalanches. This was solved by channel network module in SAGA GIS. The proposed method enabled almost automated estimation of avalanche paths. Due to the time lack and com-

puter capacity the method was used only on selected slopes.

3 RESULTS

3.1 Statistical analysis of Avalanche database summary

A statistical analysis was focused on two factors: elevation and aspect. The aim was to figure out what kind of slopes are most avalanche prone. Altogether 571 avalanches records with valid height and aspect information

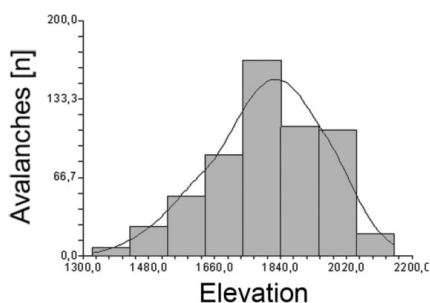


Figure 3. Avalanche distribution within elevation.

were analyzed. Elevation analyze showed that that most of the avalanches triggered from interval 1700 - 1950 m a. s. l. , Specifically 339 avalanches what represents 59.3% of all analyzed avalanches. Further insight to elevation aspect and avalanches see figure 3 and table 3.

Elevation (m a. s. l.)	No. of avalanches	% of avalanches
1200 - 1450	7	1,23
1450 - 1700	150	26,27
1700 - 1950	339	59,37
1950 - 2200	75	13,13

Table 3. Avalanche distribution within elevation.

The most avalanche prone slopes have south aspect with 137 avalanches occurred. Followed by west and south-east aspects with 117 respectively 103 avalanches. More than half of the avalanches occurred on slopes with S, W, and SE orientation. Further details see figure 4 and table 4.

Aspect	No of avalanches	% of avalanches
N	54	9,12
NE	33	5,57
E	46	7,77
SE	104	17,57
S	137	23,14
SW	71	11,99
W	117	19,76
NW	30	5,07

Table 4. Avalanche distribution within aspect

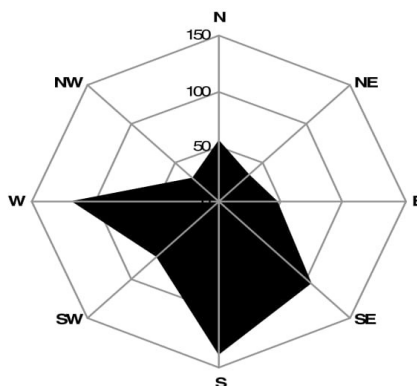


Figure 4. Avalanche distribution within aspect.

3.2 Avalanche trigger zones

Results from the model estimating probable avalanche paths correlates well with avalanche cadastre map figure 7. It was expected that trigger zones estimated by the model will occur in upper parts of historical avalanche paths. Some historical path and modeled trigger zones show some inconsistency. Field investigation and aerial imagery inspection indicated large forest succession in these places for last 25 years. Due to this succession avalanche activity was reduced to minima. Using up to date land cover maps and ortophotos as an input for the model resulted in the proper estimation of potential avalanche trigger hazard. Model revealed that 67,45% of the study area falls into the zone with small avalanche trigger potential 21,56% with medium 10,4% with high and 0,59% as very high avalanche trigger potential. See figure 5. Due to the implementing the data from avalanche and database curvature factor estimated release zones reflects the nature of avalanche triggering. It can be seen from figure 6. Ridges were properly classified as places with minimal avalanche trigger potential. On the other hand

high or very high risk potential was given to the steep gullies and vast steep slopes covered with grass.

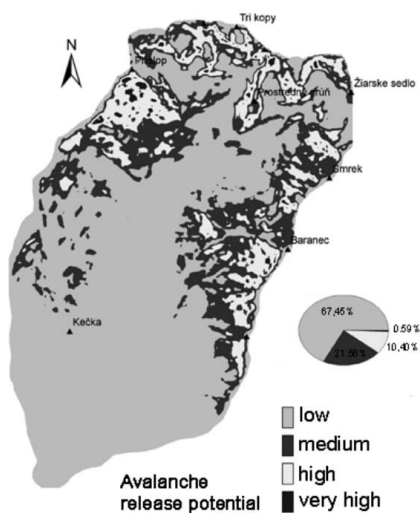


Figure 5. Avalanche release potential within study site.



Figure 6. High and very high avalanche release potential.

3.3 Avalanche run outs

GIS with the help of script language (Avenue) allowed implementing statistical run out modeling in automated way. This was done on selected slopes. The final regression equation for the Western Tatras is

$$\alpha = 0,91B - 0,04^{\circ}(3)$$



Figure 7. Output of the run-out model.

Correlation coefficient for this regression is 0,95 coefficient of determination is 0,9 and standard error of predicted α angle is 1,1. Figure 7 shows final run outs on the two of the selected avalanche paths. It can be said that in this case model outputs are in well correlation with historical avalanche cadastre map. In some other cases model failed to represent run outs naturally e. g run ups, channeled curvy run outs. Because the avalanche movement was approximated as water flow, circumstances occurred in narrow channels where all the flowlines gathered together and from certain point they flowed together. This was partially solved by channel module in SAGA. Anyway some in some extremely narrow channels satisfying results were not obtained and different methods should be used for determining avalanche width.

3.4 Conclusion

Probable avalanche trigger zones estimated by simple equation model are in good agreement with avalanche cadastre. This easy to use model is easy to implement into GIS environment. It is simple to calculate model factors and the results are in sufficient correlation with real observations represented by cadastre map. Therefore it would be suitable to introduce model in avalanche hazard zoning praxis. Therefore Alpha-beta regression model was implemented into GIS by using script which enabled automated runouts estimation. Model failed to estimate runups because the avalanche movement was modelled as flowing water. Anyway the proposed method might be par-

ticular useful in updating avalanche cadastre map on straight down sloping paths with no run-ups in the depositional area.

References

- Barka, I., Rybár, R. 2003. Identification of snow avalanche trigger areas using GIS, Ecology (Bratislava), Suppl. 2
- Bovis, M. and Mears, A., 1976: Statistical prediction of snowavalanche runout from terrain variables in Colorado. Arctic and Alpine Research, 8: 115-120.107-119.
- Hrečko, J. 1998. Avalanche hazard of the high mountain landscape in Tatras territory (in Slovak) Folia Geographica 2, Prešov, p. 348 – 352
- Lied, K., Bakkehoi, S., 1980. Empirical calculation of snow-avalanche run-out distancebased on topographic parameters. Journal of Glaciology 26 (94), 165–177
- Delparte, D., 2008. Avalanche Terrain Modeling in Glacier National Park, Canada. PhDThesis, University of Calgary, Calgary, AB, Canada, 179 pp
- Furdada, G., Vilaplana, J.M., 1998. Statistical predication of maximum avalanche run-out distances from topographic data in the western Catalan Pyrenees (northeast Spain). Annals of Glaciology 26, 285–288
- Fujisawa, K., Tsunaki, R., Kamiishi, I., 1993. Estimating snow avalanche runout distances from topographic data. Annals of Glaciology 18, 239–244.
- Maggioni, M. and Gruber, U., 2003. The influence of topographic parameters on avalanche release dimension and frequency. Cold Regions Science and Technology, 37: 407-419.
- Mitáková, H., Hofierka, J., 1993: Interpolation by Regularized Spline with Tension: II.Application to Terrain Modeling and Surface Geometry Analysis, Mathematical Geology 25, p. 657-667
- Toppe, R., 1987. Terrain models: a tool for natural hazard mapping. In: Salm, B., Gubler, H. (Eds.), Avalanche Formation, Movements and Effects (Proceedings of the Davos Symposium, September 1986). International Association of Hydrological Sciences (IAHS), Wallingford, UK, pp. 629–638.

Publication 3

Boltižiar, M., **Biskupič, M.**, Barka I.,2016, Spatial modelling of avalanches by application of GIS on selected slopes of the Western Tatra Mts. and Belianske Tatra Mts., Slovakia, Gographica Polonica, 89,79 – 90. (Scopus)



Geographia Polonica
2016, Volume 89, Issue 1, pp. 79-90
<http://dx.doi.org/10.7163/GPol.0047>



INSTITUTE OF GEOGRAPHY AND SPATIAL ORGANIZATION
POLISH ACADEMY OF SCIENCES
www.igipz.pan.pl

www.geographiapolonica.pl

SPATIAL MODELLING OF AVALANCHES BY APPLICATION OF GIS ON SELECTED SLOPES OF THE WESTERN TATRA MTS. AND BELIANSKE TATRA MTS., SLOVAKIA

Martin Boltžiar^{1,2} • Marek Biskupič^{3,4} • Ivan Barka⁵

¹ Department of Geography and Regional Development
Constantine the Philosopher University in Nitra
Trieda A. Hlinku 1, 949 74 Nitra: Slovakia
e-mail: mboltzciar@ukf.sk

² Department of Geography
J.E. Purkyně University in Ústí nad Labem
České mládeže 8, 400 96 Ústí nad Labem: Czech Republic

³ Avalanche Prevention Center
Dr. J. Gašperika 598, 033 01 Liptovský Hrádok: Slovakia
e-mail: avalanches@hzs.sk

⁴ Institute for Environmental Studies
Charles University Prague
Ovocný trh 3-5, 116 36 Prague 1: Czech Republic

⁵ National Forest Department
T.G. Masaryka 22, 960 92 Zvolen: Slovakia
e-mail: barka@nlcsk.org

Abstract

The avalanches represent a significant and very dynamic process within the Tatra high-mountain landscape. Undoubtedly avalanche run-out distances play a key role in land use planning within avalanche prone areas. The Žiarska valley and Predné Meďodoly valley are considered as one of the most avalanche prone valleys in Tatra Mts. This environment represents an excellent opportunity for studying and modelling extreme avalanche run-outs. Primarily avalanche release zones were estimated by using an existing model proposed by Hreško (1998). This model was modified and calibrated for both valleys. The alpha-beta regression model developed in Norway has been used to estimate avalanche run-outs. Data processing and model calibration have been elaborated in GIS environment. Avenue script for ArcGIS was written to perform automated run-out estimation based on alpha-beta regression model. Model managed to estimate run-outs on some slopes while it failed to model run-ups. Finally the results were visualized by creating the fly-through simulations and 3D views. Comparison between model calculation and avalanche cadastre showed correlation.

Key words

snow avalanche • GIS • run-out modelling • Western Tatra Mountains • Belianske Tatra Mountains

Introduction

Over the course of several decades, the estimation of avalanche run-outs has been carried out in some countries within Europe and North America based on topographical parameters. Early attempts were made in USA (Bovis & Mears 1976) and Norway (Lied & Bakkehøi 1980). Since then the so called alpha-beta regression model (Lied & Bakkehøi 1980) has been introduced in many countries and mountain ranges in the world (Fujisawa et al. 1993; Lied et al. 1995; Furdada & Vilaplana 1998; Johannesson 1998; Barka 2003; Jones & Jamieson 2004; Delporte 2008). Later on, with the development of computers and geoinformatics and their application for natural hazard zoning, GIS has been widely adopted. Terrain models (Toppe 1987) and GIS have been used to estimate the probable avalanche release zones (Hreško 1998; Maggioni & Gruber 2003), model avalanche run-outs (Barka 2003; Delporte 2008) or assess the protective function of forest against avalanches (Sitko 2008; Bebi et al. 2001).

Four thousand avalanche paths are registered within five Slovak mountain ranges. Several hundred of these avalanche tracks cross roads, hiking trails and places often frequented by winter travellers and backcountry skiers. Avalanches have been observed during the last 50 years and their findings have been documented either in written form or drawn into an avalanche cadastre maintained by the Slovak Centre for Avalanche Prevention (SCAP). Several disastrous avalanches with extreme run-outs have occurred in the last 15 years and most of them have gone beyond the borders of well-known avalanche paths.

So far several projects dealing with the estimation of probable avalanche trigger zones using GIS have been developed in Slovakia (Hreško 1998; Hreško & Bugár 1999; Hreško & Boltžiar 2001; Barka 2003; Barka & Rybár 2003; Kohút 2005; Boltžiar 2007; Sitko 2008) and also in Poland (Rączkowska

et al. 2013; Rojan et al. 2013; Lempa et al. 2014). Most of them were carried out as part of research in local universities or institutes. The aim of this work is to use GIS techniques to estimate probable avalanche trigger zones and model run-outs on selected slopes. A simple equation model (Hreško 1998) for release zones is developed and used to automate the mapping of release zones in GIS. The model calibration has been based on data from the avalanche database maintained by SCAP. The avalanche path model uses a statistical regression model described by Lied and Bakkehøi (Lied & Bakkehøi 1980) and is implemented into GIS by script written in Avenue programming language. Despite this, the model failed to accurately represent run-ups and curved channeled paths; it has functioned well with linear paths which run straight down slopes.

Research area

The Ziarska valley is situated in the Western Tatra Mts. and the Predne Metodoly valley is situated in the Belianske Tatra Mts. (Fig. 1). Due to their overall geomorphological character both valleys have very similar conditions for the formation of avalanches. From all the valleys in Slovakia's high mountains, they have the greatest topographic suitability for the formation of avalanches, especially in terms of size and frequency. The decisive factor is the overall morphology of avalanche gullies, especially the length and position of the cut-off zone, size of catchment area, length and slope of avalanche paths and vegetation conditions. According to the SCAP avalanche cadastre the length of avalanche paths is approximately 500-2000 m and height difference is 300-950 m. These mountains provide particularly favourable conditions due to the lowering of the upper forest boundary and destruction of the dwarf-pine zone because of very long term extensive use of these areas for grazing sheep and cattle. On the longest and steepest section of the avalanche path, i.e. from the cut-off zone to the upper forest boundary, avalanches



Figure 1. Research areas: Žiarska valley in Western Tatra Mts. and Predné Meďodoly valley in Belianske Tatra Mts.

Source: Orthophotos: © Google Earth, 2014

grow not only in size, but especially in dynamic force. Their dynamic effects cause a clear cut to be produced right through the current forest area down to the bottom of the valleys, which shows not only their occurrence but also their destructive effects (Kňazovický 1967). The effects of avalanches were continuously monitored during the field surveys conducted during which photographic documentation was produced.

Methods

Statistical analyses of the avalanche database: SLPDB

The avalanche database contains information on avalanches that have occurred within the territory of Slovakia. The database consists of information on release zones (elevation, exposition, aspect, type of snow etc.), transport zones (shape, topographic

parameters), deposition zones (shape, height, type, etc.), casualties and damage (number of people involved and injured, deceased, forest damage). The first record dates back to 1937. For the purpose of identifying release zones, relevant information (aspect and elevation of release zones) has been extracted from the database. Based on these parameters a model for avalanche trigger zones has been calibrated.

Data sources and pre-processing

The accuracy of the model results is dependent on the accuracy of data inputs. Therefore relative high accuracy of data inputs is required. Both models are based on topographical factors which require an accurate digital elevation model (DEM). Contours at 5 m intervals were used as a base for creating a DEM. For the Žiarska valley these

were scanned from "The Base Map of Slovak Republic" at a scale 1:10,000 and those for the Predné Međodoly valley were also generated by photogrammetric methods (Euro-senses s.r.o., Bratislava, SK). Consequently contour lines were vectorised and the DEM was computed using the spline function with tension (Mitášová & Hofierka 1993). Because of the presence of artificial undulations in the DEM (profile curvatures varied from concave to convex around contours), DEM preprocessing was performed. Random points with the elevation attribute were extracted from the DEM. Points from the valley bottom contours (in strips 20 m wide on each side of thalwegs) were added to random points. As a result new elevation data points were created. Compared to the general fill method, this method of DEM creation prevents the generation of depressions in the valleys. It can be argued that there are more accurate ways of creating digital elevation models e.g. digital photogrammetry, aerial or terrestrial laser scanning

or geodetic survey, but these methods are much more costly and time consuming. The land cover layer obtained by analysing the large scale vegetation maps (1:10,000) and aerial imagery were other important data inputs for estimating terrain roughness.

Model of probable avalanche release zones

An avalanche trigger or release zone can be described as an area with certain topographical features which allow deposition of snow masses. These snow masses tend to release as a snow avalanche under certain conditions. Hreško (1998) proposed a simple equation model for estimating avalanche release zones. The equation and model factors were modified according to the results of statistical analysis of the avalanche database. This step was done to calibrate real avalanche situations with the proposed model.

Table 1. Factors used to estimate trigger zones

Elevation [m a.s.l.]	Elevation factor [A]	Plan curvature	Curvature factor [f_y]	Profile curvature	Curvature factor [F]
1200-1450	0.1	-4.0(-0.2)	1.0	4.0-0.2	1.0
1450-1700	1.0	-0.2-0.2	1.0	0.2(-0.2)	1.0
1700-1950	2.0	0.2-0.5	1.0	-0.2(-0.5)	1.0
1950-2200	0.5	0.5-4.0	0.5	-0.5(-4.0)	0.5
Cover type				Roughness factor [Rg]	
Forest (coniferous, deciduous, mixed)				0.5	
Open forest with dwarf-pine, rough stony debris and slope covered by lesser blocks				1.2	
Deciduous shrub wood				1.4	
Open forest				1.5	
Dwarf-pine and slope with exposures of parent rock jutting out less than 50 cm				2.5	
Grass with sporadic dwarf-pine, and small size slope debris				2.8	
Compact grass areas and rock plates				3.0	
Slope [°]	Slope factor [S]	Aspect	Aspect factor [Ex]		
0°-10°, 70°-90°	0.0	N	0.8		
10°-19°, 60°-70°	0.4	NE	0.5		
19°-25°, 55°-60°	0.8	E	0.7		
25°-30°, 50°-55°	1.2	SE	1.5		
30°-35°, 45°-50°	1.6	S	2.0		
35°-45°	2.0	SW	1.0		
		W	1.7		
		NW	0.4		

$$Av = (Al + Ex + Fx + Fy) \cdot S \cdot Rg$$

Where:

Av - is a value estimating potential avalanche trigger zones,

Al - is the elevation factor,

Ex - is the aspect factor,

Fx - is the profile curvature factor,

Fy - is the plan curvature factor,

S - is the slope inclination factor and

Rg - is the roughness factor.

The land cover layer and DEM are the two main data inputs for calculation of the model. Each of the factors (*Al*, *Ex*, *Fx*, *Fy*, *S*, *Rg*) was classified according to Table 1 and the final grid layer (*Av*) was calculated using map algebra. The classification was based on the data extracted from the avalanche database. According to the database, the lowest avalanche frequency is observed in the interval from 1200 m-1450 m. Therefore this interval was given a score of 0.1. The same was carried out for other factors (plan and profile curvature, land cover, etc). The complete methodology of the classification can be found in studies done by Hreško, Bárka and Rybár (Hreško 1998; Bárka & Rybár 2003).

Final reclassification according to Table 2 resulted in a final grid layer which represents avalanche prone areas. Avalanche prone areas have higher values of *Av*.

Table 2. Final reclassification

Equation (1) result <i>Av</i>	Avalanche trigger hazard
0.0-15.0	low
15.0-22.5	medium
22.5-30.0	high
30.0-36.0	very high

ArcGIS was used to fully automate the estimation of probable trigger zones by using the model builder module (Fig. 2). For avalanche run out modelling based on this, zones reaching an *Av* value of at least 22.5 or more were selected. The final output was compared with the avalanche cadastre map,

visually assessed, and imported into ArcScene to create 3D bird's eye views for the Žiarska valley (Fig. 6).

Avalanche run out modelling

For the purpose of this work a model developed in Norway by Lied and Bakkehøi was implemented into GIS. The model predicts a maximal avalanche run out using the terrain parameters of the avalanche chute. Avalanche dynamics are not taken into account. The authors based the model on analyses of hundreds of well-known avalanche chutes. They chose a reference point (the so called the β point) with the angle β defined as the average gradient of the avalanche path profile from the position where the slope decreases to 10° to the trigger zone (Fig. 3).

The angle α is the angle sighting from the extreme run out position to the trigger zone. Least square regression analysis showed a correlation between the α and β angle and that the relationship has the form of an equation (Lied & Bakkehøi 1980).

$$\alpha = C0 + C1\beta$$

The model was calibrated on a dataset of 44 avalanche paths from both valleys (30 from the Žiarska valley and 14 from the Predné Medodoly valley) with well-known run-outs. With the assistance of the expert knowledge of avalanches of J. Peťo from SCAP, maximum run outs were measured on the terrain using GPS. A survey of aerial imagery accompanied the fieldwork to increase the accuracy of measurements. The topographical parameters of each path were extracted in ArcGIS and linear regression analysis was performed using a statistical package NCSS. Acquired regression coefficients together with avalanche trigger zones (where $Av \geq 22.5$) served as the input parameters for script written in Avenue for ArcGIS. This script models avalanche movement as flowing water. It creates flowlines from certain points (avalanche trigger zones), then it finds β points, calculates the β angle, and following this it estimates the α angle

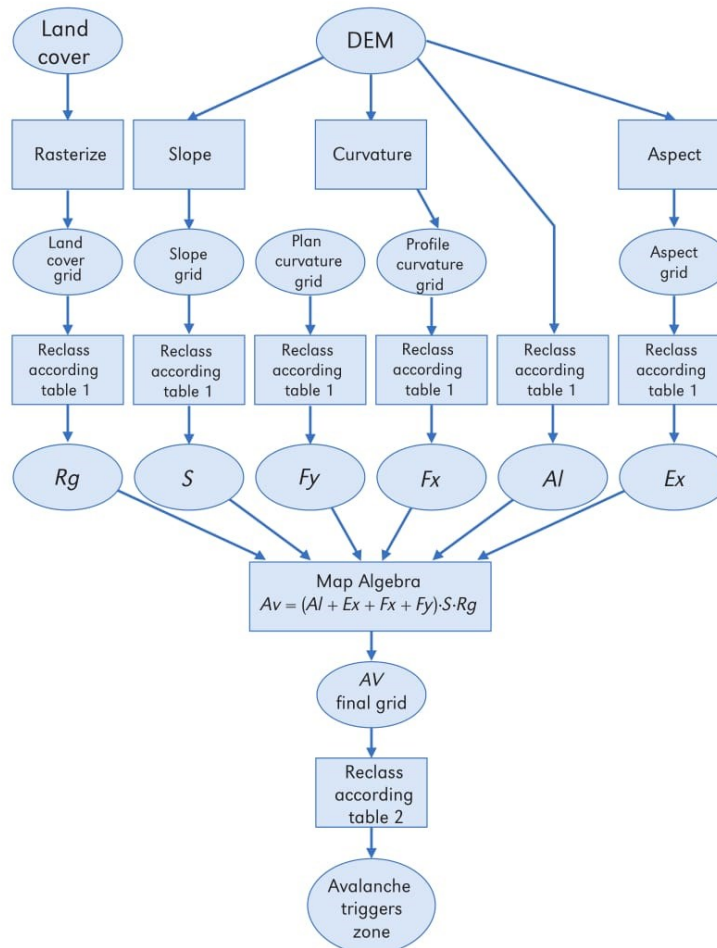


Figure 2. Workflow of the trigger zones estimation model

based on Equation 2. Later it estimates the point α and cuts the flow-line at this place. The script runs automatically and in addition to the input points, it needs DEM in the form of TIN. Because the avalanche movement is modelled as water, some problems are raised. At one point all the flowlines connected and continued as one flowline, which is the natural behaviour of water but not common in avalanches. This was solved by the channel network module in SAGA GIS. The module derives a channel network based on gridded digital elevation data and is enabled to keep all the separated flowlines in one flow simi-

lar to the flow of avalanches. The proposed method enabled almost automated estimation of avalanche paths. Due to the lack of time and computer capacity the method was only used on selected slopes.

Results

Results from the model estimating probable avalanche paths correlate well with the avalanche cadastre map (Fig.6). It was expected that trigger zones estimated by the model will occur in the upper parts of historical avalanche paths. Due to forest succession

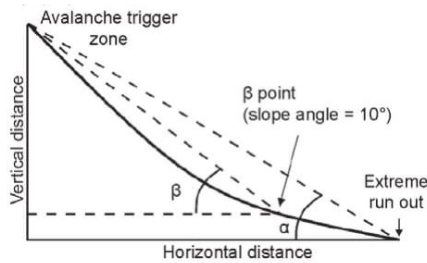


Figure 3. Topographical run-out model

10% of the avalanche trigger areas are no longer avalanche prone. This is due to the growth of mature forest on such sites forming a perfect avalanche barrier. The up to date land cover layer used in the model influenced the result so that areas with lower avalanche triggering potential were properly estimated. Field investigation and aerial imagery inspection indicated significant forest succession in these places over the last 25 years. Due to this succession, avalanche activity was reduced to a minimum. Use of the up to date land cover maps and orthophotos as an input to the model resulted in the proper estimation of potential avalanche trigger hazards. The model revealed that in the Žiarska valley, 68% of the area studied falls into a zone with small avalanche trigger potential; 21% with medium; 10% with high and 1% with very high avalanche trigger potential and in the Predné Meďodoly valley: 62% of the area studied falls into the zone with small avalanche trigger potential; 14% with medium; 14% with high and 10% with very high avalanche trigger potential (Fig. 4). Due to implementing the data from the avalanche database and the curvature factor, the estimated release zones reflect the nature of avalanche triggering (Fig. 7). Ridges were properly classified as places with minimal avalanche trigger potential (Fig. 5). On the other hand high or very high risk potential was given to the steep gullies and vast steep slopes covered with grass. This is one of the reasons why the Predné Meďodoly valley has more 'very high' avalanche release potential areas.

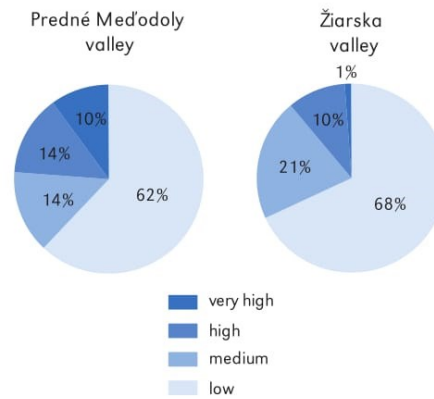


Figure 4. Comparison of avalanche release potential areas in %

Avalanche run-outs

Use of scripting language (Avenue) in GIS allowed the implementation of statistical run out modelling in an automated manner. This was done on selected slopes. The final regression equation for the Western Tatra and Belianske Tatra Mts. is

$$\alpha = 0,91\beta - 0,04^\circ$$

The correlation coefficient for this regression is 0.95, the coefficient of determination is 0.9, and the standard error of the predicted α angle is 1.1. Figure 6 shows the final run-outs on all the avalanche paths in both valleys. It can be stated that in this case the model outputs are in good agreement with the historical avalanche cadastral map. In some other cases the model failed to represent run-outs in a natural manner, e. g. run-ups and channelled curvy run-outs. Because the avalanche movement was approximated as water flow, circumstances occurred in narrow channels where all the flowlines gathered together and from a certain point they flowed together. This was partially solved by the channel module in SAGA. Unfortunately in some extremely curved channels satisfactory results were not obtained and different methods should be used for determining avalanche width.

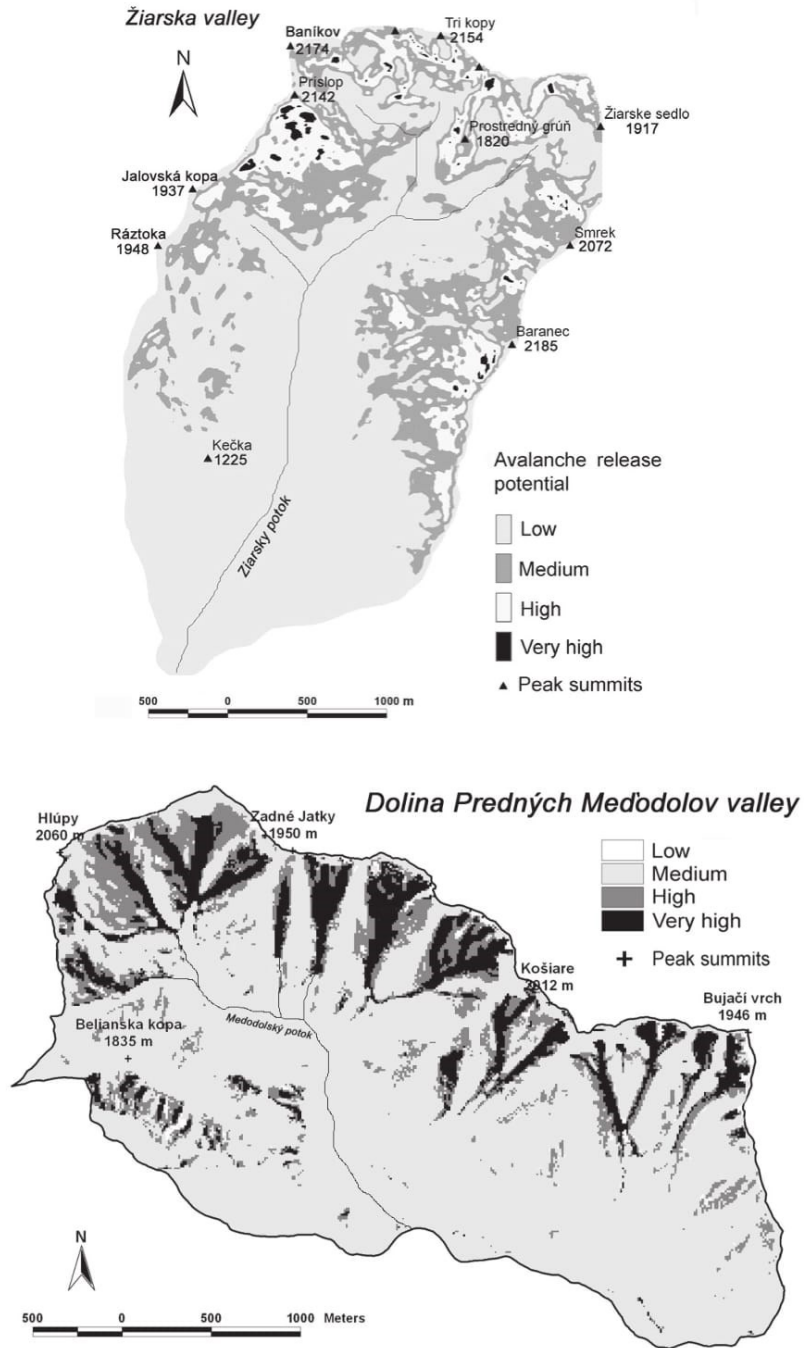


Figure 5. Avalanche release potential within the sites studied

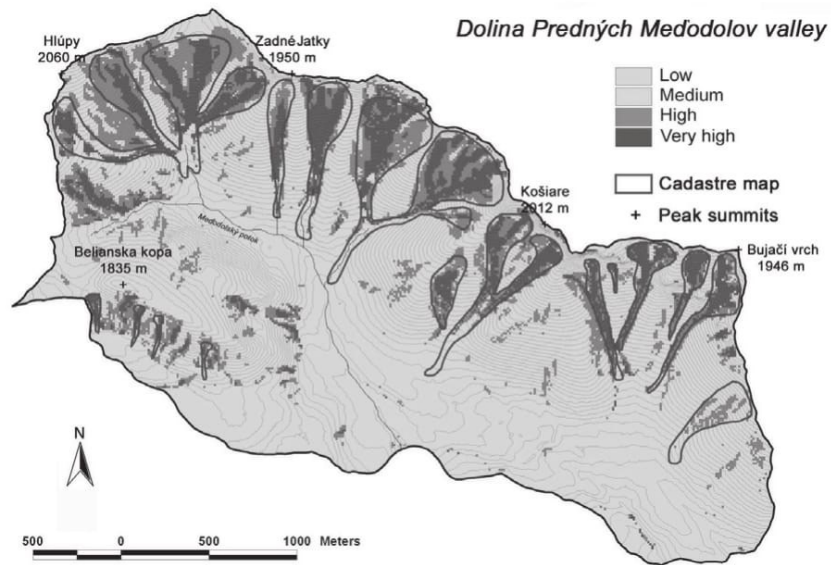
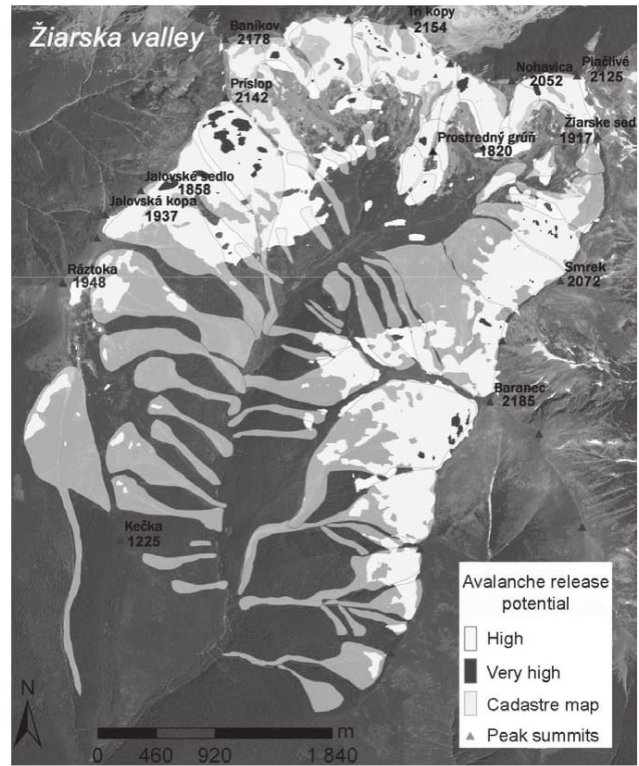


Figure 6. Avalanche release potential compared with the cadastral map

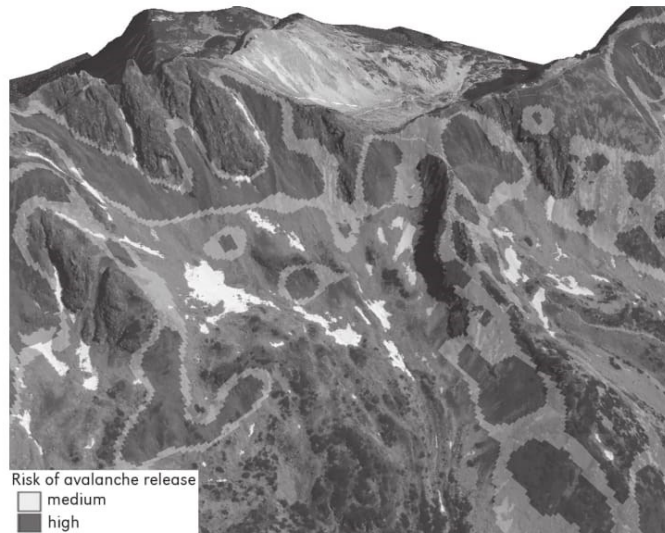


Figure 7. High and very high avalanche release potential in the Žiarska valley (3D view in ArcGIS)

Conclusions

A visual assessment of the avalanche trigger model shows agreement with the avalanche cadastre in some cases. The model did not estimate several trigger zones which were mainly located in the lower parts of the valleys. In total 91% of the pixels marked as avalanche prone areas fit in the area of the avalanche cadastre. In future, more detailed observations and the use of satellite imagery will be required to obtain data on avalanche prone locations. This can be explained by the succession undergone in these trigger zones. Field investigation proved that the trigger zones are naturally reforested and therefore avalanche activity is reduced. This conclusion is also supported by direct avalanche observations which did not report any avalanche for the last 15 years. It is crucial to use the most up to date data on land cover because only this can guarantee the proper estimation of the actual trigger areas. The release zones evolve in space and time according to the development of avalanche activity and forest succession.

The avalanche trigger model is easy to implement in the GIS environment. It is

simple to calculate the model factors and, after several improvements, the model may be used in avalanche zoning. It will be interesting to see the future development of the model. In operational use the coupling of the model with on line meteorological data could help to improve the results and it could, in particular, enable one to estimate the actual trigger zones in real time depending on the weather situation. This would be a great aid to people travelling in avalanche prone areas.

The alpha-beta regression model implemented into GIS showed several discrepancies with the real behaviour of avalanches. In many cases it was not possible to find the beta reference point. This is caused by the relative steepness of the study region. Most of the avalanches do not reach the beta point and they terminate either on the steep valley bottom or the opposite slope. The model was developed in Norway taking into account local topography which differs from topographies in the Western Tatra Mts. or Belianske Tatry Mts. It cannot be stated that the model doesn't work at all. It works, but just for specific slopes. The model is suitable for straight down sloping paths with no run-ups in the depositional area.

The method developed for avalanche zoning showed that many improvements will have to be done to use this method for land use planning. It is an advantage especially for avalanche zoning on small scales that models are implemented into GIS and can perform the simulations in an automated manner. After refinement and adjustment the method can be translated to other mountain areas. The proposed method of estimation of avalanche prone areas seems to be a good replacement of a method based entirely

on field observations. It saves time and brings more safety to the SCAP staff. On the other hand, avalanches are very difficult to predict and only relying on model outputs is not advisable. In some way or other, field observations will always be necessary.

Editors' note:

Unless otherwise stated, the sources of tables and figures are the authors', on the basis of their own research.

References

- BARKA I., 2003. *Identification of snow avalanche trigger areas and avalanche paths by the GIS*. Geomorphologia Slovaca, vol. 3, no. 2, pp. 60-63.
- BARKA I., RYBÁR R., 2003. *Identification of snow avalanche trigger areas using GIS*. Ecology, vol. 22, suppl. 2, pp. 182-194.
- BEBI P., KIENAST F., SCHONENBERGER W., 2001. *Assessing structures in mountain forests as a basis for investigating the forests' dynamics and protective function*. Forest Ecology and Management, vol. 145, no. 1-2, pp. 3-14.
- BOLTIŽIAR M., 2007. *Structure of the Tatra high mountain (large scale mapping, analysis and evaluation of changes by application of remote sensing data)*. Nitra: Fakulta prírodných vied Univerzity Konštantína Filozofa, Ústav krajiny ekológie SAV Bratislava, Pobočka Nitra, Slovenský národný komitét pre program UNESCO Človek a biosféra.
- BOVIS M., MEARS A., 1976. *Statistical prediction of snow avalanche run-out from terrain variables in Colorado*. Arctic and Alpine Research, vol. 8, no. 1, pp. 115-120.
- DELPARTE D., 2008. *Avalanche terrain modeling in Glacier National Park, Canada*. Calgary: University of Calgary [PhD thesis].
- FUJISAWA K., TSUNAKI R., KAMIISHI I., 1993. *Estimating snow avalanche run out distances from topographic data*. Annals of Glaciology, 18, pp. 239-244.
- FURDADA G., VILAPLANA J.M., 1998. *Statistical predication of maximum avalanche run-out distances from topographic data in the western Catalan Pyrenees (northeast Spain)*. Annals of Glaciology, 26, pp. 285-288.
- HREŠKO J., 1998. *Avalanche hazard of the Tatra high mountain landscape*. Folia Geographica, 2, Prešov: Prešovská univerzita, pp. 348-352.
- HREŠKO J., BOLTIŽIAR M., 2001. *The influence of the morphodynamic processes to landscape structure in the high mountains (Tatra Mts.)*. Ekológia, vol. 20, suppl. 3, pp. 141-148.
- HREŠKO J., BUGÁR G., 1999. *Avalanche risk of the SE part of Belianske Tatra Mts* [in:] T. Hrnčiarová, Z. Izakovičová (eds.), Krajinnokoekologické plánovanie na prahu 3. Tisícročia, Bratislava: Ústav krajiny ekológie SAV, pp. 268-269.
- JOHANNESSEN T., 1998. *A topographical model for Icelandic avalanches*. Reykjavik: Meteorological Office Report Vi-G980003-UR03.
- JONES A., JAMIESON B., 2004. *Statistical avalanche runout estimation for short slopes in Canada*. Annals of Glaciology, vol. 38, no. 1, pp. 363-372.
- KŇAZOVICKÝ L., 1967. *Avalanches*. Bratislava: Vydavateľstvo SAV.
- KOHÚT F., 2005. *Natural processes in high mountain landscape - Jalovecká valley*. Nitra: University of Constantine the Philosopher [PhD thesis].
- LEMPA M., KACZKA R.J., RĄCZKOWSKA Z., 2014. *Rekonstrukcja aktywności lawin śnieżnych w Białym Żlebie (Tary Wysokie) na podstawie przyrostów rocznych świerka pospolitego (Picea abies L. Karst.)*. Studia i Materiały Centrum

- Edukacji Przyrodniczo-Leśnej, vol. 16, no. 3, pp. 105-112.
- LIED K., BAKKEHØI S., 1980. *Empirical calculation of snow-avalanche run-out distance based on topographic parameters*. Journal of Glaciology, vol. 26, no. 94, pp. 165-177.
- LIED K., WEILER C., BAKKEHØI S., HOPF J., 1995. *Calculation methods for avalanche run-out distance for the Austrian Alps* [in:] F. Sivardi-ère (ed.), *The contribution of scientific research to safety with snow, ice and avalanche*. Grenoble: Association nationale pour l'étude de la neige et des avalanches, ANENA, pp. 63-68.
- MAGGIONI M., GRUBER U., 2003. *The influence of topographic parameters on avalanche release dimension and frequency*. Cold Regions Science and Technology, vol. 37, no. 3, pp. 407-419.
- MITÁŠOVÁ H., HOFIERKA J., 1993. *Interpolation by regularized spline with tension: II. Application to terrain modeling and surface geometry analysis*. Mathematical Geology, vol. 25, no. 6, pp. 657-667.
- RĄCZKOWSKA Z., DŁUGOSZ M., KACZKA R., KALAFARSKI M., ROJAN E., 2013. *Geomorphological aspects of snow avalanche activity in the Polish Tatras*. Geomorphologia Slovaca et Bohemica, vol. 13, no. 1, pp. 67-68.
- RĄCZKOWSKA Z., DŁUGOSZ M., GADEK B., GRABIEC M., KALAFARSKI M., ROJAN E., 2014. *Environmental conditions, dynamic and multiproxy records of snow avalanches in the Tatra Mts* [in:] IGU 2014 Book of Abstracts, Kraków: IGU, pp. 1.
- ROJAN E., RĄCZKOWSKA Z., KALAFARSKI M., DŁUGOSZ M., KACZKA R., GADEK B., 2013. *Avalanches in relation to relief of the Tatra Mountains* [in:] *Geomorphology and Sustainability*. Paris, 27-31 August 2013. 8th International Conference (AIG) on Geomorphology. Abstracts volume, p. 1066.
- SITKO R., 2008. *Identification, classification and assessment of forest function with the use of geoinformatics*. Zvolen: Technical University [PhD thesis].
- TOPPE R., 1987. *Terrain models: A tool for natural hazard mapping* [in:] B. Salm, H. Gubler (eds.), *Avalanche formation, movements and effects* (Proceedings of the Davos Symposium, September 1986), International Association of Hydrological Sciences (IAHS), no. 162, pp. 629-638.



Publication 4

Frauenfelder, R., Lato, M. J., Biskupič, **M.**, 2015, Using eCognition to automatically detect and map avalanche deposits from the spring 2009 avalanche cycle in the Tatra mts., Slovakia, Int. Arch. Photogramm. Remote Sens. Spatial Inf. Sci., XL-7/W3, 791-795. (Scopus)

USING ECOGNITION TO AUTOMATICALLY DETECT AND MAP AVALANCHE DEPOSITS FROM THE SPRING 2009 AVALANCHE CYCLE IN THE TATRA MTS., SLOVAKIA

R. Frauenfelder ^{a,*}, M. J. Lato ^b, M. Biskupič ^{c,d}

^a Norwegian Geotechnical Institute, P.O. Box 3930 Ullevaal Stadion, 0806 Oslo, Norway – Regula.Frauenfelder@ngi.no

^b BGC Engineering Inc., Ottawa ON, Canada – mlato@bgcengineering.ca

^c Avalanche Prevention Center, Dr. J. Gašperika 598, 033 01 Liptovský Hrádok, Slovakia – avalanches@hzs.sk

^d Institute for Environmental Studies, Charles University, Ovocný trh 3-5, 116 36 Praha 1, Czech Republic

KEY WORDS: Avalanche debris detection, Tatra Mountains, Slovakia, eCognition

ABSTRACT:

Here we present results from ongoing work where we apply an object oriented mapping algorithm developed in eCognition in order to automatically identify and digitally map avalanche deposits. The algorithm performance is compared with respect to a selected number of manually digitized avalanche outlines mapped by avalanche experts.

1. INTRODUCTION

1.1 The March 2009 avalanche cycle in the High Tatras

The Tatra Mountains, located in the border region between Slovakia and Poland, experienced several severe avalanche cycles during spring 2009. The peak was reached between March 25-31, 2009, when an estimated number of more than 200 avalanches were observed in the area of the Tatra national park on an area of approximately 738 km².



Figure 1: Avalanches in the Žiarska valley, photograph taken on April 1, 2009. Source: <http://hzzssp.blogspot.sk/2014/03/5-rokov-od-padu-storocnej-laviny-v.html?q=2009>

Avalanches were observed in almost every gully and on many slopes. They ranged in size from small to large (cf. Figure 1, 2), with the largest ones having a return period of approximately 100 year.



Figure 2: Avalanches in the area of the Belianske Tatry, photograph taken on April 1, 2009. Source: Slovakian Avalanche Prevention Center.

Several huts, bridges, two automatic weather stations and 1,000,000 m² of forest were destroyed. Some of the avalanches were mapped using field based GPS instruments by staff of the Slovakian Avalanche Prevention Center (APC). Yet, much of the affected area is remote and knowing exactly where avalanches had released was a challenge for the authorities.

Very High Resolution (VHR) satellite imagery was fast recognized as potentially being an important source of information to map avalanches which had released in more remote areas. Therefore, the APC acquired WorldView-1 imagery from April 2, 2009, covering parts of the Tatra

* Corresponding author

Mountains, in order to detect and map avalanches in regions that were inaccessible for the field teams.

1.2 Avalanche mapping techniques

1.2.1 Traditional methods: With few exceptions in densely studied areas (e.g., around avalanche research stations), snow avalanches are, in general, relatively poorly mapped. This is commonly due to the remote location of their occurrence. Often avalanches are only reported if they caused fatalities, led to an obstruction to public infrastructure, damage to personal property, or are witnessed and reported by local observers. However, decisions regarding, e.g., the closure of roads and the setting of warning levels, rely on information derived from knowledge of historic events in combination with meteorological data of the recent past and expected future.

The general practiced routine for mapping snow avalanches relies on two main techniques: a) the first technique involves a field mission to map the extent and location of avalanche start-zones and runout-zones by hand, by amateur photographs, or with a GPS device. Problems related to this method are poor accessibility of the terrain due to avalanche danger, that only small areas can be surveyed, and that surveys only can be conducted in good weather. b) The second commonly used technique for mapping snow avalanches is the visual analysis and digitising of aerial photographs or optical remote-sensing imagery (Scott, 2009). Both methods require expert involvement and visual identification of an occurred snow avalanche.

Identified and mapped avalanches are usually used to nourish avalanche data bases, also known as avalanche cadastres. A small section of an avalanche map based on data from the Slovakian avalanche cadastre (accessible online at <http://mapy.hiking.sk/>) is visualised in Figure 3. In this map, the length of the avalanche paths is the longest ever recorded in a given avalanche path.



Figure 3: Slovakian avalanche map, example from the Žiarska valley. Blue colour = slopes with an infrequent occurrence of avalanches; yellow = slopes with frequent occurrence of avalanches; red = slopes with very frequent occurrence of avalanches. Triangular shapes in orange, red and yellow within a given avalanche frequency zone mark avalanche paths with a higher frequency than the respective zone they are located in would indicate. (Map source: Copyright © HZS, hiking.sk, SHOcart)

Such maps are used to estimate regional susceptibility, to perform risk assessments and, eventually, to design hazards maps which directly link to policy making, i.e., to land use planning and land use regulations. More frequent information

on avalanche occurrences provides decision makers with knowledge of the frequency of avalanches as well as details regarding the size and extent of such events. It becomes, therewith, evident that the more and better observations that are available, the more reliable avalanche databases and avalanche maps can become.

1.2.2 Applying VHR optical imagery: The ability to automatically identify snow avalanches using VHR optical imagery greatly assists in the development of such accurate, spatially widespread, detailed maps and databases of areas historically prone to avalanches.

Recent developments in the field of imaging sensors and data processing techniques in the last two decades have resulted in the use of remotely sensed data for various and diverse applications for hazard mapping. Advancements in data collection techniques are producing imagery at previously unprecedented and unimaginable spatial, spectral, radiometric and temporal resolution. The advantages of using remotely sensed data vary by topic, but generally include safer evaluation of unstable and/or inaccessible regions, high spatial resolution, spatially continuous and multi-temporal mapping capabilities (change detection) and automated processing possibilities. Of course, as with every method, there are also disadvantages involved with the use of remotely sensed data. These are generally in relation to the lack of ground truth data available during an analysis and to data acquisition costs.

Recent publications in the literature on the use of optical remote sensing for hazard applications include, among others: landslide and rockfall evaluation (e.g., Mantovani et al., 1996; Rössner et al., 2005; Miller et al., 2012); flood mapping and modelling (e.g., Townsend and Walsh, 1998; Sanyal and Lu, 2004), glacier- and permafrost related hazard assessments (e.g., Kääh et al., 2005) and avalanche detection (Bühler et al., 2009; Lato et al., 2012). An extensive list of various satellite and airborne sensors with sufficient resolution for such analyses is given in, for example, Lato et al. (2012).

2. DATA AND RESULTS

The Slovakian Avalanche Prevention Center (APC) acquired WorldView-1 imagery from April 2, 2009, which covered large parts of the Tatra Mountains. While the eastern part of the imagery (Figure 4) was totally cloud-free, featuring a stunning quality, the western part was largely cloud-covered, thus, hampering its further use for avalanche detection, both for manual and automatic detection.

2.1 Algorithm training

The algorithm that we applied was originally designed to perform on data from a multi-band, 12-bit opto-electronic pushbroom scanner by Leica (ADS40-SH52; cf., Bühler et al., 2009) and on VHR optical imagery from the QuickBird satellite (cf., Lato et al., 2012). The algorithm was subsequently trained further on WorldView-1 imagery from Norway (not discussed here) and using the south-eastern third of the Slovakian imagery (marked with a blue rectangle in Figure 4).

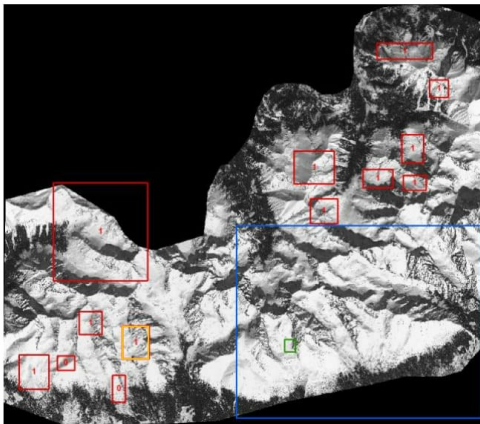


Figure 4: Eastern part of the WorldView-1 imagery from April 2, 2009. Blue rectangle = algorithm training area; green rectangle = location of example shown in Figure 5; red rectangles = randomly selected test areas for validation (0 = no avalanches present; 1 = avalanches present); orange rectangle = location of example shown in Figures 7, 8. (Satellite image: Copyright © DigitalGlobe/WorldView-1; courtesy of Slovakian Avalanche Prevention Center).

Even though the results of the first training runs looked seemingly satisfactory when just analysing a small portion of the imagery, the algorithm did not perform satisfactory on larger subsets of the data. On the one hand side the mapped avalanche debris was punctuated by small holes (i.e., errors of omission); at the same time many areas, especially wind-blown areas and rock outcrops, were falsely classified as avalanche debris (i.e., errors of commission).

Analysing the Slovakian imagery more closely, we observed a distinct "rake" pattern in many lower-lying areas of the imagery. We found that the rake pattern is more pronounced at lower altitudes, with the 1700 m a.s.l. contour line approximately delineating the height below which the problem starts occurring. The features showed to be the result of melting processes, caused either by a rain-on-snow event or even just by increasing air temperatures. Therefore we had to adapt the algorithm in order to eliminate these features prior to the actual avalanche debris mapping.

Figure 5 shows an example of the performance of the adapted algorithm enabling the differentiation between the "rake" pattern snow and avalanche debris.

For the time being, refinement of the algorithm based on training data is completed. Figure 6 shows an overview of the processing results for the entire training area.

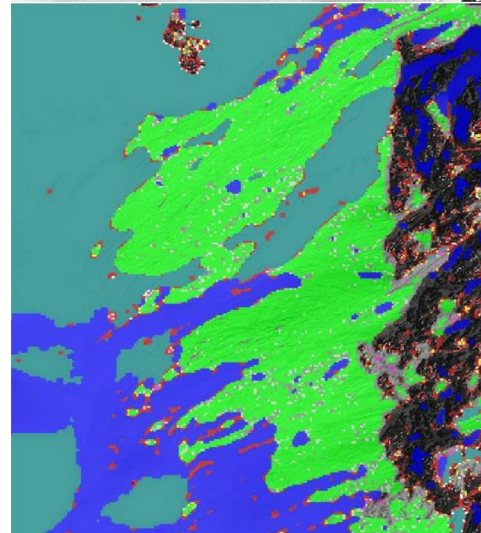
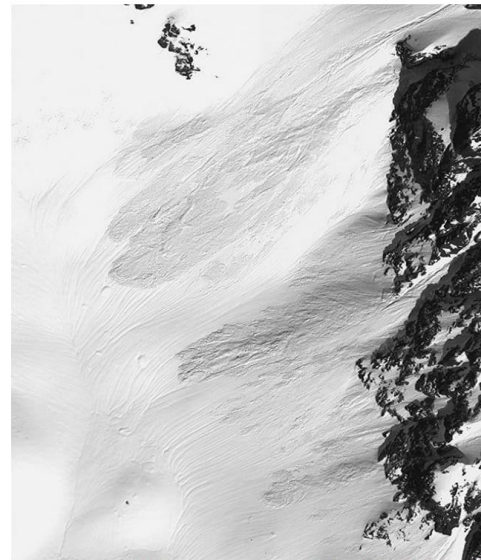


Figure 5: Classification result with the refined algorithm trained to differentiate the "rake" pattern from avalanche snow; the shown training section corresponds to the green rectangle in Figure 4. Top) raw image; bottom) automatic classification: green = avalanche debris; turquoise = glare and non-avalanche snow without rake pattern; blue = rake pattern; red = rock outcrops (Satellite image: Copyright © DigitalGlobe/WorldView-1).

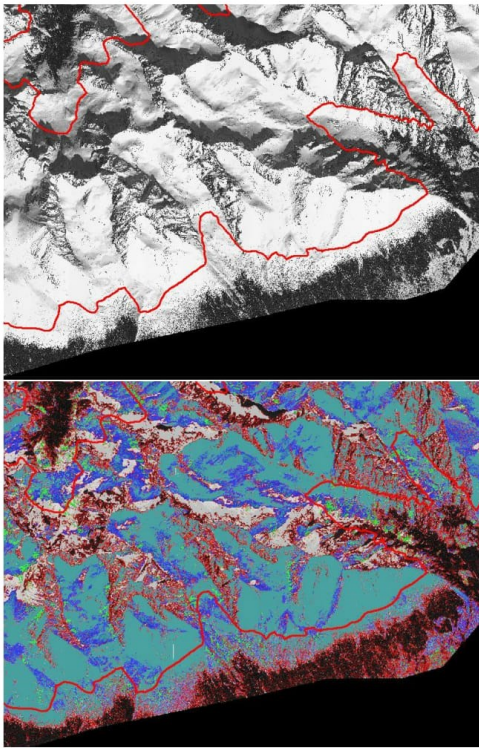


Figure 6: Automatic avalanche detection for the entire Slovakian training area. Top) raw image; bottom) green = avalanche debris; turquoise = glare and non-avalanche snow without rake pattern; blue = rake pattern; red = rock outcrops and forested areas; red line = 1700 m a.s.l. contour line which approximately delineates the height below which the "rake pattern" problem starts occurring in this data set. (Satellite image: Copyright © DigitalGlobe/WorldView-1).

2.2 Algorithm testing

Currently, we are testing and validating the trained algorithm in randomly selected test areas of the Slovakian data set (red rectangles in Figure 4). In order to quantitatively assess the performance of the algorithm, all avalanches in the test areas were visually identified and manually digitized by an avalanche expert. An example of the manually digitized avalanches is shown in Figure 7b.

A qualitative comparison between expert mapping and automatic classification by the algorithm seems to indicate that the algorithm struggles in areas with strong pixel saturation. This finding is not surprising as such, as this has already been reported by both Bühler et al. (2009) and Lato et al. (2012). However, oversaturation seems to be more of an issue in WorldView-1/2 imagery than in previously explored data sets such as QuickBird imagery and airborne pushbroom scanner data. Indeed, of recent WorldView-1 acquisitions over Norwegian terrain (not further discussed here), oversaturation was an issue in three out of four acquired data sets and one

recently acquired WorldView-2 data set was not analysable at all due to oversaturation over large and critical areas of the imagery.

It also has to be noted that the manual avalanche mapping was demanding, especially the delineation of the release areas of the point release avalanches (which account for a large proportion of the avalanches in the eastern part of the Slovakian imagery) and the mapping in shadow areas posed challenges. So in principle, neither the results by the human observer nor those by the algorithm give the entire "true" picture. But for the sake of a first evaluation of the algorithm performance, the human mapping was considered as representing the "true" situation.

The quantitative comparison of the algorithm performance with respect to the expert mapping shows a good overall performance with comparable rates of errors of omission and errors of commission if one takes the expert mapping as the "true" situation (Table 1; Figure 8). However, the processed test area is small and the overall algorithm performance on the WorldView-1 imagery can first be assessed when all the selected test areas have been processed.

Table 1. Accuracy (in percent) of the avalanche classification algorithm versus the manual digitizing method in one of the randomly selected test areas (orange rectangle in Figure 4).

Overall correct detection rate	84.2
- No avalanches (transparent areas in Fig. 8)	69.4
- Avalanches (blue areas in Fig. 8)	14.7
Omission error (red areas in Fig. 8)	7.3
Commission error (yellow areas in Fig. 8)	8.6

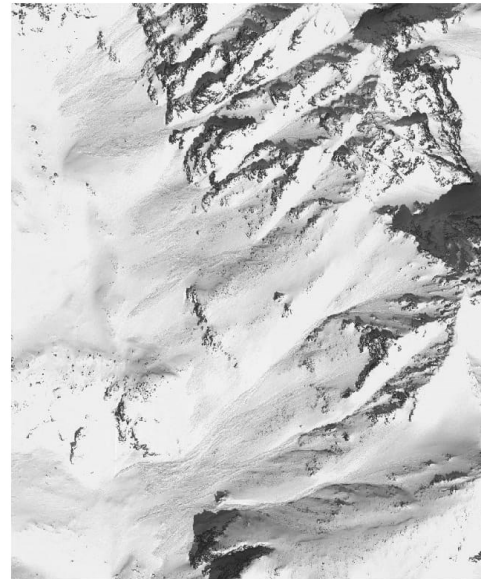


Figure 7a: Qualitative comparison between expert mapping and algorithm performance: Raw image. (Satellite image: Copyright © DigitalGlobe/WorldView-1)

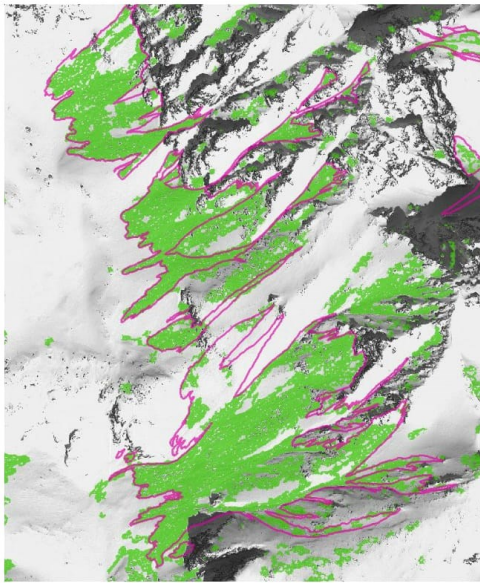


Figure 7b: Qualitative comparison between expert mapping and algorithm performance: manually digitized avalanche outlines (in pink) superimposed on the automatically classified avalanches (in green). (Satellite image: Copyright © DigitalGlobe/WorldView-1)

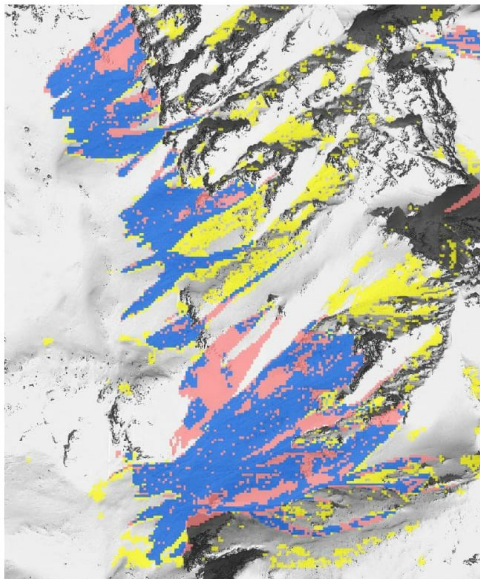


Figure 8: Quantitative comparison between expert mapping and algorithm performance. Blue = mapped as avalanche snow by both methods; red = only mapped as avalanche snow by manual method; yellow = only mapped as avalanche snow by algorithm. (Satellite image: Copyright © DigitalGlobe/WorldView-1).

3. CONCLUSIONS

We presented results of avalanche debris detection by an automatic detection algorithm implemented within eCognition.

The method described and illustrated above is flexible and easily adaptable to different sensors and image quality, however it requires further testing and validation before, e.g., implementation in an operational setting is possible.

ACKNOWLEDGEMENTS

This contribution was partly funded by the ESA PRODEX project ASAM ("Towards an automated snow property and avalanche mapping system"; contract no. 4000107724). The satellite image from the Tatra Mountains was obtained with the support of the Slovakian Ministry of Interior, Department of Scientific and Technological Development. Kristine Ekseth (NGI) is acknowledged for her help during an early phase of the algorithm training and Galina Ragulina (NGI) for her meticulous manual mapping of the numerous avalanches in the presented data set.

REFERENCES

- Bühler, Y., Hüni, A., Christen, M., Meister, R., Kellenberger, T. 2009. Automated detection and mapping of avalanche deposits using airborne optical remote sensing data. *Cold Reg. Sci. Technol.*, 57, 99–106.
- Kääb, A., Huggel, C., Fischer, L., Guex, S., Paul, F., Roer, I., Salzmann, N., Schlaefli, S., Schmutz, K., Schneider, D., Strozzi, T., Weidmann, Y. 2005. Remote sensing of glacier- and permafrost-related hazards in high mountains: an overview. *Nat. Hazards Earth Syst. Sci.*, 5, 527–554, doi:10.5194/nhess-5-527-2005.
- Lato, M., Frauenfelder, R., Bühler, Y. 2012. Automated detection of snow avalanche deposits: segmentation and classification of optical remote sensing imagery. *Nat. Haz. And Earth. Syst. Sci.*, 12, 2893–2906. doi:10.5194/nhess-12-2893-2012.
- Mantovani, R., Soeters, R., van Western, C. J. 1996. Remote sensing techniques for landslide studies and hazard zonation in Europe. *Geomorphology*, 15, 213–225.
- Miller, P.E., Mills, J.P., Barr, S.L., Birkinshaw, S.J., Hardy, A.J., Parkin, G., Hall, S.J. 2012. A Remote Sensing Approach for Landslide Hazard Assessment on Engineered Slopes. *Geoscience and Remote Sensing, IEEE Transactions*, 50(4), pp. 1048, 1056, doi: 10.1109/TGRS.2011.2165547.
- Roessner, R., Wetzel, H.-U., Kaufmann, H., Sarnagoev, A. 2005. Potential of Satellite Remote Sensing and GIS for Landslide Hazard Assessment in Southern Kyrgyzstan (Central Asia). *Natural Hazards*, 35(3), 395–416.
- Sanyal, J., Lu, X.X. 2004. Application of Remote Sensing in Flood Management with Special Reference to Monsoon Asia: A Review. *Natural Hazards*, 33(2), pp. 283–301.
- Townsend, P.A., Walsh, S.J. 1998. Modeling floodplain inundation using an integrated GIS with radar and optical remote sensing. *Geomorphology*, 21(3–4), pp. 295–312.

Publication 5

Publication 5: Richnavský, J., **Biskupič, M.**, Mudroň, I., Devečka, B., Unucka, J., Chrustek, P., Lizuch, M., Kyzek, F., Matějček, L., 2011, Using Modern GIS Tools to reconstruct the avalanche: A case study of Magurka 1970. GIS Ostrava 2011 Proceedings p. 175 - 185. (reviewed)

USING MODERN GIS TOOLS TO RECONSTRUCT THE AVALANCHE: A CASE STUDY OF MAGURKA 1970

Jozef, RICHTAVSKÝ¹, Marek, BISKUPIČ², Ivan, MUDROŇ¹, Branislav, DEVEČKA¹, Jan,
UNUCKA¹, Pawel, CHRUSTEK⁴, Milan, LIZUCH³, Filip, KYZEK³, Luboš, MATĚJÍČEK²

¹Institute of Geoinformatics, Faculty of Mining and Geology, VŠB – Technical University of Ostrava, 17.
listopadu 15, 708 00, Ostrava Poruba, Czech Republic
jozef.richnavsky@vsb.cz, ivan.mudron@vsb.cz, branislav.devecka@vsb.cz, jan.unucka@vsb.cz

²Institute of Environmental studies, Faculty of Science, Charles University in Prague, Benátská 2,
12801, Praha 2, Czech republic
mabis@seznam.cz, lubos.matejcek@gmail.com

³Avalanche Prevention Centre of Mountain Rescue Service, Jasná 84, 032 51 Demänovská dolina, Slovak
Republic
slp@hzs.sk

⁴Institute of Geography and Spatial Management, Faculty of Biology and Earth Sciences, Jagiellonian
University, Gronostajowa 7, 30-387, Cracow, Poland
p.chrustek@annapasek.org

Abstract

A huge avalanche released on 14 March 1970 from the saddleback of Ďurková below the Low Tatras mountain ridge, which ran down through the whole valley and stopped close to the settlement of Magurka. The length and height of the avalanche path was enormous reaching 2,2 km and 22 meters high respectively. Taking other parameters into consideration (the length of the avalanche, the height of the avalanche release zone, total volume of snow) it can be categorised among the greatest avalanches ever observed in Slovakia. The major causes for such a big avalanche were unfavourable long-lasting snow and weather conditions. However, the starting mechanism was, as in most cases, a man. RAMMS model was used for avalanche reconstruction. It allows modelling the height of avalanche deposition, the speed of an avalanche flow and also the maximum pressure that was reached. All the required input data were derived from historical information, photographs and maps and also from the statements of the witnesses of this avalanche event. The avalanche has been successfully simulated and reconstructed. The total volume of deposited snow (relative deviation 0.16%) revealed that the simulated released area and other input parameters were precisely approximated. Small deviation between simulated and measured avalanche runout zone refers to good calibration of friction parameters. The result of the modelling will enable us a better understanding of the complete progress and action of this avalanche during its motion. The results can be also applied to planning and constructing of anti-avalanche structures and to minimizing the negative consequences of similar avalanche in the future.

Keywords: avalanche, modelling, reconstruction, Magurka, runout zone

INTRODUCTION

For centuries, people have been altering the Earth's surface to produce food and gain material or energy through various activities. The urban areas are being enlarging backcountry skiing areas spreading fast etc. Over the last years, more people are coming to the mountains, building new cottages and cabins underneath, spending more time in the countryside. Magurka surroundings are no exceptions. The mountains are becoming overcrowded and the fact that people are dramatically enhancing the avalanche risk is well known. This was also the case of the Magurka 1970 tragedy, when four skiers triggered the avalanche. Three of them died. To avoid the risk of tragedies in the mountains of Slovakia, it is important to undertake more studies involving GIS. This paper deals with avalanche reconstruction applying the avalanche dynamics program RAMMS. Modern numerical simulation tools are frequently used for avalanche prevention in USA, Canada and some alp countries, especially in Switzerland and Austria. On the other side, in Slovak Republic as well as in Czech Republic, these tools have not been used yet. The aim of the paper is

to show that this historical process can be reconstructed with modern technologies and give some useful information, which can be used nowadays

DESCRIPTION OF AVALANCHE EVENT

Weather conditions were good on March 14, 1970. Four skiers came to the saddleback of Ďurková passing the main ridge from Chopok. One of them was slightly injured, so they decided to go down all the way to Magurka settlement. They started to traverse to the right crest, and so releasing one of the greatest avalanches in Slovak history. The total amount of deposited snow was 65 000 m³, i.e. about 200,160 tons of snow. This snow deposition was stretching over 1.8 km and the front was from 20 to 25 m high. This mass of snow did not melt the following summer. The avalanche was 2.2 km long and was extending on the total area of 35.8 ha. The release area was 340 metres wide and the vertical drop between the top of the release and avalanche front was 620 m. The released snow layer varied from 1.8 metres on side ridges to 12 metres in gullies. In this mass of snow the rescue team (517 rescuers) could not find the victims for 26 days. The last victim's body was found on 6 June.

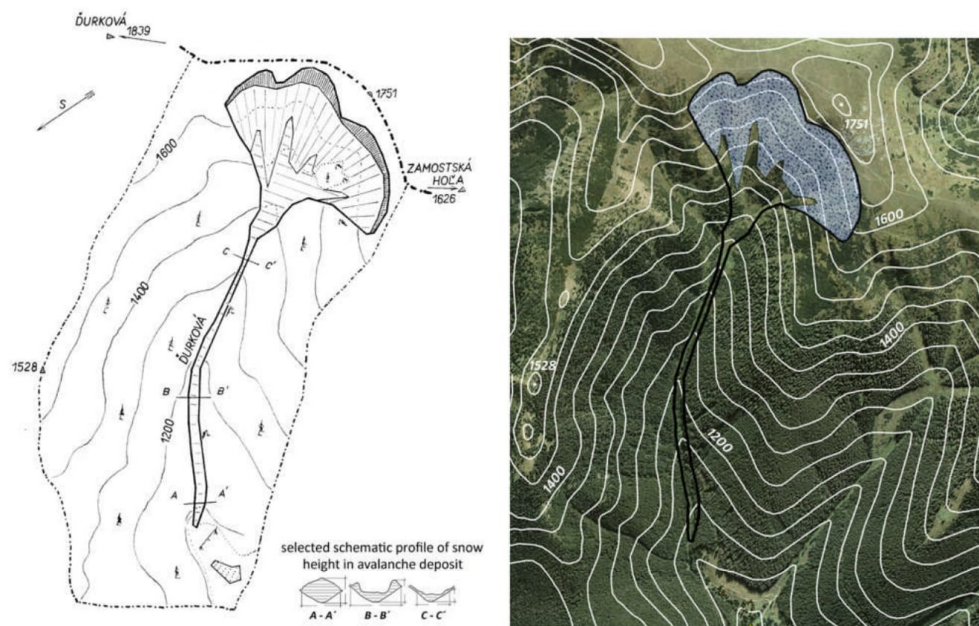


Fig. 1. Schematic location outline and its presentation in ArcMap software

AVALANCHE SIMULATION

Modern numerical simulation software package RAMMS was used for avalanche simulation. RAMMS (*Rapid Mass MovementS*) model calculates the motion of geophysical mass movements (including snow avalanches) from initiation to runout in three-dimensional terrain (Christen, 2010). It has been developed at the WSL Institute for Snow and Avalanche Research SLF in Davos. Model RAMMS can be used for accurate prediction of avalanche runout distances, flow velocities and impact pressures of avalanches. For this case of study, we have used this model for calculating the snow height in avalanche deposition and for understanding the avalanche motion. Input data were gained from historical records, studies and photos. The same data were used also for calibrating the model (calibration of friction parameters) to obtain sufficiently accurate simulation. Required input data for model RAMMS are mentioned below. Well prepared data are essential for the quality of the model results.

Release zone

Sufficiently precise reconstruction of avalanche release's parameters has the biggest influence on exactness of simulated result. The characteristics of release determine directly the volume of avalanche snow mass. They determine the velocity of avalanche and the kinetic energy of avalanche together with the influence of terrain attributes. Hence, the reconstructed allocation of release, its shape and length of the avalanche has to be done correctly not to derive incorrect inputs. The reconstruction was deduced from schematic location outline, historical records and pictures. The main attributes of avalanche release are mentioned in Table 1. The maximum of 12 m height release were recorded in the channel due the weather conditions. Snow accumulation is taking place, especially in channels or smaller gullies under the main range. So, 12 m height is not a rare value. According to the attributes, primarily to the length, it is one of the largest avalanches observed in Slovakia. Fig. 1. shows the location outline of avalanche area, which was geotransformed and subsequently vectorised in ArcMap.

Table 1. Basic parameters of avalanche release

length of fracture line	maximal snow height	minimal snow height
1500 m	12 m	1.8 m

One of the fundamental problems in avalanche modelling is an accurate definition of release zones. It is very difficult to define release areas with responsible release heights in three-dimensional terrain. In avalanche modelling, it is common to set one release height for whole release area because of ease, simplicity and rate of calculation. In this case we have tried to simulate and reconstruct historical avalanche with big span of threshold release heights (1.8 m – 12 m). With consideration to the biggest approximation to the reality, our approach the release area was to divide it into few smaller areas with different release heights.

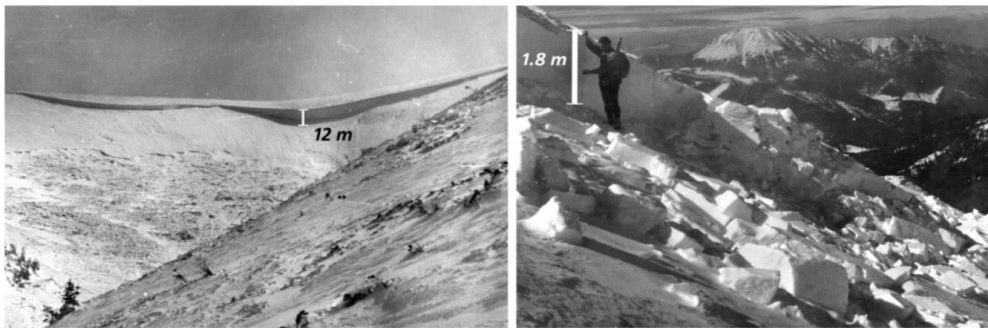


Fig. 2. Big differences in release snow height in range 1.8 up to 12 m

Terrain parameters

A terrain is considered to be a permanent, stationary factor in avalanche forecasting. So, we can use present terrain parameters also for simulation of historical avalanche events. We do not assume that there were some considerable changes in terrain proportions between years 1970 and 2010. We used digital elevation model of the study area for simulation in model RAMMS. It was derived from contours in a basic topographic map of research area with scale 1:10 000. Spatial resolution of DEM was set to 2 m (this is the value recommended for detailed avalanche simulation in RAMMS). This is accurate enough for including small terrain features, like big boulders, gullies, needles and depressions into the simulation. A good digital representation of the topography is crucial for the accuracy of the model results, especially in sensitive

areas, such as small gullies and mountain ridges (Haeberli, 2004). In this case, interpolation method Topo to Raster in ArcMap software was used to determine the digital terrain model of study area.

Forest cover

The forest cover significantly inhibits or even stops avalanche flow. Thus, it significantly influences avalanche flow direction, flow velocity, and subsequently also the resulting shape of an avalanche path. To reach the most precise reconstruction of the avalanche, impact of the given forest cover was also needed to be included into the simulation. But, when the impact pressure of avalanche is more than about 100 kPa (threshold value for uproot mature spruce), inhibiting effect of the forest cover become insignificant. Large avalanches often break trees and develop into a mixed flow of snow and trees, creating greater mass with increasing damage potential. As we wanted to include information about the forest cover into the simulation, we needed to obtain this information from the date before March 1970. For this purpose the basic topographic map from the year 1956 was used. The comparison between the forest cover before simulated avalanche and the present state of the forest cover is shown in Fig. 3. Forty years are quite a long term and differences in the forest cover are significant. Therefore it is so important to use adequate information about the forest cover for avalanche modelling. Other important factors related with the forest cover (cover density, height of trees, species diversity) have influence, but the forest occurrence is sufficient for precise modelling results using model RAMMS (boolean raster layer: 0 for no forest, 1 for forest areas).

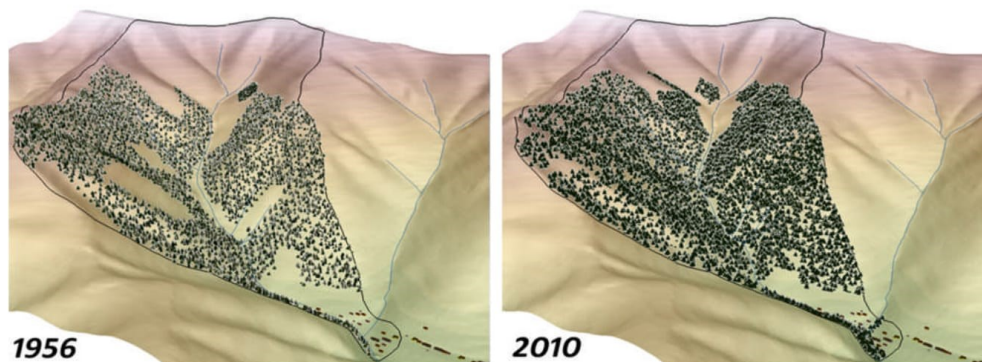


Fig. 3. Differences in forest cover in years 1956 and 2010

Inhibiting and obstacle effect of dwarf pine was not considered into this calculation due to extensive height of snowpack. The dwarf pine cover influences avalanche formation only in case, when the height of the snowpack is smaller than the height of the dwarf pine cover.

Snow density of release area

The density of released snow is another important factor linked with avalanche modelling and with model RAMMS. There are no precise measurements of snow density in historical records. However, it can be assumed that reconstructed avalanche was a hard dry slab avalanche. This precondition was derived on the grounds of historical photos (Fig. 4). A hard slab usually has large chunks of debris in the deposit. They are evidently recognized on these photos. A sharp bounded breakaway wall of top periphery of the slab is another characteristic feature for dry slab avalanches. It is also visible on these figures. Large amount of snow in gullies is the result of snow transporting due to blowing wind. Wind packing can produce dense, cohesive snow, which aids in slab formation (McLung & Schaerer, 2006). These slabs are usually very brittle with low cohesion with the snow layer beneath. Generally speaking, most slabs consist of cohesive wind-deposited or well-bonded old snow. Average density for such snow is about 200 kg/m^3 with the range of 50 to 450 kg/m^3 (McLung & Schaerer, 2006). From the sample on Fig. 4., nearly 90% of these avalanches have average densities between 100 and 300 kg/m^3 . Densities below and above this range are rare. The value 200 kg/m^3 was set as the best estimation and was used in the avalanche simulation in model RAMMS. Dry

slabs are responsible for most of the damage and fatalities from avalanches. According to world injury statistics, 90 % of these slab avalanches were triggered by mountain visitors themselves.

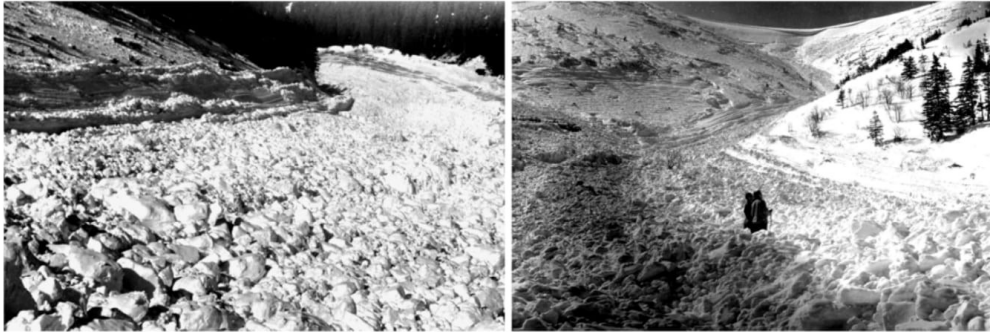


Fig. 4. Large chunks of debris in the deposit, typically for dry slab avalanches

SIMULATION ACCURACY

Simulation accuracy is given by comparison of the simulated results with the real measured data obtained by the field research in 1970. The differences between the simulated results and the measured values are shown in the Table 2. It is necessary to mention that the precise measurement of parameters (volume, area) in 1970 was difficult. Still, it is impossible today to make precise measurements of such a big avalanche without using GIS technologies (LIDAR, modelling, etc.). Due to proper calibration method close approximation of real measured avalanche runout zone (Fig. 5.) was reached. The deviation from the real measured runout zone was statistically insignificant as well as the deviation of total avalanche volume. In spite of this, the height of avalanche front was not successfully restored (Fig. 6.). The real height of avalanche front exceeds simulated value considerably. The difference in the total avalanche area is observed mainly on the upper right part of the slope. This is due to inaccuracies in DEM representation and in localization of release area. Comparisons of all simulated results with real measured data are shown in Table 2. The relative deviation from the measured data was calculated as the ratio of difference to the measured value in 1970. The value of total area was set to recalculated data from 1970 using GIT (39.1 ha). Sequences of avalanche simulation in different computing time steps are shown in Fig. 7. A single sequence is showing the maximum height of moving snow. Profile B (Fig. 5.) is revealing a significant unevenness in the deposit surface. It was testified by eyewitnesses and historical photos.

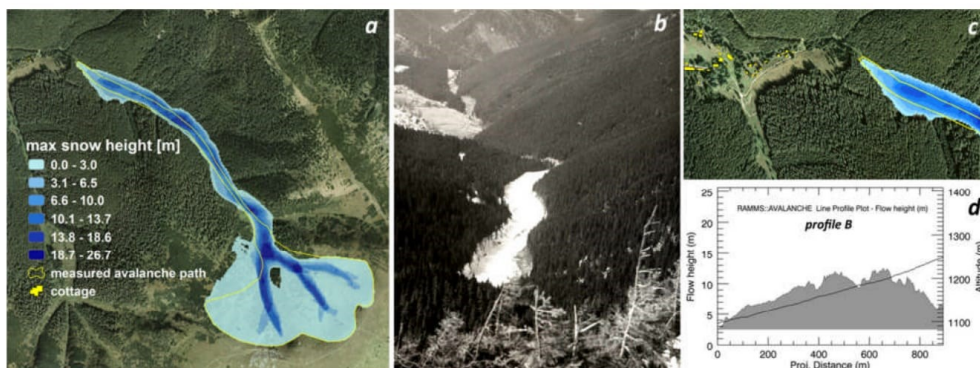


Fig. 5. Maximal snow height from avalanche simulation (a) and comparison of its runout zone with real measured data (c). Simulated snow height in longitudinal profile of avalanche deposit (d), which is captured in the historical photo (b)

Table 2. Comparison of the simulated results with real measured data

Parameter name	Measured 1970	Simulated 2010	Difference	Relative deviation
Avalanche length	2 200 m	2 221 m	21 m	0.95 %
Snow deposition length	1 800 m	1 725 m	75 m	4.17%
Snow deposition volume	625 000 m ³	626 028.7 m ³	1028.7 m ³	0.16 %
Front height	20 – 25 m	4 – 5 m	16 – 20 m	80.00%
Total area	35.8 ha (39.1 ha)	51.38 ha	12.28 ha	31.41 %
Vertical drop	620 m	622 m	2 m	0.32 %

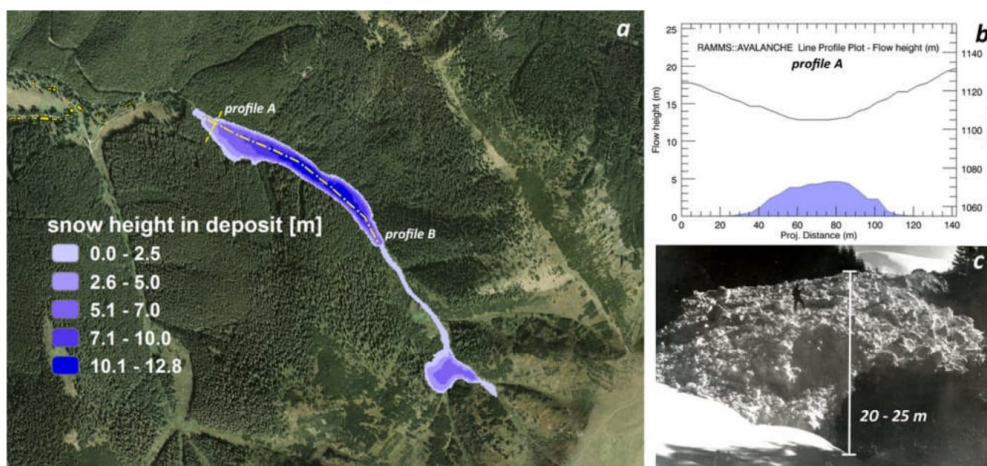


Fig. 6. Snow height in avalanche deposit and lines of cross and longitudinal profiles A and B (a). Real snow height of avalanche front (c) exceeds simulated value in profile A (b) considerably

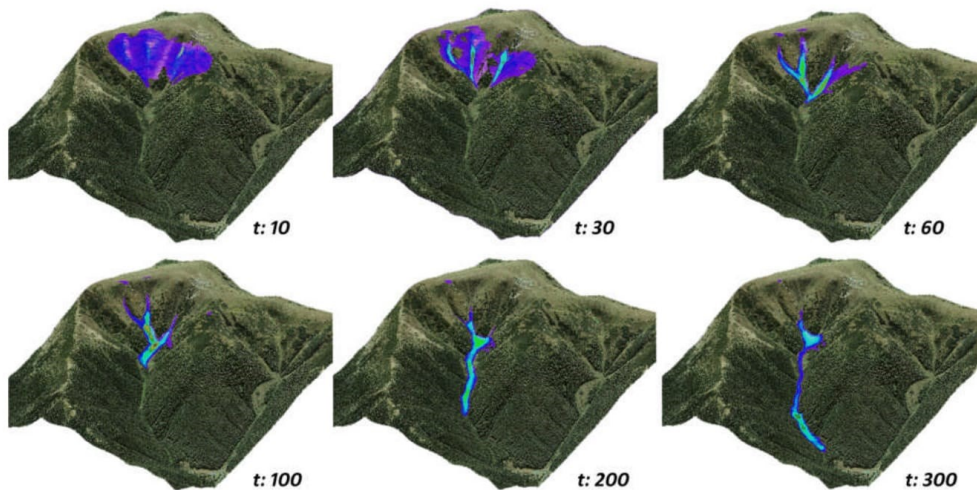


Fig. 7. Sequences of simulation in different time steps of calculation (t: 10 – t: 300)

RESULTS APPLICATIONS

One way of simulation results applications is determining established calibration friction coefficients (μ , X_i). These friction coefficients determine the surface friction in different heights. Coefficients, which were determined and used in one valley, can also be used in avalanche simulations in the adjacent valleys. There is a big probability that surface resistance to the avalanche flow will be similar in adjacent valleys as well. This piece of knowledge was used for modelling potential avalanche events in the valley of Viedenka, which is situated to the west of Ďurková valley. In contrast with the reconstructed avalanche in the Ďurková valley, similarly great avalanche in the valley of Viedenka will affect significantly the urban space of Magurka settlement. Many cottages in this settlement will be damaged or ruined as a consequence of destructive power of a similar avalanche. In this locality, some experimental simulations were calculated with different heights of potential release zones. Fig. 8. shows results of particular cases of these simulations. It is obvious that a fracture height more than 2 m causes a significant spreading of the runout and more cabins are endangered.

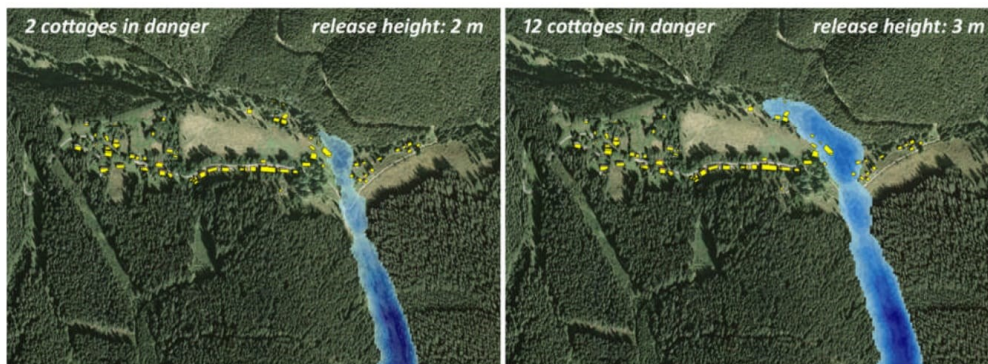


Fig. 8. Comparison of conclusions from potential avalanche with different release heights

We have alluded to prevention until now. Now, we turn to the usage of avalanche reconstruction when endangered areas are revealed. In practice, there are cases, when infrastructure, important facilities or parts of urban sprawl are a part of an endangered area. Model RAMMS can be a useful tool for designing and allocating anti-avalanche barriers, such as an avalanche dam. Parameters of these dams can be included into the digital representation of topology. Avalanche simulation can be undertaken in different scenarios with or without these barriers. A well-placed and designed avalanche dam manages to stop or divert the direction of the potential avalanche flow in order to protect the lower situated infrastructure. For facilities placed in avalanche path, it is the only way of protection.

CONCLUSION

The introduction of GIS technology opened up new perspectives to mapping and assessing hazards from snow avalanches. The purpose of mapping snow avalanche hazards is to consider avalanche risks with respect to land use planning (Haeberli, 2004). Numerical models (like RAMMS), coupled with field observations and historical records are especially helpful in understanding avalanche flow in complex terrain (Christen et al., 2008). They are very helpful in avalanche research in the given region. Simulations, like this in this case of study, are useful in understanding of all processes and actions, which are connected with avalanche. The avalanche modelling is particularly important and applicable in the avalanche protection. The results can be applied to planning and constructing of anti-avalanche structures and in this way they can minimize the negative results of a similarly destructive avalanche in the future. It is obvious that the simulated result differs from the phenomenon measured in 1970, although the deviation is not serious. The most important attribute for the avalanche hazard mapping is the length of the avalanche, which was successfully modelled. There are more reasons why differences in other attributes appeared. First of all, we

have to mention that RAMMS simulation result is a model, which cannot include whole complex reality. The next reason is the input data; especially, the digital elevation model uncertainties leading to greater divergence. There will never be a model as same as the true state of nature. It is impossible to include every small bush, the precise distances between the trees etc. in the forest cover, or include every small depression in the valley, which is filled by additional snow. Next is the fundamental modelling problem such as definition of release areas in three-dimensional terrain. The difficult estimation of snow entrainment, which greatly affects overall snow mass, contributes too. One of the other drawbacks is the estimation of the height of stauwall and the other heights (volume) of released snow. Just because of these drawbacks, it is impossible to make a perfect fit. There are much more reasons, which influence the result e.g. the historical documents (sketches, sampling etc.) were made in the era, when no computers and other advanced tools could help. Despite all these reasons, modern GIS numerical tools are able to truly reconstruct an avalanche event and this research was a good demonstration of it.

ACKNOWLEDGEMENTS

We would like to acknowledge the SGS project SV5480051/2101 from VSB TU-Ostrava. Special acknowledge belongs also to the Avalanche Prevention Centre of Mountain Rescue Service in Jasná and to Mr. Ladislav Milan for provision of historical photos and records of this avalanche event.

REFERENCES

Gruber, U. (2001) Using GIS for avalanche hazard mapping in Switzerland. Proceedings of the 2001 ESRI International User Conference, San Diego, s. 21.

Haeberli, W., et al. (2004): GIS applications for snow and ice high-mountains areas: Examples for the Swiss Alps in Geographic Information Science and Mountain Geomorphology. Chichester, UK, pp. 381 - 402

Christen, M, et al. (2010) RAMMS User manual v 1.01 : A modeling system for snow-avalanches in research and practice. Davos, Švajčiarsko.

Christen, M, et al. (2010) Back calculation of the In den Arelen avalanche with RAMMS: interpretation of model result. In Annals of Glaciology, vol. 52 issue 54, International Glaciological Society. 161 – 168.

Christen, M, et al. (2008) Calculation of dense snow avalanches in three-dimensional terrain with the numerical simulation program RAMMS. In International Snow Science Workshop. Whistler, BC, CAN, pp. 192 - 211.

McLung, D; Schaerer, P. (2006) Avalanche Handbook. The mountaineers book, Seattle, USA.

Publication 6

Biskupič, M., Richnavský J., Lizuch M., Kyzek, K., Žiak I., Chrustek, P., Procter, E., 2012, Three different shapes of avalanche balloons a pilot study, International Snow Science Workshop, Proceedings, 482-487.

THREE DIFFERENT SHAPES OF AVALANCHE BALLOONS – A PILOT STUDY

Marek Biskupič^{1,2*}, Jozef Richnavský¹, Milan Lizuch¹, Filip Kyzek¹, Igor Žiak¹, Pawel Chrustek³, Emily Procter⁴

¹Avalanche Prevention Center, Demänovská Dolina, Slovakia

²Faculty of Science, Charles University, Prague, Czech Republic

³Anna Pasek Foundation, Cracow, Poland

⁴EURAC Institute of Mountain Emergency Medicine, Bolzano, Italy

ABSTRACT: Flotation devices are more and more frequently used. Their efficacy has already been demonstrated by field tests (Tschirky and Schweizer 1996; Kern et al. 2002; Meier and Harvey 2010) and retrospective studies (Tschirky et al. 2000; Brugger and Falk 2002; Brugger et al. 2007).

There are several systems on the market that differ in release mechanism and balloon shape. In general three different balloons shapes exist. In the winter season of 2011/2012 a pilot study of three differently shaped floatation devices was made for the first time. The aim of this study was to investigate the behavior of each inflated system during an avalanche event. Three human-weighted dummies were positioned on the slope and an avalanche was triggered with explosives. Several video cameras, installed on and beside the avalanche path, recorded the movement and final deposition of the dummies. The track of each dummy was measured with high accuracy GPS (<1m) and avalanche flow properties (flow height, velocity and pressure) were simulated with the Rapid Mass Movements (RAMMS) tool. The video material together with the GPS measurements and numerical simulation was used to analyze the behavior of different floatation systems. The burial grade differed for each dummy and none of them were completely or partially-critically buried. From this pilot study we cannot draw conclusions about the efficacy of the different shapes; further tests are needed for an in-depth comparison of the devices.

KEYWORDS: Avalanche balloon packs, avalanche airbags, field trial

1. BACKGROUND

The purpose of an avalanche airbag is to prevent complete burial. Currently, there are three different shapes of avalanche balloons produced by four manufacturers. One system uses a dual bag (ABS), the three other systems are mono bags (Mammut/Snowpulse, BCA, Warry). The packs differ in shape and place from which they inflate. The avalanche balloon packs have been previously tested using dummies in various conditions. Past field trials used:

- (i) ABS mono airbags (Tschirky and Schweizer 1996),
- (ii) ABS mono airbags, ABS dual airbags and Avagear collar mono type airbag vest (Kern et al. 2002)
- (iii) ABS dual airbags and Snowpulse collar type mono airbags (Meier and Harvey 2010).

* Corresponding author address:

Marek Biskupič, Avalanche Prevention Center,
dom HS č.84, 032 51 Demänovská Dolina Slovakia
tel: 00421 903 624 664
fax: 00421 44 5591 637; email: avalanches@hzs.sk

The volume of the chambers for dual bags is approx. 170 L and for mono bags approx. 150 L.

So far there has been no field trial using all three balloon shapes mentioned. The aim of the field test was to observe how the differently shaped avalanche airbags behave in an avalanche with specific attention on the grade of burial.

2. METHODS & TEST SITE INSTRUMENTATION

The three following packs were chosen because each of them differs in shape of the balloon(s).

Snowpuls/Mammut Lifebag is a collar type mono balloon backpack. When the pack is inflated, it creates a balloon around the backside of the neck and shoulders. The aim of this system is to prevent burial and simultaneously provide trauma protection for the head and neck.

Backcountry Access (BCA) Float is also a mono balloon pack with the balloon positioned behind

the head. Besides preventing burial it provides some trauma protection for the head and neck.

The only dual airbag system tested was the ABS Vario. The system consists of two balloons located at the side of the backpack. Both airbags have an overall volume of 170 L (2x85 L) (www.abs-airbag.de).

The field test took part in Jasna, Slovakia, where numerous easily approachable gullies and couloirs can be found.

The test site was instrumented with 3 crash test dummies with a weight of 80 kg. The joints were adjusted to simulate the flexibility of real humans. The dummies were positioned by a ropeway system in a northeast orientated slope, 40 m below the snow cornice. Each dummy was instrumented with an avalanche balloon pack and they were placed side by side in one line. One dummy was equipped with the Snowpulse/Mammut Lifebag Guide 30 L backpack, one with BCA Float 18 L and one with ABS Vario 25 L. All three backpacks were deployed 60 seconds prior to the avalanche release.

The upper part of the avalanche path had an inclination of 37°. The release area was a snow cornice with a height ranging from 0.5 m to 3 m. The track was open and the run-out was smooth with no depression or terrain traps.

The position of the dummies was measured with high accuracy GPS (<1m) before and after the avalanche. Several cameras and point of view cameras were placed either in the track or across the track to shoot the movement of the dummies. Photographers were situated along the track to document the trial.

3. RESULTS

The explosion released the cornice and initiated an avalanche of size 2 (US avalanche size classification). Additional snow masses were entrained in the main flow and formed a decent avalanche. The turbulent front hit the dummies after 4 seconds after release. The first dummy that was hit was wearing the BCA Float backpack and the other dummies were hit 0.25 s thereafter. Immediately all the dummies disappeared in the snow mass and were rotated and twisted, falling over the small cliff. A moment later all dummies were visible and floating on the avalanche surface. When the avalanche slowed down and snow

deposition started, the dummies were segregated aside from the main flow.

The dummy equipped with the BCA Float stopped first and within a few seconds the dummy with the ABS and Snowpulse/Mammut Lifebag stopped also (Figure 1).



Figure 1. Position of the dummies after the avalanche stopped.

3.1. *Assessing the avalanche burial*

The grade of burial was classified according to Observational Guidelines for Avalanche Programs in the United States (Greene et al. 2010).

The dummy with the Snowpulse/Mammut Lifebag was dragged by the avalanche for 132 m in 20 s. The average speed was 6.6 ms^{-1} (23.76 kmh^{-1}) while it reached a maximum speed of 17.8 ms^{-1} (64.08 kmh^{-1}). Acceleration occurred over 89m with an average velocity of 3.56 ms^{-2} . When the avalanche stopped moving, this dummy was buried from the hips down (Figure 2). The lower part of the body was anchored in the snow deposit and the whole body was partially buried in a tilted position. This was a partial-not critical burial, the airways were not obstructed and the head was not impaired by the snow. The balloon was clearly visible on the avalanche surface.



Figure 2. Burial position of the dummy wearing the Snowpulse/Mammut Lifebag.

The dummy equipped with ABS Vario system was carried over 123 m in 18 s. The maximum velocity reached by this dummy was 18.6 ms^{-1} (66.96 kmh^{-1}) while the average speed was 6.9 ms^{-1} (24.84 kmh^{-1}). The avalanche reached the highest speed at 9 s. At 9 s the dummy had been carried 93 meters from its starting point, reaching an acceleration of 3.36 ms^{-2} . The dummy was deposited in a horizontal face-up position lying on its back with the head pointing down the slope. There was a block of snow (approximate diameter 70 cm) lying on its abdomen and additional snow laterally. The grade of burial was between partially buried and not buried. It is questionable if a human being would be capable of freeing himself in this position without additional help from companions. Important is that the airways were not obstructed and the head was not impaired with snow. One leg was visible and the balloons were clearly visible as well (Figure 3).



Figure 3. Burial position of the dummy with the ABS backpack.

The dummy wearing the BCA Float balloon was carried along the shortest distance of 114m with an average velocity of 8.1 ms^{-1} (29.16 kmh^{-1}). The dummy reached a maximum speed of 16.8 ms^{-1} (60.48 kmh^{-1}) with an acceleration of 3.72 ms^{-2} after 84 m. From this moment the dummy started to decelerate until the point of stopping in a supine

position (Figure 4). The head and the airways were free of snow except and only a few small snow chunks were deposited on the trunk. Probably a human could free himself with no additional help. Based on this the burial was classified as no burial. The surrounding chunks of snow left the airways unobstructed and the head was not impaired by the snow. Both legs and one arm were sticking out from the deposited snow. The balloon was clearly visible on the snow surface.



Figure 4. Burial position of the dummy with the BCA backpack.

The grade of burial was different for each dummy. The dummy which travelled furthest was the most seriously buried and the one with the shortest path had the least serious grade of burial. This was due to the fact that the dummy with the Snowpulse/Mammut Lifebag was transported closer to the main flow and therefore closer to the front of deposition zone than the others. The dummies stopped within 88 m to 116m of the deposition front (BCA Float 116 m, ABS Vario 96 m and Snowpulse/Mammut Lifebag 88 m).

The extremities of the dummies were twisted and positioned in unnatural positions. In the case of real human beings, they would probably have suffered injuries. On the other hand, no dummy accurately represents a real human example in an avalanche and humans may, for example, try to actively escape from the main flow. The short trailer from the field test can be found on: <http://www.youtube.com/lavinyH2S>.

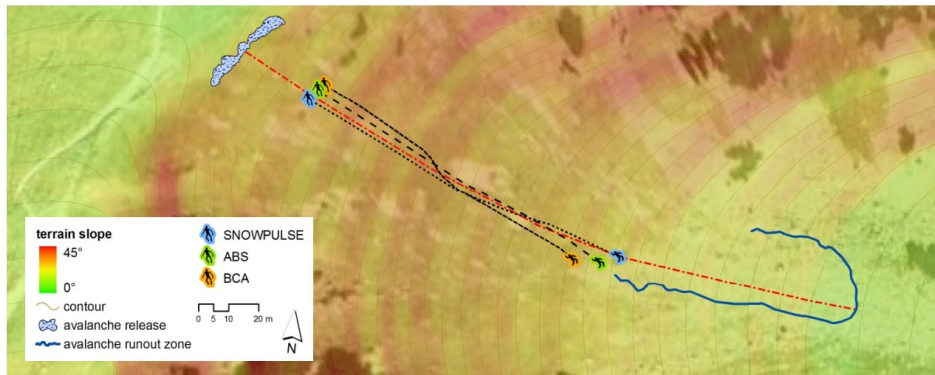


Figure 5. Tracks of the avalanche and dummies.

Dummy equipped with:	Movement duration	Track	Average speed	Max. speed	Acceleration	Grade of burial
BCA Float 18L	14 s	114 m	8.1 ms ⁻¹	16.8 ms ⁻¹	3.72ms ⁻²	not buried
ABS Vario 25L	18 s	124 m	6.9 ms ⁻¹	18.6 ms ⁻¹	3.36ms ⁻²	partially/not buried
Snowpulse/Mammut Lifebag 30L	20 s	132 m	6.6 ms ⁻¹	17.8 ms ⁻¹	3.56ms ⁻²	partially buried–not critical

Table 1. Overview of the of track lengths, speeds, accelerations and burial grades.

3.2. About the avalanche

The triggered avalanche was a snow cornice fall type avalanche which loaded underlying snow. The cornice was 40 m long with a height from 0.5 m to 3 m. The maximum width of the avalanche

Initial snow volume	Track	Avg. deposition depth	Max. pressure	Max. speed	Run-out size
280m ³	250m	1,5m	125,13 kPa	18.6ms ⁻¹	130m x 30m

Table 2. Basic information on triggered avalanche.

track was 60 m and 25 m in the most confined section. The predominant snow which created the avalanche was moist. The initial volume of the snow mass used to trigger the avalanche was estimated as 280 m³. The total distance of the avalanche was 250 m. Numerical simulation showed that the avalanche reached a maximum speed of 18.6 ms⁻¹ (66.96 kmh⁻¹) and a maximum pressure of 125.13 kPa (Figure 6). The deposition area was 30 m wide and 130 m long with an

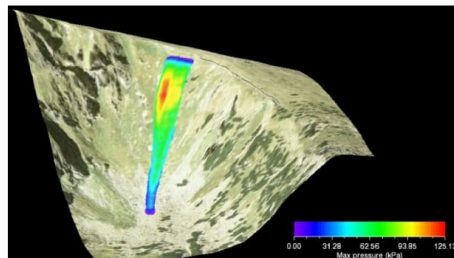


Figure 6. Pressure simulation of the triggered avalanche. average height of 1.5 m. Basic information is in Table 2.

Impact pressure (kPa)	Potential damage
1	Break windows
5	Push in doors
30	Destroy wood – framed structures
100	Uproot mature spruce
1000	Move concrete structures

Table 3. Impact pressure and damage potential of avalanches. (after McClung and Shear 2012)

4. CONCLUSION

The field testing consisted of only one trial and there were no reference dummies (without an airbag). It is plausible that a reference dummy would have been buried, but this is speculative and cannot be tested. Thus, the results of the test are applicable for this particular avalanche. The most important result is that none of the dummies were completely buried. In all cases the heads were free from snow, the airways were not obstructed and the balloons were clearly visible on the surface of the avalanche. In this particular trial the grade of burial was more serious for the dummies which were carried further down the slope. This can vary in other cases and real life situations. However, this also is only true for this particular situation (terrain and avalanche conditions) and test results are not applicable to all other avalanches. Regardless of having an avalanche airbag backpack, one can be completely buried with all the associated consequences. Based on this trial we are not able to judge the efficiency and floating capabilities of the used avalanche backpacks. In future more field trials will be necessary to properly assess the various shapes of avalanche balloon packs

5. ACKNOWLEDGEMENTS

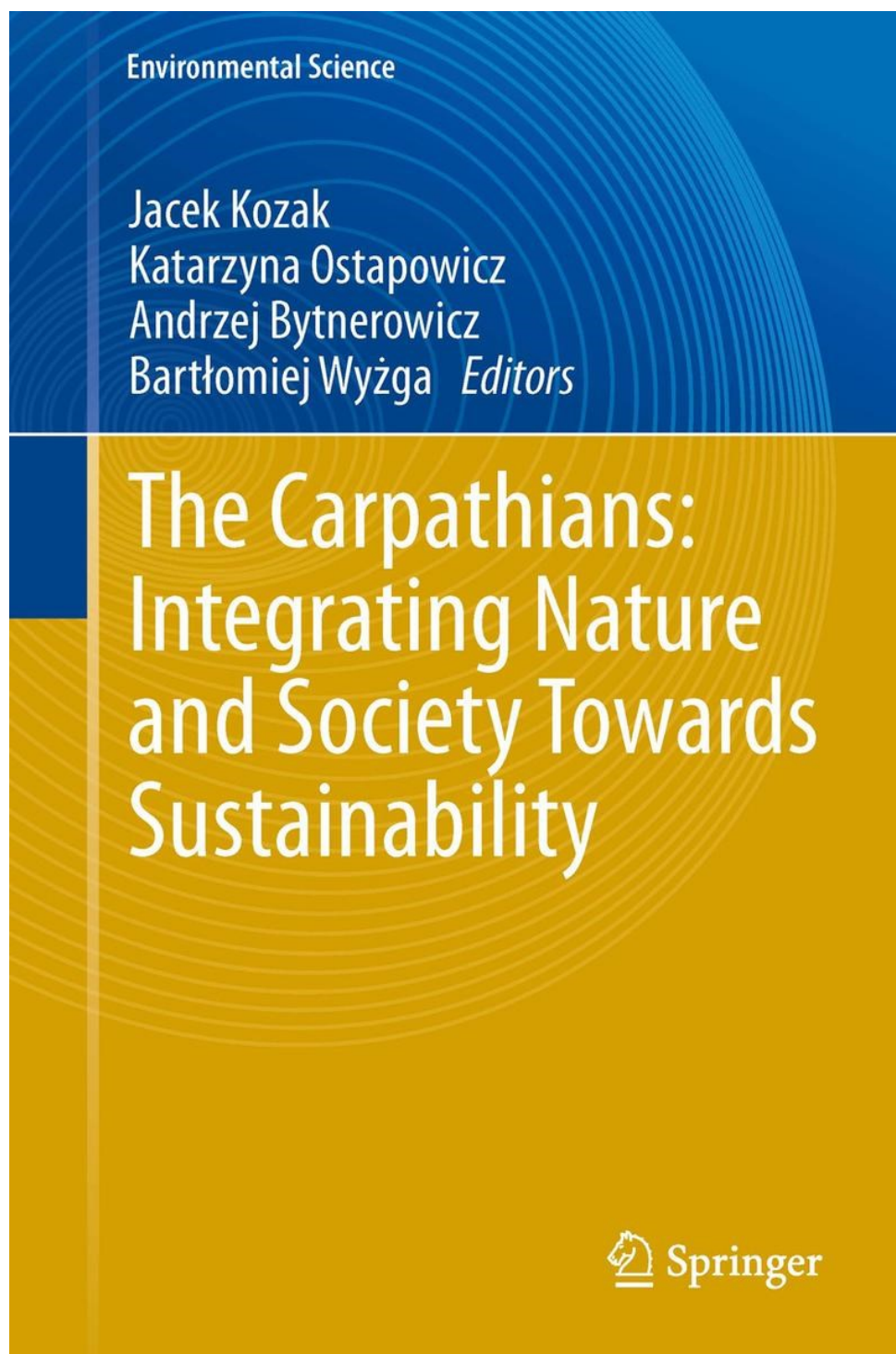
The following institutions and people deserve great thanks: Gustav Kasanicky and Igor Dirnbach from the Institute of Forensic Engineering for providing the dummies, Lukas Neklan from Signing Rock for support, Rado Michalica from the Institute of Forensic Sciences, all the staff of the Avalanche Prevention Centre and the Mountain Rescue Service in Slovakia, Rasto Hatiar for shooting the movie and Gabriel Liptak for taking the pictures.

6. REFERENCES

- Brugger, H., Etter, H.-J., Zweifel, B., Mair, P., Hohlirieder, M., Ellerton, J., et al. (2007). The impact of avalanche rescue devices on survival. *Resuscitation*, 75, 476–483.
- Christen, M., Kowalski, J., Bartelt, P. (2010) RAMMS: Numerical simulation of dense snow avalanches in three-dimensional terrain. *Cold Regions Science and Technology* (63) 1-2, pp. 1 – 14.
- Brugger, H., Kern, M., Mair, P., Etter, H.-J., Falk, M. (2003). Effizienz am Lawinenkegel. *BergUndSteigen*, 03/4, 60–65.
- Greene, E. M., Atkins, D., Birkeland, K. W., Elder, K.C., Landry, C., Lazar, B., McCammon I, M., Moore, Sharaf, D., Sterbenz, C., Tremper, B., and Williams, K. (2010). *Snow, Weather and Avalanches: Observation guidelines for avalanche programs in the United States*. 2nd ed. Pagosa Springs, Colorado: American Avalanche Association, 2nd printing.
- Kern, M. (2000). Inverse grading in granular flow. PhD Thesis, École Polytechnique Fédérale de Lausanne, Lausanne, Switzerland. [available online at http://biblion.epfl.ch/EPFL/theses/2000/2287/EPFL_TH2287.pdf].
- Kern, M., Tschirky, F., Schweizer, J. (2002). Field tests of some new avalanche rescue devices. Paper presented at the International Snow Science Workshop, Penticton, BC.
- McClung, D., Shaerer, P. (2011) *The Avalanche Handbook*. Seattle, WA: The Mountaineers Books. ISBN 0898863643.
- Meier, L., Harvey, S. (2011). Feldversuche mit Lawinen-Notfallgeräten Winter 2010/11. WSL Institute for Snow and Avalanche Research SLF, Davos, Switzerland. Accessed at: http://www.slf.ch/praevention/verhalten/notfallausruestung/ReportAirbagTests_v4_Meier_Harvey.pdf
- Radwin M.I., Grissom C. K. (2002). *Technological Advances in Avalanche Survival*. *Wilderness and Environmental Med.* 2002; 13(2):143-52
- Tschirky, F., Schweizer, J. (1996). *Avalanche Balloons- Preliminary Test Results*. Paper presented at the International Snow Science Workshop, Banff, AB.
- Tschirky, F., Brabec, B., Kern, M. (2000). *Avalanche rescue systems in Switzerland: Experience and limitations*. Paper presented at the International Snow Science Workshop, Big Sky, MT.

Publication 7

Chrustek P., Wężyk P., Kolecka N., Marek **Biskupič** M., Bühler Y., Christen M., 2012 Using high resolution LiDAR data for snow avalanche hazard mapping in Kozak, J., Ostapowicz, K., Anna (Eds.) Integrating Nature and Society towards Sustainability, Springer, 290 p. (book chapter)



Using High Resolution LiDAR Data for Snow Avalanche Hazard Mapping

Paweł Chrustek, Piotr Wężyk, Natalia Kolecka, Marek Biskupič, Yves Bühler and Marc Christen

Abstract Each year in the Carpathian Mountains and the Sudety Mountains snow avalanches cause a great number of accidents. Avalanches also threaten buildings and affect the environment. The latest studies in Poland aim to implement advanced snow avalanche hazard mapping procedures, which would allow the creation of complex cartographic products for the location of avalanche hazard areas. These preliminary studies showed that results of these procedures strongly depend on the quality of the input digital surface data. The main goal of this study is to investigate this problem in detail through comparison of different types of Digital Elevation Models (DEMs), putting stress on high resolution DEMs generated from airborne and terrestrial laser scanning, in the context of estimating potential avalanche release areas and making run-out calculations. Test sites in the Tatra Mountains in the Carpathians and in the Karkonosze Mountains in the Sudety Mountains were selected for this study. The analysis was performed using Swiss Rapid Mass Movements (RAMMS) model and modified script on delineation automated release area. The study recognized that not only quality but also

P. Chrustek (✉) · N. Kolecka
Institute of Geography and Spatial Management, Jagiellonian University,
Gronostajowa 7, 30-387 Kraków, Poland
e-mail: p.chrustek@annapasek.org

P. Chrustek · P. Wężyk · M. Biskupič
Anna Pasek Foundation, Małobądzka 101 42-500 Będzin, Poland

P. Wężyk
Agricultural University in Kraków, Faculty of Forestry, Al. 29 Listopada 46,
31-425 Kraków, Poland

M. Biskupič
Charles University in Prague, Faculty of Science, Albertov 6, 12843 Praha, Czech Republic

Y. Bühler · M. Christen
WSL Institute for Snow and Avalanche Research SLF, Flüelastr. 11,
7260 Davos, Switzerland

J. Kozak et al. (eds.), *The Carpathians: Integrating Nature and Society*
Towards Sustainability, Environmental Science and Engineering,
DOI: 10.1007/978-3-642-12725-0_42, © Springer-Verlag Berlin Heidelberg 2013

597

resolution of a digital surface models influence the accuracy of release area and volume estimation, calculated topography parameters, location of avalanche track and other parameters calculated by dynamic models.

1 Introduction

Avalanche hazard mapping is a set of procedures used by land planning authorities as a tool to prevent settlements, roads and railways being constructed in areas that are endangered by avalanches (Gruber 2001). It has proven to be one of the most economic effective hazard mitigation measures in Switzerland (Gruber and Margreth 2001). The goal of the procedure is to estimate the areas exposed to the avalanche hazard and related risk.

Hazard mapping started early as first large and extreme avalanches threatened human settlements, caused life losses and serious damages. In the early attempts run-outs were simply plotted on topographic maps and so called avalanche cadastres were created. With the development of knowledge about avalanche flow and rheology more sophisticated approaches were used. Nowadays in the Alps many guidelines for avalanche hazard zoning have been established, most of them based on avalanche dynamics simulations (Jamieson 2008). These numerical simulations coupled with tools for delineation of release areas, historical avalanches and snow depth records are undoubtedly the crucial part of avalanche hazard mapping (Maggioni 2005).

Generating potential release areas is the first and crucial step in the avalanche hazard mapping process. It determines their location and helps to calculate release volumes used as input parameters for further dynamics calculations. A method for automated delineation of snow avalanche release area was described by Maggioni (2005). The procedure based on geographic information systems (GIS) classifies release areas based on vegetation and such topographic parameters as inclination, planar curvature, altitude generated from digital elevation model (DEM). The method finds widespread application in mountainous regions where historical avalanche events have been poorly documented (or no documentation exists at all) (Maggioni 2005). However, it has a tendency for some generalization, mainly because the results are used for analyzing extremely large avalanches. Developing a reliable automated release method and adapting it to smaller avalanches, however, requires extensive testing with various numerical models. The impact of initial conditions (release location, dimension and volume) on model results (run out distance and flow) must be extensively tested in various regions.

In the course of several decades the estimation of avalanche run-outs has been the scope of scientific investigations in both Europe and North America. To predict avalanche speed and run-out, dynamic models use physical laws (conservation of momentum, conservation of mass). Numerical modeling requires data on initial avalanche conditions (dimensions of release zones, snow cover entrainment and

friction parameters). The complexity of terrain makes avalanche flow simulations a very demanding and challenging task. Many simplifications and assumptions have to be implemented.

First attempts to simulate the avalanche flow were done in the former Soviet Union in Tbilisi. Dry friction and force increasing linearly with speed were introduced as frictional forces (Salm 2004). According to Salm (2004), the implementation of the Coulomb law of friction in avalanche dynamics is one of the most ingenious theories in this field. In 1955, in a chapter *Über die Zerstörungskraft von Lawinen* (On the destructive force of avalanches) dealing with dense snow avalanches Voellmy assumed that their flow was similar to fluids and proposed to include in the avalanche model two parameters: Coulomb friction and turbulence. Salm and others adapted the model to better fit observed run-outs and included the back pressure due to the deceleration in the run-out zone (Salm et al. 1990). This model is well known as the Voellmy-Salm model and allows to estimate the flow depth at a given flow width. It has been used widely across Europe to design avalanche hazard maps.

For many years various dynamic models have been developed (e.g. Perla et al. 1980; Sampl and Zwinger 2004) but only two of them: AVAL-1D and RAMMS (Rapid Mass Movements) (Christen et al. 2002, 2010a) were released as a commercially available solution by the WSL Institute for Snow and Avalanche Research SLF in Davos, Switzerland. Using them, however, requires experience in avalanche science and GIS technology. A DEM is the basic input for all these models; its quality directly affects the result of calculations.

Technological developments have also facilitated quick and more efficient acquisition methods of detailed geodata. The LiDAR (Light Detection And Ranging) has been known from the last decade as a rapid, accurate and adaptable method for 3-dimensional (3D) surveying of the Earth surface and profiling the atmosphere via either satellite laser scanning (SLS), airborne laser scanning (ALS) or terrestrial laser scanning (TLS). All these technologies deliver information which can be integrated with other sensors, like airborne digital cameras (e.g. CIR orthophotomaps), hyperspectral linear scanners or thermal imaging cameras (Wężyk 2006).

Several advantages of using high resolution LiDAR data for better understanding natural processes in complex terrain and obtaining snow and avalanche data were found (e.g. Vallet et al. 2000; Deems and Painter 2006; Jörg et al. 2006; Prokop et al. 2008; Vallet 2008), however, detailed studies about its influence on hazard mapping process and procedures (including dynamics calculations) have not been published yet. Introduction to this kind of studies, but mainly in the context of estimating release area delimitation, was presented by Chrustek and Wężyk (2009) and McCollister and Comey (2009).

Mountains in Poland (above 500 m a.s.l.) cover only 3.1% of the total country area, so avalanches are a less serious problem than in the Alpine regions. This does not make it less important. Each year Polish mountains witness a few fatal accidents caused by avalanches. The greatest tragedy took place on the 28th of March, 1968, when the avalanche in the Karkonosze Mountains area killed nineteen

people. Moreover, snow avalanches in Poland bring significant damages to forested areas. During winter seasons of 2008/2009 and 2009/2010 many new avalanche paths in the Tatra Mountains were activated and caused many fatalities and infrastructure damages. It confirmed the importance of implementation of avalanche mapping procedures for this region (Chrustek and Biskupič 2010).

Considering current technological progress e.g. global positioning system (GPS) receivers integrated with handheld computers or mobile GIS software implemented into cell phones that are brought into general use in mountain exploring, it seems that avalanche mapping showing a range of avalanche risk/hazard areas might be very useful in future in safety context. Not only for planners, engineers or administrators of recreational areas, but also for mountain rescuers, specialists during their field work and tourists performing a wide range of winter mountain activities.

However, preliminary studies in Poland (Chrustek 2005, 2009) recognized that results of hazard mapping procedures strongly depend on the quality of the input digital surface data. DEM quality and its resolution influences determining release areas, release volumes, simulated avalanche flow and consequently precision of the hazard zoning, especially when analyzing smaller avalanches in a more complex terrain. This impact is not obvious thus detailed analysis must be performed, before avalanche hazard mapping procedures can be fully implemented in the region of the Sudety Mountains and the Carpathians.

The chapter is part of this research and its main goal is to compare different types of DEMs, in particular high resolution DEMs generated from ALS and TLS data, in the context of estimating potential avalanche release areas and making run-out calculations, that are fundamental steps of hazard zonation. The analysis was performed using the Swiss RAMMS model and modified script for release area delineation.

1.1 Test Areas

Goryczkowy test site (surroundings of the Kasprowy Wierch peak) in the Polish Tatra Mountains was chosen as a main test site (Fig. 1). The region has a high frequency of snow avalanches due to the presence of long and steep slopes. On the other hand, it has been a very popular tourist destination for a long time, and has highly developed tourist infrastructure (mountain hotels, ski lifts and ski routes). Therefore, the highest number of incidents related to avalanches is recorded in this region. Part of the analysis was made in the Mały Staw test site located in the Karkonosze Mountains, Poland (the Western Sudety Mountains) (Fig. 1). Here frequent avalanche accidents are caused mainly by small and medium avalanches in a more complex terrain.

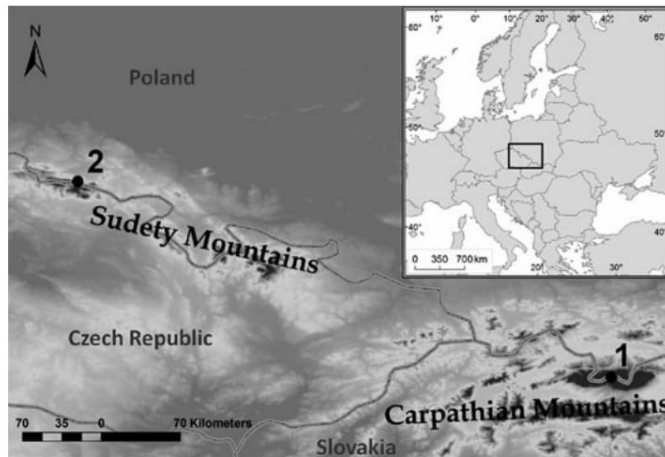


Fig. 1 Location of the test sites. (1) the Goryczkowy test site in the Polish Tatra Mountains (Western Central Carpathians). (2) the Mały Staw test site located in the Karkonosze Mountains, Poland (the western Sudety)

2 Materials

As already indicated, DEM is a fundamental dataset for avalanche hazard mapping. Higher-resolution DEMs are required for channeled and inhomogeneous terrain, especially for small avalanche events (volumes $< 25,000 \text{ m}^3$). Large, extreme events, travelling at high speed, appear not to react to small scale terrain features, suggesting that some simulations can be performed on low-resolution DEMs and yield realistic results. High-resolution DEMs seem to be crucial for small and frequent avalanches. In the same way wet snow avalanches, travelling at a lower speed than dry snow avalanches, may require a higher DEM resolution than dry snow avalanches (Christen et al. 2010a). The most suitable values of the DEM resolution in step are not standardized thus for the comparison we used three types of surface data which were finally resampled to spatial resolutions of 1, 5, 10 and 25 m.

2.1 ALS Data

The ALS system used in August 2007 over the Tatra Mountains was based on two LMS-Q560 (full waveform) scanners (Riegl) mounted on a special platform under the DA42 airplane. Those two scanners (forward and backward looking) allowed obtaining very dense point cloud, even up to 40 laser beams on 1 m^2 of the ground. Dedicated RiscanPro Software (Riegl) allowed generating the first (FE for digital surface model, DSM, generation) and the last echo (LE for DEM generation) from

the full waveform signal. The matching of 33 separate scans was conducted on planar surfaces (buildings' roofs with minimum 6 points) measured with dGPS receiver (Leica 1230) and tachimeter (Leica 407 power). The EUPOS-ASG network was used as a reference signal for geoprocessing. The accuracy of the point cloud in the 3D space was approximately 0.06, 0.02 and 0.01 m in X, Y and Z, respectively, when measured on the planar roof surfaces (Wężyk et al. 2008). The whole matched point cloud was cut into 500×500 m tiles for the purpose of a ground filtration and generation of the DEM (1×1 m GRID) based on the Axelsson (2000) algorithm with the Terrasolid software. A similar approach was used to create the DEM for Mały Staw test site.

2.2 TLS Data

The Laser Profile Measuring System LPM-321 (Riegl), used by authors in the Polish Tatra Mountains in July 2009, allowed long range 3D profiling up to 6,000 m with the high accuracy. The distance meter comprises of the state-of-the-art digital signal processing and echo waveform analysis, enabling precise distance measurements even under reduced visibility conditions. The scanner can detect up to 3 target distances per measurement. The combination with mounted high resolution digital camera calibrated and accurately orientated makes a hybrid sensor system, which allows to obtain colored point clouds. The scan range of the LPM-321 is -20 to 130° vertically, and 360° horizontally. The accuracy of the measurements is 25 mm (Riegl 2010).

Because of the large size of the Goryczkowy test site, it was divided into three parts to make scanning more efficient. TLS data pre-processing consisted of point cloud denoising and decimation, removing redundant and isolated points, meshing and mesh cleaning (VRMesh 2010). Three point clouds had to be merged and registered in the global coordinate system. The procedure comprised of an approximate manual registration of input point clouds, followed by automatic alignment based on least square matching (Shan and Toth 2008; Heritage and Large 2009). Positioning in the global coordinate system was achieved by means of automatic alignment of the TLS points to the existing photogrammetric model. There were more than 1 million points in the merged cloud, with average spacing of 0.803 m.

One of the characteristic features of the TLS technology are occlusions, that cause some gaps within the data. In the Goryczkowy dataset two significant holes appeared. Therefore, the primary TLS model was updated with the altitude information obtained from the photogrammetric model (Fig. 2). TLS data for Mały Staw test site were not available.

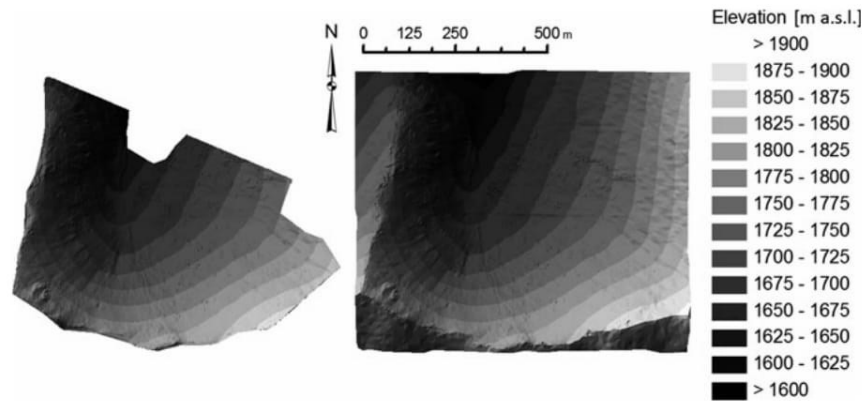


Fig. 2 TIN of the Goryczkowy test site produced out of the TLS point clouds only (*left*) and updated with the altitude data from the photogrammetric model (*right*)

2.3 Topo Data

Topo data were derived from the TIN model based on contour lines with 5 m intervals (digitized from topographic maps 1:10,000), mass points and structure lines obtained from aerial images processing. This type of data covers large areas in Polish mountainous regions and is the fundamental part of public administration GIS databases at the moment.

3 Methodology

Comparative analyses were performed based on two distinct avalanche hazard mapping procedures: generating potential release areas (PRAs) and avalanche dynamic calculations (including potential extreme event calculations based on the generated PRAs and “back calculations” based on the recorded historical avalanche). Each procedure is presented in detail below.

3.1 Generating Potential Release Areas

Automatic procedure for release area delineation proposed by Gruber et al. (2002) and Maggioni (2005) was used for the analysis at the Goryczkowy test site. This method is not directly adaptable to such areas as the Polish mountains (Chrustek 2005) thus some steps were changed due to morphological differences between mountain ranges in Poland and Switzerland. Upgrade procedure was written by the authors using the Python Script and implemented in the ESRI ArcInfo ver. 9.3.

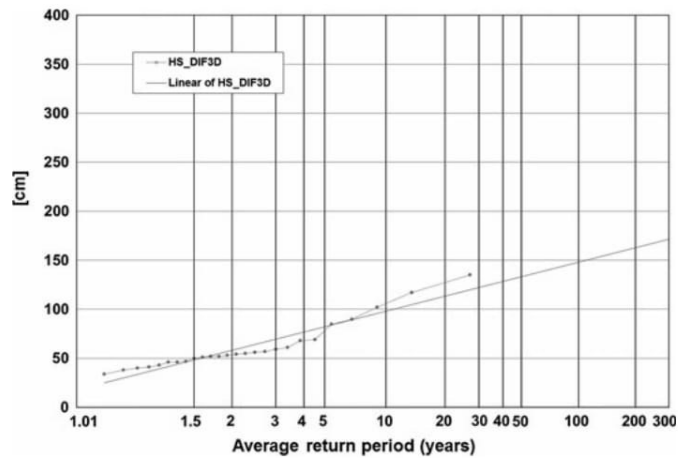


Fig. 3 Data and Gumbel statistics extrapolation of the maximum annual value of HS_DIF3D of the Kasprowy Wierch High Mountain Observatory (1,987 m a.s.l., 26 winters)

Besides 1 m resolution, spatial resolutions of the DEMs used in this analysis are the most widely used spatial resolutions for generating release areas (e.g. Gruber 2001; Gruber et al. 2002; Gruber and Bartelt 2007; Pagliardi et al. 2009). Generating PRAs from ALS and TLS LiDAR with DEM spatial resolution higher than 1 m is possible but it does not seem to be justified, as such a precise terrain differentiation disappears under snow cover, which causes natural process of “smoothing” the surface.

All of the release areas in the ESRI shape file format derived from the automatic procedure and their base DEM models were loaded into Swiss RAMMS model (Christen et al. 2010a) and then release parameters like areas, mean angle, mean altitude, estimated release volumes or mass were calculated. Estimated release height value was calculated according to the Swiss guidelines for avalanche hazard mapping (Salm et al. 1990). This procedure assumes that the maximum yearly increase of snow cover within three days (HS_DIF3D) is representative for the fracture depth of the avalanche. For hazard mapping purposes, the yearly maxima of HS_DIF3D were extrapolated using Gumbel extreme-values statistics (Reiss and Thomas 1997) and the data from the Kasprowy Wierch High Mountain Observatory which is situated about 1 km away from the Goryczkowy test site (Fig. 3).

The calculated value was corrected using the cosine of slope angle, elevation difference value and snow drift statistics. Finally, the value of 113 cm for 100 years return period was derived.

3.2 *Avalanche Dynamics Calculations*

RAMMS model solves the depth-averaged equations governing avalanche flow with accurate second order solution schemes. RAMMS deals with the avalanche flow using two different approaches: the standard Voellmy-Salm approach or random kinetic energy model (RKE). The Voellmy-Salm model is implemented in RAMMS through its AVAL-1D code. Coupled with an easy to use interface it is an invaluable tool for avalanche engineers dealing with hazard zoning and mitigation (Christen et al. 2010a,b).

Three model inputs must be specified to perform a numerical calculation: (1) a digital elevation model (DEM) (2) release zone area and fracture height and (3) model friction parameters.

3.2.1 Calculating Potential Extreme Avalanche Event

The goal of this comparison test was to recognize the influence of the different types of DEMs (spatial resolutions with 1 and 25 m) and relation between avalanche volumes on the calculation results.

PRAs in the ESRI shapefile format generated from different ALS and Topo DEMs for the Goryczkowa test site were used in the dynamics calculations using RAMMS model. TLS data was not used in this analysis because of the limited spatial extent of the dataset.

Generated PRAs extents, their topographic parameters and predicted extreme fracture height in 100 year return period were assumed as input parameters for modelling extreme run-outs. The input variable friction parameters were calculated using automatic procedure implemented in the RAMMS model. The procedure classifies terrain features like slope angle, planar curvature and altitude into categories such as open slope or flat, terrain or channelled or gully and forested or non-forested areas (Christen et al. 2010a). Some of the default parameters (like avalanche volume which influences calculated friction parameters) were slightly modified based on the calibrating analysis for this region. Assumed snow density was constant and equal to 300 kg/m^3 . In each case the 5 m spatial resolution was used for the calculation.

3.2.2 Back Calculation Based on the Recorded Historical Avalanche

The final step of the analysis was an evaluation how the type and resolution of the DEMs influences dynamics analysis results, with particular emphasis on small avalanches in a more complex terrain. For this study a documented avalanche event from Mały Staw test site in the Karkonosze Mountains was chosen. On 26 January 2003 it killed one climber and caused serious injuries to two another. The avalanche with estimated release volume about 550 m^3 and 300 m length was



Fig. 4 Documented avalanche track from 26 January 2003 (the Mały Staw test site)

released close to the ridge and then flowed down through the rocky couloir (Fig. 4). Following parameters were used for the release area in further dynamics calculation: 2D area ($1,215 \text{ m}^2$), mean angle (39.9°), mean altitude ($1,349.1 \text{ m a.s.l.}$), release height (35 cm), estimated avalanche volume (555 m^3), snow density (300 kg/m^3) and release mass (166.5 tons).

Input friction parameters were calculated in the same way as in the previous analysis. ALS and Topo data were used, with two different resolutions (1 and 25 m). Measured release height (35 cm) and release area (drawn on the map based on the accident documentation) were used for the calculation. In each case 1 m resolution was used for the calculation.

4 Results and Discussion

4.1 Results of Generating PRAs

Results of all calculations are presented in Table 1. When comparing automatically generated values for such topographic parameters as mean angle and mean altitude, there are no noticeable quantitative differences.

The biggest differences are observed for area, volume and mass parameters. The differences were caused both by the types of input DEMs and their spatial resolutions. Calculated values for ALS and TLS data related to the area are very similar but the values for Topo DEMs are always smaller than the other. For example, if an assumption is made that area values for ALS data are 100% , then percentage differences are between $0.2\text{--}2.2\%$ (when comparing ALS and TLS

Table 1 Automated generated PRAs for Goryczkowy test site with release parameters calculated in RAMMS model

Type of PRA	2D Area (m ²)	Mean angle (degree)	Mean altitude (m a.s.l.)	Estimated volume (m ³)	Mass (t)
ALS 1 m	83,500	34.5	1,744.4	1,14,511	34,353.3
TLS 1 m	82,300	34.5	1,743.1	1,12,811	33,843.3
Topo 1 m	79,200	34.6	1,744.5	1,08,779	32,633.7
ALS 5 m	84,000	34.4	1,744.8	1,15,005	34,501.5
TLS 5 m	84,200	34.3	1,744.5	1,15,158	34,547.4
Topo 5 m	79,200	34.5	1,745.2	1,08,620	32,586.0
ALS 10 m	84,700	34.1	1,744.6	115,644	34,693.2
TLS 10 m	83,100	34.1	1,742.4	1,13,416	34,024.8
Topo 10 m	80,100	34.3	1,743.1	1,09,564	32,869.2
ALS 25 m	79,000	33.2	1,734.3	1,06,650	31,995.0
TLS 25 m	77,300	33.7	1,737.6	1,05,018	31,505.4
Topo 25 m	76,500	34.1	1,737.2	1,04,426	31,327.8

results – minimum value refers to the 5 m and maximum value to the 25 m spatial resolution of DEM) and 3.2–5.7% (when comparing ALS and Topo results – minimum value refers to 25 m and maximum to 5 m spatial resolution of DEM).

Degrading spatial resolution of the DEMs causes reduction of differences between the area, volume and mass values. On the other hand calculated values decrease pixel size with the increasing spatial resolution of the DEMs. Degrading resolution of LiDAR (ALS and TLS) DEMs from 1 to 25 m causes bigger differences in calculated release values (areas, volumes, mass) than of Topo DEMs. (e.g. for the release mass 6.86 % for ALS, 6.91 % for TSL and 4 % for TOPO).

Recognized maximum differences appear to be quite large, especially when it is assumed that these values describe release parameters for a single extreme avalanche.

4.2 Results of Avalanche Dynamics Calculations

4.2.1 Results of Calculations of the Potential Extreme Avalanche Event

For various input DEM resolutions maximum velocity, flow height and pressure were calculated (Table 2).

The quantitative differences between output parameters calculated for different DEMs with different resolution do not seem to be significant but more discrepancies were noticed when analyzing their spatial variations (Fig. 5).

Analyzed examples showed that ALS models allow to predict avalanche flow process more precisely (even after reducing the model resolution) than Topo models, including also such terrain as the surrounding of the Goryczkowy test site where topographic surface is not very complex.

Table 2 Selected output parameters for 100 year return period avalanche calculated using RAMMS model (for Goryczkowy test site)

Type of the input dataset used in calculation	Max velocity (m/s)	Max flow height (m)	Max pressure (kPa)
ALS 1 m	30.67	16.71	282.16
Topo 1 m	30.01	14.50	270.13
ALS 25 m	30.21	15.55	273.87
Topo 25 m	29.62	14.52	263.13

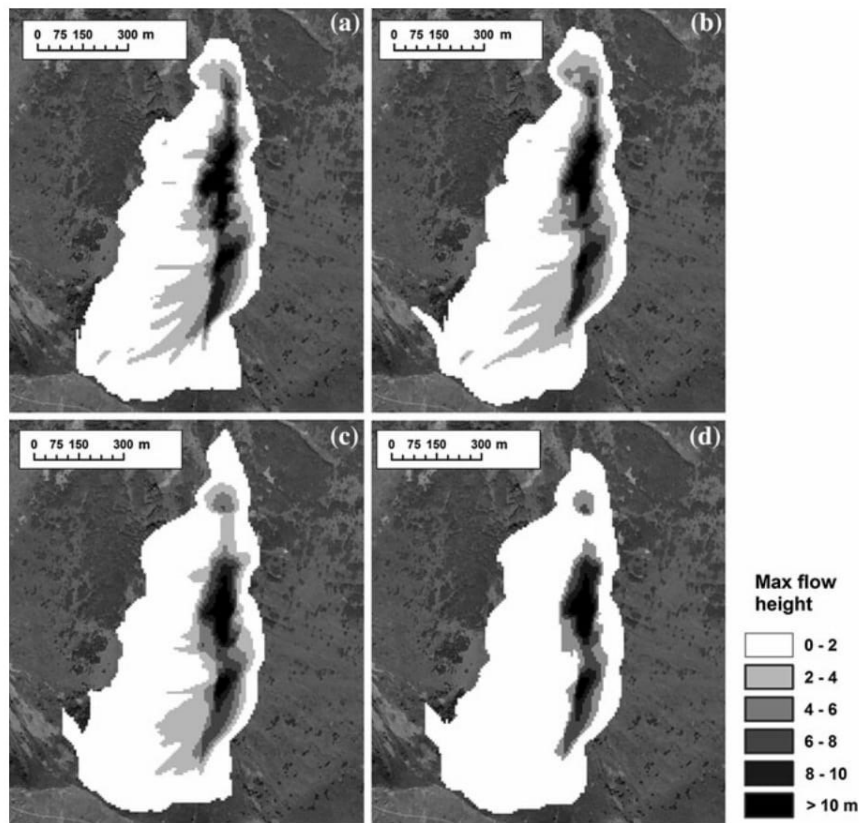


Fig. 5 Maximum flow height of predicted avalanche in the Goryczkowy test site, calculated in the RAMMS model: **a** 1 m ALS dataset, **b** 1 m Topo dataset, **c** 25 m ALS dataset, **d** 25 m Topo dataset

The influence of various DEM types and different resolutions on the maximum distance was also investigated. When comparing 1 m ALS and 1 m Topo data differences between calculated distances were about 25 m (distance for Topo dataset was greater, Fig. 5a, b). The same comparison for 25 m resolution datasets

showed that the difference was much bigger – about 40 m (distance for ALS dataset was greater, Fig. 5b, c). The biggest difference was obtained after changing resolution in ALS dataset. Difference between maximum flow distance for 1 and 25 m was about 50 m (distance for ALS 25 m was greater, Fig. 5a, c). The same comparison for Topo dataset showed difference that was about 30 m (distance for Topo 1 m was greater, Fig. 5b, d).

Based on the results presented in Table 2 it can be stated that parameter differences between calculated PRAs are noticeable during dynamics calculation as well. This test showed that differences were bigger when spatial resolution were changed for ALS data. These discrepancies for Topo data were less noticeable. However, direct relation between estimated volume and maximum distance calculated by the model was not investigated (when comparing results from different resolutions). Interesting results were obtained when analyzing ALS data. Despite of much lower estimated volume (by 5.4%, 2,358.3 t less), calculated distance for 25 m dataset was 40 m longer than for 1 m dataset. It means that smoothing the

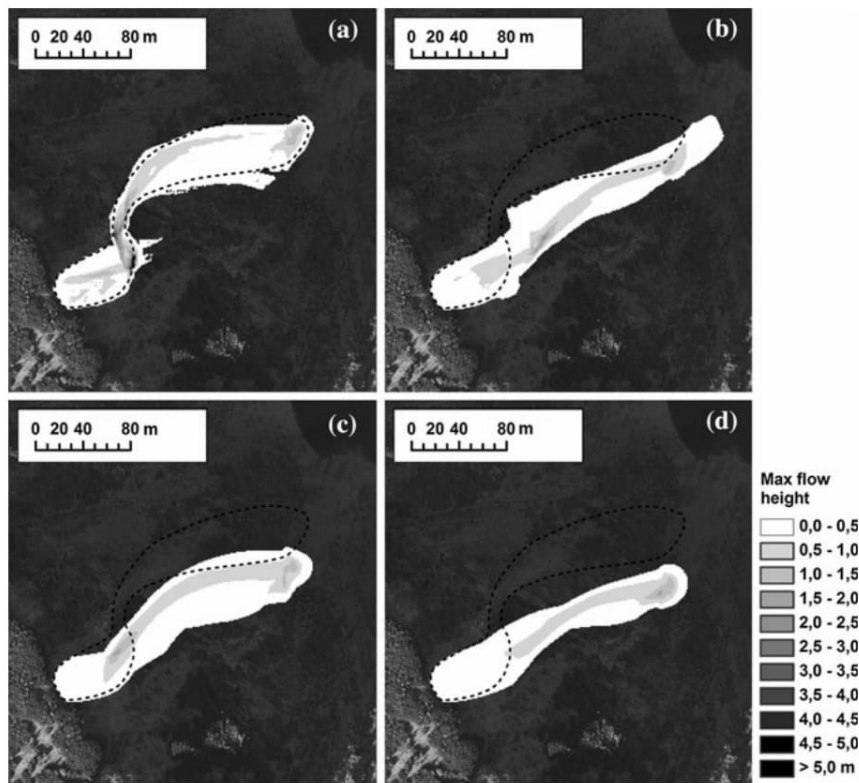


Fig. 6 Maximum avalanche flow height in the Mały Staw test site calculated in the RAMMS model: **a** 1 m ALS dataset, **b** 1 m Topo dataset, **c** 25 m ALS dataset, **d** 25 m Topo dataset; dashed line shows extents of the documented avalanche

Table 3 Selected output parameters for simulation of the documented avalanche calculated using the Swiss model RAMMS (for Mały Staw Lake test site)

Type of the input dataset used in calculation	Max velocity (m/s)	Max flow height (m)	Max pressure (kPa)
ALS 1 m	20.67	5.18	128.20
Topo 1 m	24.41	2.23	178.79
ALS 25 m	21.25	1.63	135.42
Topo 25 m	19.78	1.56	117.40

topography while decreasing the spatial resolution, strongly influences calculation results. This influence is more significant when analyzing LiDAR data.

4.2.2 Results of the Back Calculations

In this example, quantitative differences between calculated parameters are significant (Table 3) but the biggest discrepancies were observed when analyzing tracks of the avalanche flows (Fig. 6). High similarity of the simulated track with observed track was obtained only from high resolution ALS data (1 m resolution). ALS data resampled to smaller 25 m resolution lost important surface details, however, its simulated avalanche profile is more similar to the documented avalanche than the one obtained from 1 m Topo model. Results from Topo models are completely unsatisfactory (Fig. 6) as calculated avalanche flows were completely different from the observed one.

5 Conclusions

Presented tests proved that many variables influence hazard mapping results. One of the most important factors is a quality of DEMs. It influences the precision of the release area estimation, calculated topography parameters, calculated release volume, location of avalanche track and another parameters calculated by dynamic models. DEMs generated from LiDAR data (ALS or TLS) introduced new quality for avalanche modeling but influence of this improvement on all hazard mapping procedures must be extensively tested. When comparing automatically generated PRAs from Topo and LiDAR models (for common spatial resolutions of 1, 5, 10 and 25 m), it was observed that reduction of the spatial resolution causes reduction of PRA areas. It affected also directly the calculated release volume. Based on the presented test, differences between results obtained from 1 and 25 m resolution could achieve up to 7%.

Using DEMs with different resolutions only slightly affected calculation of such topographic parameters as: mean angle and mean altitude. There were no noticeable quantitative differences between these parameters computed for various

DEMs, which seems very important as they directly affect calculations of an avalanche release volume.

Presented example for the Mały Staw test site showed that only high resolution DEMs obtained from LiDAR data were able to simulate proper avalanche flow for small events which in case of the Carpathian Mountains and the Sudety Mountains kill more people every year than large catastrophic events with large return periods. For extreme events, the relation between DEM spatial resolution and avalanche model accuracy is not so obvious. When analyzing the extreme scenario for the Goryczkowy test site, significant influence of DEM spatial resolution on the final results was noticed. The resolution changes affect calculation results more significantly, when basing on LiDAR data. This relation was noticed both while analyzing release areas and performing dynamic calculations. It may prove quite important for avalanche specialists who deal with hazard mapping, because different analysis steps require different spatial resolutions of DEMs. However, it is still uncertain how differences between calculated avalanche volume, type of input DEM and its resolution can influence simulated avalanche flow and calculated avalanche maximum distance. To better understand of this problem, more tests in different regions have to be performed.

While the high resolution terrain data is still available for selected regions only, the future studies should also contain an analysis based on free of charge elevation data which is acquired by a satellite-borne sensors (like SRTM or ASTER). This data are easily downloadable and cover all mountainous regions on Earth. Spatial resolution of these data is not higher than 25 m, therefore they have a limited applicability in studies of small avalanches in a more complex terrain. However, they may be useful for large scale avalanche hazard mapping, especially for the region without access to any other digital elevation data.

Acknowledgments We would like to express our gratitude to the Foundation for Polish Science for financial support of Paweł Chrustek. Performing analyses was possible mainly thanks to the VENTURES program organized by the Foundation of Polish Science and co-funded by the European Regional Development Fund under the Operational Program Innovative Economy 2007–2013. We would also like to thank to the Anna Pasek Foundation for additional financial support. Natalia Kolecka is a grant holder of “Doctus” Programme. We would like to also thank the Karkonosze National Park, ProGea Consulting Company and Kraków Branch of the Institute of Meteorology and Water Management (IMGW) for deriving the Geodata (ALS, GIS, Meteo data), Andrzej Brzeziński and Jakub Radliński from the Mountain Rescue Services (GOPR), for assistance in collecting data and materials concerning avalanches in the Karkonosze Mountains and Marek Świerk from the Anna Pasek Foundation in Poland, for assistance in collecting field data.

References

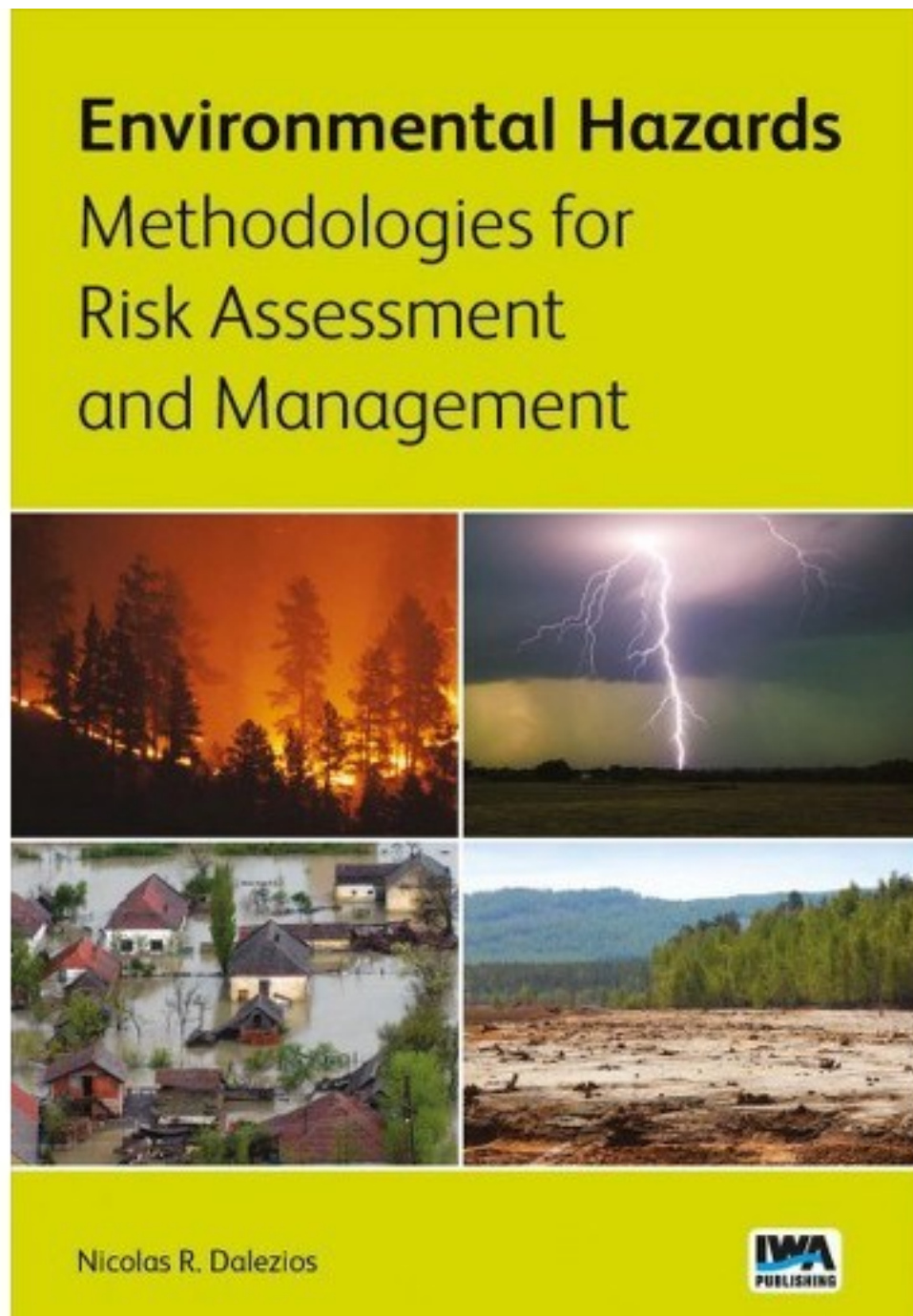
- Axelsson P (2000) DEM generation from laser scanner data using adaptive TIN models. *Int Arch Photogram Remote Sens* 33/4B:203–210
- Christen M, Bartelt P, Gruber U (2002) AVAL-1D: an avalanche dynamics program for the practice. *Interpraevent 2002. Matsumoto - Japan. Congress publication* 2:715–725

- Christen M, Kowalski J, Bartelt P (2010a) RAMMS: Numerical simulation of dense snow avalanches in three-dimensional terrain. *Cold Reg Sci Technol* 63:1–14
- Christen M, Bartelt P, Kowalski J (2010b) Back calculation of the In den Arelen avalanche with RAMMS: interpretation of model results. *Ann Glaciol* 51(54):161–168
- Chrustek P (2005) Zastosowanie GIS w typologii obszarów potencjalnego występowania lawin śnieżnych na przykładzie rejonu Kasprowego Wierchu w Tatrach. MSc Thesis. Jagiellonian University, Kraków
- Chrustek P, Wężyk P (2009) Using high resolution LiDAR data to estimate potential avalanche release areas on the example of polish mountain regions. In: Schweizer J, Van Herwijnen A (eds) *International Snow Science Workshop. 27 Sep to 2 Oct 2009, Davos, Switzerland. Proceedings. Swiss Federal Institute for Forest, Snow and Landscape Research Birmensdorf*
- Chrustek P, Biskupič M (2010) Extreme snow avalanche events in Tatra Mountains. In: Ostapowicz K, Kozak J (eds) *Conference proceedings of the 1st forum carpaticum, integrating nature and society towards sustainability, Cracow, Institute of Geography and Spatial Management, Jagiellonian University, Kraków*
- Deems J, Painter T (2006) Lidar measurement of snow depth: Accuracy and error sources. In: *proceedings of the international snow science workshop, 1–6 October 2006, Telluride, CO, USA*
- Gruber U (2001) Using GIS for avalanche hazard mapping in Switzerland. In: *proceedings of the 2001 ESRI international user conference, July 9–13, 2001, San Diego, USA*
- Gruber U, Bartelt P (2007) Snow avalanche hazard modelling of large areas using shallow water numerical methods and GIS. *Environ Model Softw* 22(10):1472–1481
- Gruber U, Maggioni M, Stoffel A (2002) Definition and characterization of potential avalanche release areas. In: *Proceedings of the 22nd ESRI international user conference, October 15, 2002, San Diego, USA*
- Gruber U, Margreth S (2001) Winter 1999: a valuable test of the avalanche-hazard mapping procedure in Switzerland. *Ann Glaciol* 32:328–332
- Heritage GL, Large ARG (2009) *Laser scanning for the environmental sciences. Blackwell Publishing Ltd, West Sussex*
- Jamieson B, Margreth S, Jones A (2008) Application and limitations of dynamic models for snow avalanche hazard mapping. In: *Proceedings of the ISSW 2008, Whistler, Canada*
- Jörg P, Fromm R, Sailer R, Schaffhauser A (2006) Measuring snow depth with a terrestrial laser ranging system. In: *proceedings of the international snow science workshop, 1–6 October 2006, Telluride, CO, USA*
- Maggioni M (2005): *Avalanche release areas and their influence on uncertainty in avalanche hazard mapping. PhD Thesis, Department of Geography, University of Zurich UZH, Switzerland*
- Maggioni M, Gruber U (2003) The influence of topographic parameters on avalanche release dimension and frequency. *Cold Reg Sci Technol* 37:407–419
- McCollister CH, Comey R (2009) Using LiDAR (light distancing and ranging) data to more accurately describe avalanche terrain. In: Schweizer J, Van Herwijnen A (eds) *international snow science workshop. 27 Sep to 2 Oct 2009, Davos, Switzerland. Proceedings. Swiss federal institute for forest, snow and landscape research, birmensdorf*
- Pagliardi M, Barbolini M, Corradeghini P, Ferro F (2009) Identification of areas potentially affected by extreme snow avalanche combining expert rules, flow-routing algorithms and statistical analysis. In: Schweizer J, Van Herwijnen A (eds) *International snow science workshop. 27 Sep to 2 Oct 2009, Davos, Switzerland. Proceedings. Swiss Federal Institute for Forest, Snow and Landscape Research, Birmensdorf*
- Perla R, Cheng TT, McClung D (1980) A two-parameter model of snow-avalanche motion. *J Glaciol* 26(94):197–207
- Prokop A, Schirmer M, Rub M, Lehning M, Stocker M (2008) A comparison of measurement methods: terrestrial laser scanning, tachymetry and snow probing for the determination of the spatial snow-depth distribution on slopes. *Ann Glaciol* 49:210–216
- Reiss R, Thomas M (1997) *Statistical analysis of extreme values. Birkhäuser Verlag, Basel*

- Riegl (2010) Data sheet of the LPM-321 http://www.riegl.com/uploads/tx_pxpriegldownloads/10_DataSheet_LPM-321_18-03-2010.pdf. Accessed 20 October 2010
- Salm B (2004) A short and personal history of snow avalanche dynamics. *Cold Reg Sci Technol* 39(2–3):83–92
- Salm A, Burkard A, Gubler HU (1990) Berechnung von Fliesslawinen eine Anleitung für Praktiker mit Beispielen. Eidgenössisches Institut für Schnee und Lawinenforschung Technical Report 47, Davos
- Sampl P, Zwinger T (2004) Avalanche simulation with SAMOS. *Ann Glaciol* 38:393–398
- Sauermoser S, Illmer D (2002) The use of different avalanche calculation models practical experiences. In: International congress Interpraevent, Matsumoto, Japan
- Shan J, Toth CK (ed) (2008) Topographic laser ranging and scanning. Principles and Processing, Taylor & Francis Group, Boca Raton
- Vallet J, Skaloud J, Koelbl O, Merminod B (2000) Development of a helicopter-based integrated system for avalanche mapping and hazard management. *Int Arch Photogramm Remote Sens Spatial Inf Sci* 33:565–572
- Vallet J (2008) High precision LiDAR mapping for complex mountain topography. In: Hurni L, Kriz K (eds) Proceedings of the 6th ICA mountain cartography workshop 11–15 February 2008, Zurich, Switzerland
- Voellmy A (1955) Ueber die Zerstörungskraft von Lawinen. *Schweiz Bauztg* 73:159–285
- VRMesh (2010) <http://www.vrmesh.com/>. Accessed 14 October 2010
- Wężyk P, Borowiec N, Szombara S, Wańczyk R (2008) Generation of digital surface and terrain models in Tatra based on point cloud from airborne laser scanning (ALS). *Archive of photogrammetry, Cartography and remote sensing*. ISBN 978-83-61576-08-2, Szczecin, 18b, 651–661
- Wężyk P (2006) Introduction to the laser scanning technology in forestry. *Annals of Geomatics* 4:119–132

Publication 8

Liščák, P., **Biskupič**, M., Richnavský, J., Bednařík, P., Geological hazards, in Dalezios, N., R., (Eds.) Environmental Hazards Methodologies for Risk Assessment and Management, IWA Publishing, London, (book chapter)



Chapter 10

Geological hazards

*Pavel Liščák, Marek Biskupič, Josef Richnayvsky
and Martin Bednarik*

10.1 MASS MOVEMENT HAZARDS

Two main counter-forces are shaping the morphology of the Earth's surface – Earth's internal heat vs gravity. While the internal energy of the Earth drives orogenic processes of mountains formation, the gravitational force is acting in the sense of surface levelling. These gravity-induced processes are termed as mass wasting. They include erosion, abrasion, sliding, etc. and the transporting agents are water, air and ice.

10.1.1 Slope deformations

Slope deformation (synonyms: slope failure, gravitational slope deformation, gravitational re slope failure) is a resulting form of slope movement generated by gravitational force, which led to a formation of a body differing from the surrounding rock environ due to change in shape, location or volume, or internal structure.

Landslide is a type of slope failure, which evolved as a result of gravitation movement of rock or soil masses along one or several shear planes. The main parts of landslide are depicted in Figure 10.1.

Slope movement is a geodynamic process, during which transport of rock masses occurs as a result of the effect of gravitational force of the Earth or the Moon. The result of the process is a slope failure. In civil engineering, *sensu stricto*, the slope movement doesn't comprise the cases, when the rock masses are transported by transportation media (water, ice, snow or wind).

Sliding a relatively short-term, glide down-slope movement of rock mass along one or a series of shear planes, in which a part of sliding masses is relocated above intact rocks, thus creating a landslide accumulation.

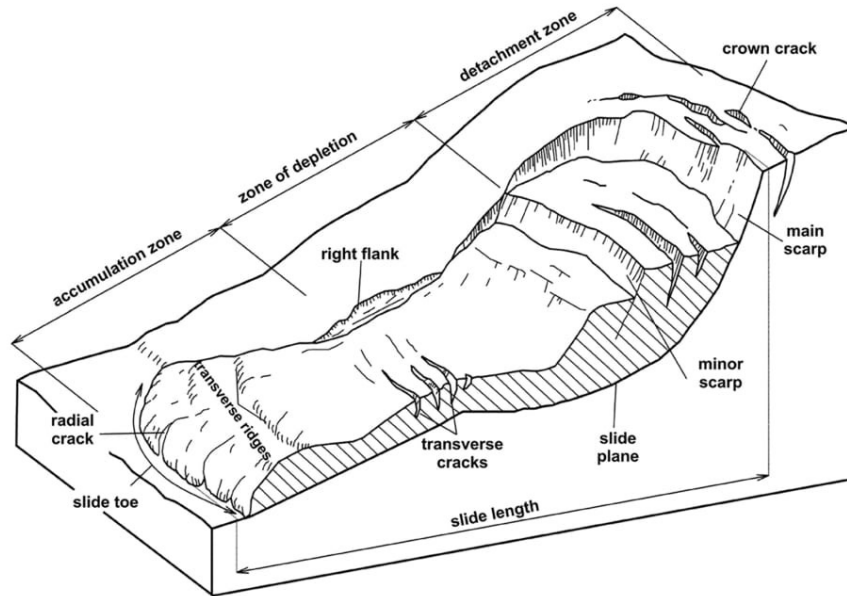


Figure 10.1 Landslide and its major morphologic signs (modified according to Petro *et al.* 2008)

Slope stability is a capability of natural or artificial slope (cut, embankment, levee, etc.) to sustain certain angle. Slope stability is affected by geometric (slope angle, bedding etc.), hydrogeological and climatic (groundwater table level, precipitation totals, effective precipitation, etc.) conditions and engineering geological conditions (bulk gravity, shear strength). Slope stability is assessed in the form of stability degree.

Slope stability degree is a numerical expression of a ratio between passive forces – friction strength, which act against rock disturbance, and the active forces – shearing stress, tending down-slope pull. Slope stability degree is marked by a symbol F and is calculated by the following formula:

$$F = \frac{\sum P}{\sum A} \quad (10.1)$$

where $\sum P$ is a sum of passive forces acting in the slope, $\sum A$ is a sum of active forces acting in the slope.

10.1.2 Snow avalanches

Snow avalanches are typical mass downslope movements and are a part of bigger group called natural hazards. Mass of snow moving downslope driven by

340 Environmental Hazards Methodologies for Risk Assessment

gravitational force is usually referred to as snow avalanche. Snow avalanches can range from only a few meters long, almost harmless sluffs, to several kilometres long, disastrous avalanches capable of destroying a whole village.

Topography of the slope and meteorological condition are the most important factors and, thus, determine when and where the naturally triggered avalanches will be released. On the other hand, human triggered avalanches include a third factor, which is us, the human being. There are two basic types of snow avalanche classification based on the following:

- (1) type of triggering mechanism and motion (loose snow, slab and glide avalanche);
- (2) type of snow in avalanche (wet, powder and mixed avalanches).

Despite the fact that snow avalanches do not have the impact of large natural hazards as earthquakes, floods and volcanic eruptions, they still can be a threat to humans and infrastructure in mountainous areas. Worldwide annual statistics count approximately 250 fatalities caused by snow avalanches. An example of one of the biggest avalanches is shown in Figure 10.2.



Figure 10.2 One of the biggest avalanches in Carpathian mountain range was released from the slopes of Prislop in Žiarska valley (Western Tatras) in March 2009.

10.1.3 Ice avalanches

Ice avalanches are common glacial hazard occurring in glaciated areas. They belong to typical gravity driven mass wasting process. Ice avalanche occurs when a large mass of ice breaks off from a glacier, drops downslope and bursts into pieces of ice (Alean, 1984; Margharet & Funk, 1999). Many high alpine hanging glaciers produce ice avalanches as normal ablation process on steep slopes. The main preconditions for ice avalanching are: steep slope (critical $> 25^\circ$), sufficient ice mass and certain degree of instability within the ice mass (Salzman *et al.* 2004). Most of the hanging glaciers fulfil the required conditions. Hanging glaciers are small type of glaciers originating from the steep mountain faces or wall of the glacier valley. Large ice masses do not detach from steep hanging glaciers very often. Such cases are extremely rare, occurring usually during the melt season, when the stability reaches its critical state. Ice avalanches are comparable to snow avalanches, however, they occur less frequently.

Combined ice – snow avalanches together with rock falls can gain high destructive potential with very long run-outs (Margharet & Funk, 1999). Major ice avalanche catastrophes usually draw public attention. In 1970, earthquake in Peru induced rock/ice avalanche from the slopes of Nevado de Huascarán. The consequent mass wasting process killed approximately 20,000 people (Plafker, 1978). Another large scale combined rock/ice was recorded in Northern Caucasus – Kolka region in September 2002. This event took the life of 140 people and caused large destruction (Kääb *et al.* 2003).

Despite the fact that occurrence of ice avalanche is low compared to other geological hazards in combination with other mass wasting processes, they can have disastrous potential. It can be assumed that with ongoing climatic change and glaciers retreat, it is expected to hear more about ice avalanches in the near future.

10.2 LANDSLIDES

Mass movements can be divided according to major (mechanism of movement, rate of movement) and minor features (age, activity degree, genesis, slope structure) into groups and types. In Slovakia the most adopted classification is according to Nemčok *et al.* (1974), which distinguishes slope movements based on the rate of the movement: creeping, sliding, flowing and falling.

10.2.1 Landslides classification

Worldwide, the most adopted is the classification by Cruden and Varnes (1996), which distinguishes six groups (Table 10.1).

Falls are abrupt movements of masses of geological materials, such as rocks and boulders, that become detached from steep slopes or cliffs, undercut by eroding agents like stream, glacier, ocean, lake or wind loaded with aeolian sediments. The fall is the fastest of slope movement types with velocities reaching

342 Environmental Hazards Methodologies for Risk Assessment

100–200 km hour⁻¹ (terminal velocity). Separation occurs along discontinuities, such as fractures, joints, and bedding planes, and movement occurs by free-fall, bouncing, and rolling. Falls are strongly influenced by gravity, mechanical weathering, and the presence of interstitial water. Repeated falls in one place over certain time period result in an accumulation of fragments and blocks termed as talus.

Table 10.1 Schematic landslide classification adopting the classification by Cruden and Varnes (1996).

Movement type		Type of Sliding Material		
		Rocks	Soils (Engineering Soils)	
			Non-Cohesive in Prevail	Cohesive in Prevail
Fall		Rock fall	Debris fall	Soil fall
Topples		Toppling of stony blocks	Debris topple	Soil topple
Sliding	Along rotational shear plane	Rock slide	Rock slump	Earth slide
	Along planar shear plane		Earth block slide Earth slide	
Lateral movement (block displacement)		Rock spread	Rock spread	Earth spread
Flow		Rock flow, rock avalanche	Debris flow, debris avalanche	Earth-flow, (soil creep)
Complex – combination of two or more prevailing types of movement				

Toppling failures are distinguished by the forward rotation of a block about some pivotal point, below or low in the block, apart from the rock massif, under the actions of gravity and forces exerted by adjacent blocks, by fluids in cracks (freezing and thawing), by temperature changes or by wedge effect of roots.

There are five basic categories of **flows** that differ from one another in fundamental ways.

Debris flow. Sudden channelled flows of large masses of weathered material (sand, clay, fragments of rock), vegetation and water in a form of a slurry down the slope due to extremely intense precipitation (long-term rainfall, heavy rains) or by a sudden snow melt. The debris flows are often accompanied by landslides and rock avalanches. The debris flows are formed mainly in high mountains with steep slopes over 30°.

Debris avalanche. This is a variety of very rapid to extremely rapid debris flow, often related to the catastrophic collapses from an unstable side of a volcano.

Earthflow represents a movement of colluvial fine-grained material, substantially wetted and saturated with water, forming a bowl or depression at the head.

Mudflow is a much faster earthflow consisting of material that is wet enough to flow rapidly and that contains at least 50 percent sand-, silt-, and clay-sized particles. They are triggered by extremely heavy rains or snow thawing.

Creep or **flowage** is the imperceptibly slow, steady, downward movement of slope-forming soil or rock. Its ultimate cause is gravity. Movement is caused by shear stress sufficient to produce permanent deformation, but too small to produce shear failure. Typical manifestations of creep are curved tree trunks (“drunken forest”), bent retaining walls, fractured engineering structures, tilted poles or fences, and small soil ripples or ridges.

Lateral spreads occur typically on very gentle slopes or flat terrain. The dominant mode of movement is lateral extension accompanied by shear or tensile fractures. The failure is caused by liquefaction of sensitive clays or sandy clays, usually triggered by rapid ground motion, for instance due to an earthquake.

10.2.2 Landslide causes

Essentially the mass movement occurs whenever the downward acting gravity and resulting shearing stress overcomes the forces resisting the sliding or flow – shear and friction strength. When shearing stress exceeds friction or shear strength, sliding occurs. This scenario may occur both due to naturally generated change of stability conditions and improper anthropogenic interventions into the slope.

10.2.2.1 Geological causes

The following list may be used: (a) weak or sensitive materials, (b) weathered materials, (c) sheared, jointed, or fissured materials, (d) adversely oriented discontinuity (bedding, schistosity, fault, unconformity, contact, and so forth), (e) contrast in permeability and/or stiffness of materials, and (f) earthquake.

10.2.2.2 Morphological causes

This class may include the following: (a) tectonic or volcanic uplift, (b) glacial rebound, (c) fluvial, wave, or glacial erosion of slope toe or lateral margins, (d) subterranean erosion (solution, piping), (e) deposition loading slope or its crest, (f) vegetation removal (by fire, drought), (g) thawing, (h) freeze-and-thaw weathering, and (i) shrink-and-swell weathering.

10.2.2.3 Human causes

This class may include: (a) excavation of slope or its toe, (b) loading of slope or its crest, (c) drawdown (of reservoirs), (d) deforestation, (e) irrigation, (f) mining, (g) artificial vibration, (h) water leakage from utilities.

10.3 SNOW AVALANCHES

Avalanches are usually released on the slope, where the gravitational force on the snowpack exceeds the internal cohesive force between the individual snow layers and the mass of snow starts to move downslope. Basically, there are two types of avalanches: (1) avalanches starting from a single point – **loose snow avalanches** and (2) avalanches in a form of cohesive snow layer – **slab avalanches**. The slab avalanches are the ones, which are the most dangerous to people and property. As a consequence of various precipitation events, the snowpack consists of several layers. The main prerequisite for triggering the slab avalanche is the presence of weak layer within the snowpack. The weak layer consists of snow grains, which have very low internal cohesion within the layer. On contrary, with normal snow layers, weak layers are usually not as hard and they tend to collapse easily. Release of snow slab starts with fracture, which propagates within the weak layer across the snowpack and the so-called snow slab is triggered. Consequently, the snow mass of a slab is triggered and driven downslope by gravitational force. The causes of initial fracture can be various ranging from precipitation, temperature change, cornice fall or additional load by winter traveller or explosive. The snow is the main substance in snow avalanches, but during their motion the avalanche entrains other substances, such as air, soil, rock debris, trees, etc. Multiple avalanche experiments have confirmed that dry slab avalanches can gain speeds of 50–100 km/h depending on terrain topography. However, powder avalanches are the ones that can reach maximum velocities of 200–300 km/h (Figure 10.3).

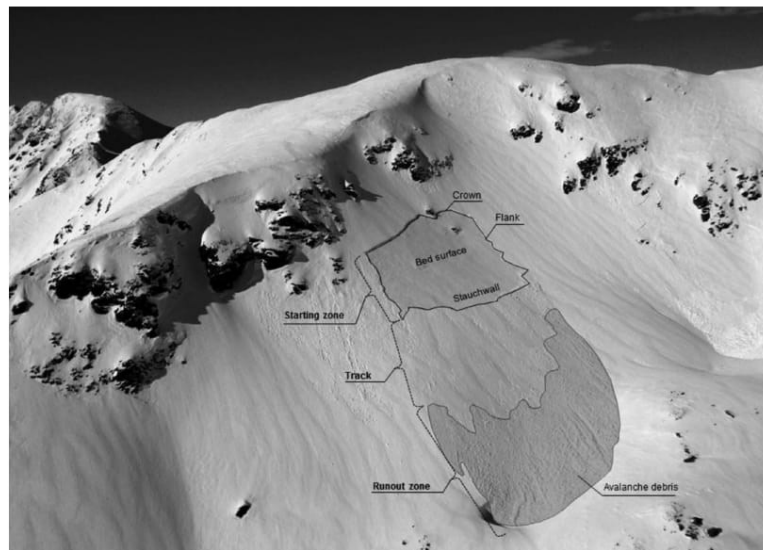


Figure 10.3 Parts of an avalanche slide path.

Besides the snow avalanches in the mountains, roof avalanches occur equally, however, these types are far less of a concern. No snow avalanche would ever be triggered without a steep avalanche-prone slope. While the snow is the sliding medium, mountain slopes provide sliding surface for every avalanche. The vast majority of avalanches are released from slopes with an angle between 30°–45°. Usually, slopes less steep than 30° are just not steep enough to produce an avalanche, but they might be avalanche-prone only during extremely unstable conditions or for special avalanche types (e. g. slush flows). Slopes steeper than 45° are subject of frequent sluffs and small avalanches and they do not collect enough snow to trigger large snow avalanches. According to worldwide statistics (Jamieson, 2000) the most avalanche-prone slopes are 30°–45° with 37° as prime avalanche angle. Other factors, which affect the avalanche predisposition of certain slope are: aspect, land cover, slope shape curvature and elevation.

Avalanche starts in starting zone also sometimes referred to as a release or trigger zone. After the fracture propagates in the snow, slab starts to move and gain speed. Crown face height and crown length have great importance, thus, they determine the volume, which gives initialization to the slab. Avalanches gain the highest velocities in track and here they entrain more snow, soil or rocks. In a very steep terrain, large slab avalanches can turn into very destructive powder avalanches. Mixture of air and snow at high velocities create an air blast with very destructive force. When the slope becomes less steep or surface friction exceeds certain limits the avalanche starts to decelerate. This happens in the runout zone, where the avalanche stops and thus creates avalanche debris. Depending on the size of avalanche (Table 10.2), avalanche debris can range from tens of centimetres to tens of meters.

10.3.1 Types of snowpack

Snow is the crucial building material of every avalanche and thus it influences the triggering and avalanche motion. The type of snowpack greatly depends on climate. In general, there are three different snowpack types based on climate: maritime, intermountain, and continental. Snow packs in maritime climate are usually thick, strong and warm. On the other hand, continental snowpack's are thin, cold and weak. Intermountain snowpack are somewhere in between of maritime and continental. Of course, there are no strict boundaries and in certain period of winter season there might be continental thin and cold snowpack in coastal mountains and vice versa. This phenomenon is often visible on small scale, when it is possible to find two different snowpack types just a few meters from each other. For example, wind scoured areas can show presence of continental snowpack and just below the ridge on the lee side there is a maritime thick snowpack.

According to many previous studies and observations, snowpack in coastal mountains tends to be over 3 meters deep with relatively warm temperatures near to freezing point (–5°C to +5°C). The new snow falls at high rates with high

densities while avalanches occur immediately during or just after the storms. The weak layers often form at the transition between new and old snow and include low cohesion layers or graupel with a short life span. The intermountain snowpack is, on the average, 1.5 to 3 meters deep with temperatures ranging from -15°C to -3°C . Weak layers, such as faceted snow or buried surface hoar, can persist for several days. Also the avalanche activity and snowpack instabilities can remain for longer periods (weeks). The thinnest (<1.5 metres) and the coldest (-10°C to -30°C) snowpack is the one in continental climates. The new snow falls at low rates and low densities. The most common weak layers consist of faceted snow, depth and surface hoar, which can last for prolonged periods of time. Even many days after the storms, either naturally or human triggered avalanche activity can be observed.

Table 10.2 Classification of avalanches by size.

Classification/ Size		Destructive Potential	Run-Out	Typical Length and Volume
Size 1	Sluff	Typically does not bury a person, could carry a person away (danger of falling)	Stops typically before the end of a slope	<50 m 100 m^3
Size 2	Small avalanche	Could bury, injure or kill a person	Stops typically at the end of a slope	$50\text{--}200$ m 1.000 m^3
Size 3	Medium avalanche	Could bury and destroy a car, damage truck, destroy a small building or break a few trees	Could traverse a flat terrain (considerably below 30°) over a distance of typically less than 50 m	$200\text{--}600$ m 10.000 m^3
Size 4	Large avalanche	Could destroy a railway, large truck, several buildings or a small forest area of approx. 4 hectares	Could traverse a flat terrain (considerably below 30°) over a distance of typically more than 50 m	1 km 100.000 m^3
Size 5	Very large avalanche	Could gouge the landscape, catastrophic destructive potential	Reaches the valley floor, the largest run out distances known	$2\text{--}3$ km $>100.000\text{ m}^3$

10.3.2 Avalanche formation and motion

Generally, avalanches can be triggered either as loose snow or a slab. In the second case, the slab is released after fracture propagates across certain area and creates initial volume that starts to slide downslope. As a result of bed roughness, slabs break into smaller blocks and particles. As the avalanche motion continues, the particles become smaller due to their collision among themselves and surface. As the velocity increases, the particles become smaller and smaller. After the particles are broken into fine elements or the avalanche runs for longer distance, the motion develops into a flow. High density material of snow particles and air flow at the bottom of the avalanche creates the so-called core. In the case of dry snow entrained in avalanche, the low density dust cloud is being created around the core. It has been estimated that one third to one half of the volume of the core represents the snow particles and the rest is the air. On the contrary, in the dust cloud, only about 1% of the space is filled with snow particles and 99% is air. Estimating the speed of avalanche and its impact, pressures is subject of exhaustive research and studies. Basically, the speed depends on the terrain roughness, resistive forces between the core and surface and resistance between the dust and air. Of course, most of the frictional resistive forces are generated at the bottom of the avalanche between the core and sliding surface. All the rubbing and collision between particles generate heat that results in the production of small amount of water. Avalanche decelerates and stops in the runout zone. Water causes snow particles to freeze together. This results in debris hard to penetrate with shovels and probes making avalanche rescue very demanding. It is well known that avalanche motion plays a crucial role in avalanche modelling and estimating runout distances. Figure 10.4 shows the sequence of an avalanche motion in different time steps calculated by numerical model RAMMS.

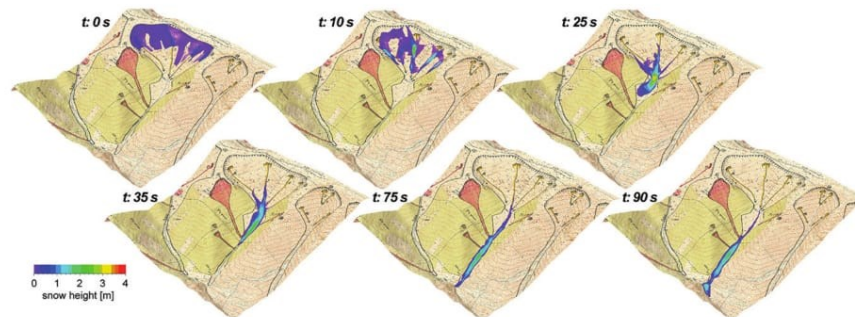


Figure 10.4 Sequence of an avalanche motion in different time steps calculated by numerical model RAMMS.

Snow avalanches usually entrain a large amount of snow from the slope during their motion (Sovilla *et al.* 2001). The entrainment affects the motion and it should

be taken into account by the model. The mechanisms of entrainment can be different depending on the avalanche type (whether it is a heavy dense avalanche or a light dry one, or a powder one). In the same avalanche there can be various mechanisms of entrainment (Gauer & Issler, 2004). The entrainment mechanism for heavy dense avalanches differs from that for light dry ones. Numerous studies have shown that avalanches can entrain 10 times more of snow than the initial slab volume.

10.4 SLOPE MOVEMENTS MITIGATION

Depending upon the infrastructure under threat of slope failure and the magnitude of slope failure, the measures are implemented to safeguard the slope stability, or to protect a slope. In the case of sudden slope failures, **emergency remedial measures** are realized immediately. The aim is to stop or at least slow down the slope movement and to alleviate the damage to a minimum scale. The principal strategy is to reduce the water content, or pore pressure, in the sliding masses and thus to increase the frictional resistance to sliding. The prevention against infiltration of surface water in the sliding masses can be reached by covering the surface with impervious material, by clogging the cracks in the landslide body with impervious material and diverting surface runoff above the slope by system of drainage ditches. The subsurface water content can be reduced by intense pumping of water from the existing wells. In the case of relatively pervious rocks a system of sub-horizontal drainage wells can also help to carry the water out of the slide area.

In the case of small-scale landslides the stability can be increased by additional surcharge material at the toe of the slope. In the case of large investments, for instance construction of highways, tunnels, railways or development of urban areas, **remedial measures** are implemented. They are usually preceded by mapping and survey, which shall clarify the engineering geological conditions and identify areas at risk and shall suggest effective stabilizing measures.

Among the essential measures belongs the **slope modification**. This includes (1) reduction of the slope angle, (2) additional support of the slope foot (accumulation zone) by material surcharge, and (3) reduction of load on the slope by removal of a certain portion of the sliding material from the detachment zone and zone of depletion.

Slope drainage includes both surface and subsurface dewatering of the slope. The surface drainage shall prevent the slope against infiltration of precipitation water into the slope and divert the water from the parts above the sliding slope. The subsurface drainage is realized by sub-horizontal boreholes, sometimes combined with gravel drainage piles or walls.

Technical stabilization measures involve anchoring combined with (micro) pile retaining walls. In the case of smaller slides in silty- and clayey rock masses the stabilizing-drainage ribs are often applied combined with gabion walls. Rock bolts are used to stabilize rockslides and rocky slopes. As a passive measure on

steep rocky slopes, mainly above the communications, protective barrier or catch fences are used. They are made of flexible mesh so that the energy of debris flow is dissipated. The protective galleries are built as overshoots above roads to prevent them from debris flows and snow avalanches. Material simply slides over the roof of the protective structure and continues down the hillside.

Protection of near surface soil against weathering and erosion includes ground covers or other vegetation planted. The most preferred are fast growing plants with sturdy and extensive root systems. The alternative protection offer thin sheets of concrete, gravel or geotextile.

10.5 AVALANCHE MITIGATION

It is very demanding and so far impossible to forecast avalanches with very precise timing. As the avalanches occur very suddenly there is no way to expect them in advance of days or weeks. Therefore, the mitigation and protection measures have to be adapted to the very specific avalanche behaviour. Avalanches failing in remote uninhabited locations do not pose serious threat to human settlements and infrastructure. The mountain settlements, roads and mountain infrastructure are the most vulnerable to avalanches. Damage from interaction of avalanches and human activities can be prevented by controlling the avalanches either by explosives and permanent structure placing into avalanche path or evacuations (Figure 10.5).



Figure 10.5 Snow fences placed in the release zone are used prevent avalanche to trigger.

The aim to avalanche control by explosives is to artificially and periodically trigger smaller avalanches by exposing the snowpack to the air blast from explosion.

350 Environmental Hazards Methodologies for Risk Assessment

Explosion, which is most effective over the snowpack, creates forces, which put additional loading and stress on the snowpack, which tends to slide and create avalanches (Figure 10.6). Regular control by explosives prevents the creation of large and disastrous avalanches, which could threaten human infrastructure. Artificial avalanche triggering can be done either by using permanent installations (towers mast or lifts) with reserve of explosives, which are usually remotely triggered. These installations are placed in the release zones of avalanche paths. The advantage is that they can be used in almost any kind of weather unless the lower placed infrastructure (road, lifts etc.) are not in use or operation. Another and more flexible approach is to carry explosives by helicopter, but this way is limited by weather and flight conditions. Sometimes, hand charges are being used mostly around ski slopes and lifts.



Figure 10.6 Hand charges assembled in to the area of avalanche starting zone.

Permanent structures, which are placed either in release or run-out zones are often used to protect human settlements and roads. Installations in run-out zones (snow fences, supporting structures) tend to prevent avalanche initiation, while the installations in track and run-out zones (deviation, retarding dams, snow sheds, galleries, and splitting wedges) tend to deflect and decelerate avalanche in motion or they directly protect from the influence of avalanches. These installations are the ones most expensive and they do have large impact on the nature. On the other hand, they are the most effective. By far the most nature friendly method is to use forest and its natural avalanche protection feature. However, this requires reforestation in the avalanche path, which can be done only until the upper border of treeline and it is rather cost and time-consuming.

10.6 MASS MOVEMENT HAZARD AND RISK ASSESSMENT

The assessment of landslide hazard and risk is predominantly important in urbanised zones included into land use plans, which assume certain socioeconomic and technological progress of a region. Especially, during the last decade, a number of scientific works have been devoted to statistical approaches to landslide hazard using map algebra tools implemented within the geographic information systems. This methodology includes the assessment of landslide hazard, identification of the elements at risk, assessment of vulnerability and the assessment of landslide risk (Figure 10.7). The application of Geographic Information Systems (GIS) represents an innovative, modern and prospective approach in the assessment of hazards and risk for larger territorial units. This section is focused on the theoretical description of the most common quantitative methods used for landslide hazard or susceptibility assessment.

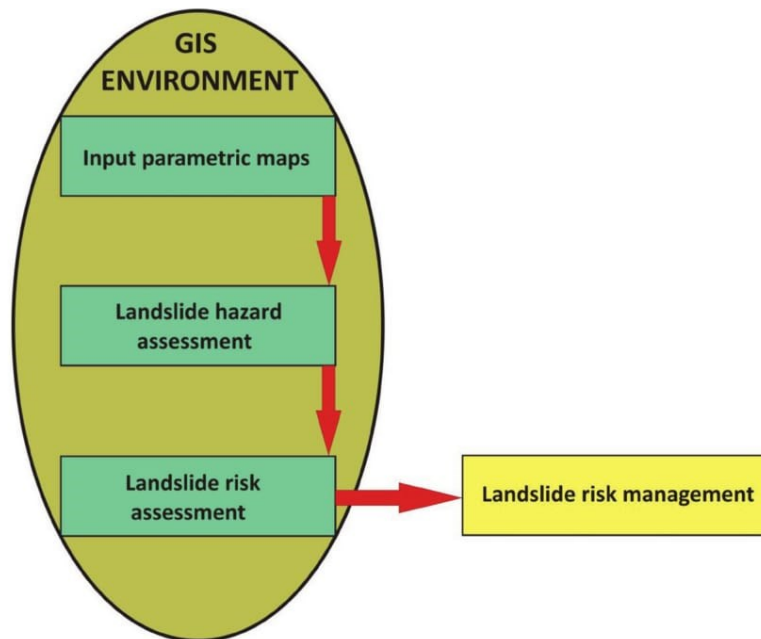


Figure 10.7 Flowchart of processing the landslide risk issue.

10.6.1 Risk terminology

The terminology used here is based on the conventional terminology according to Varnes (1978, 1984), van Westen (1993), and Aleotti and Chowdhury (1999).

Landslide hazard is defined as the probability of occurrence of landslide event within specific area and time period. **Vulnerability** reflects the capacity of the system and its elements to react to the occurrence of a harmful phenomenon in the form of a loss or damage. **Element at risk** is an element of the assessed system, where loss and damage may appear during the occurrence of a potentially harmful phenomenon. **Risk** represents probable losses and damage on the endangered elements of the environment caused by the occurrence of a potentially damaging phenomenon. Leroi (1996) defines the risk as an expected loss (toll of casualties, loss of property and interrupted economic activities) due to a specific hazard in a given area and time period. As a mathematical expression, the risk is a product of hazard and vulnerability. Four basic axioms are needed before we start to assess landslides hazard:

- (1) landslide will occur under identical geological, geomorphological, hydrogeological and climatic conditions as in the past;
- (2) the triggering factors of landslides may be defined and analysed;
- (3) the degree of landslide hazard must be quantifiable;
- (4) slope deformations must be classifiable.

10.6.2 Methods of landslides hazards assessment

Generally, the methods of landslide hazard assessment (Figure 10.8) can be divided into qualitative and quantitative. This section covers the group of the quantitative methods, particularly the statistical analyses, deterministic approach, application of fuzzy logic and neural networks. The most applied and verified statistical methods are the multivariate statistical analysis and the bivariate statistical analysis, respectively.

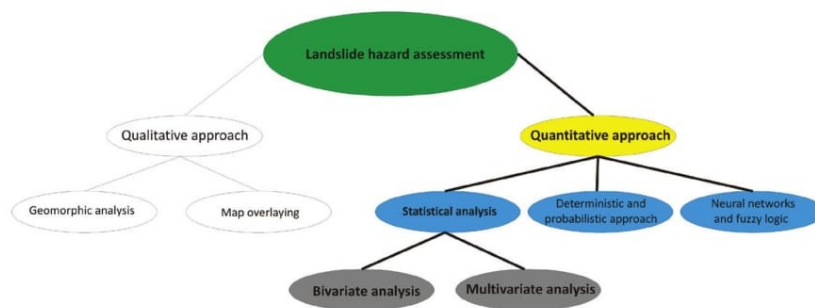


Figure 10.8 Methods of landslide hazard assessment.

The task of predicting the landslide hazard is to delimitate a certain degree of probability, the spatial delimitation of the occurrence of a landslide event as well as its intensity and time frequency. The spatial delimitation of landslides may be predicted with high probability, based on the analyses of relevant factors, using mentioned quantitative methods.

10.6.2.1 Bivariate statistical analysis

This method presents a statistical combination of each input parametric map with the landslide inventory map. The bivariate statistical analysis works with one dependent variable – landslide inventory map and one independent variable – the individual input parametric maps. The result of the combination is the delimitation of the total number of grid cells with or without landslides within the individual classes of input parametric maps, calculated as areal units or as percentage. The double combinations are stored in a table form, where one of the numbers represents the parametric map class and the second shows the presence or absence of landslides (0–false, 1–true).

Based on the combinations, each parametric map must be reclassified secondarily. During the secondary reclassification the existing classes in each parametric map are attributed with new numerical values representing statistically defined landslide probability. The top numerical value is attributed to the most landslide susceptible class and the lowest numerical value means that the class is the least susceptible to landslides. The consistency of the technical preparation of the parametric maps, especially the differences in the position accuracy, superposition and grid geometry, has a great influence on the accuracy of the results. The result of the bivariate statistical analysis is the landslide hazard map which is a weighted sum of the secondarily reclassified parametric maps. The equation for the final sum is as follows:

$$y = \sum_{i=1}^n C * V_i \quad (10.2)$$

where: y – the value in the final landslide hazard map, i – the individual parametric maps, C – class value, V_i – weight of the relevant parameter.

There are different approaches to the determination of input parameter weights. In principle, they may be divided into two major groups. The first group is the subjective approach based on expert opinion – analytical hierarchy process (AHP), Fuller triangle; and the second group is based on the mathematical approach – entropy model, frequency ratio (FR).

The result of the weighted sum is a continuous interval of values representing the landslide hazard value in the study area. The continuous interval must be classified as a level of landslide hazard. The most convenient are five classes corresponding to very low, low, medium, high and very high degree of landslide hazard (Bednarik *et al.* 2010; Constantin *et al.* 2010). The literature contains the following classifications:

- (a) Expert-based classification – it is based on expert experience, is very subjective and very misleading when applied within large regions.
- (b) Binary classification – it uses the 0.5 threshold in distinguishing two extreme cases, the presence or absence of landslides. However, this approach does not define more prone or less prone zones to landslides.

354 Environmental Hazards Methodologies for Risk Assessment

- (c) Natural breaks classification – a conventional classification method, mainly in the case of data with evident breaks and discrete data.
- (d) The standard deviation – it works with the mean determining the class median and uses the standard deviation (+ and –) to determine the extent of the individual landslide susceptibility classes.
- (e) The equal interval method – it equally distributes the final sum into three or five used classes.

Figure 10.9 below provides the principle of the bivariate analysis determining the parameter weight values.

10.6.2.2 Multivariate statistical analysis

The most used multivariate analyses are the conditional analysis and logistic regression analysis, both provide a comparable and satisfactory prediction.

10.6.2.2.1 Conditional analysis

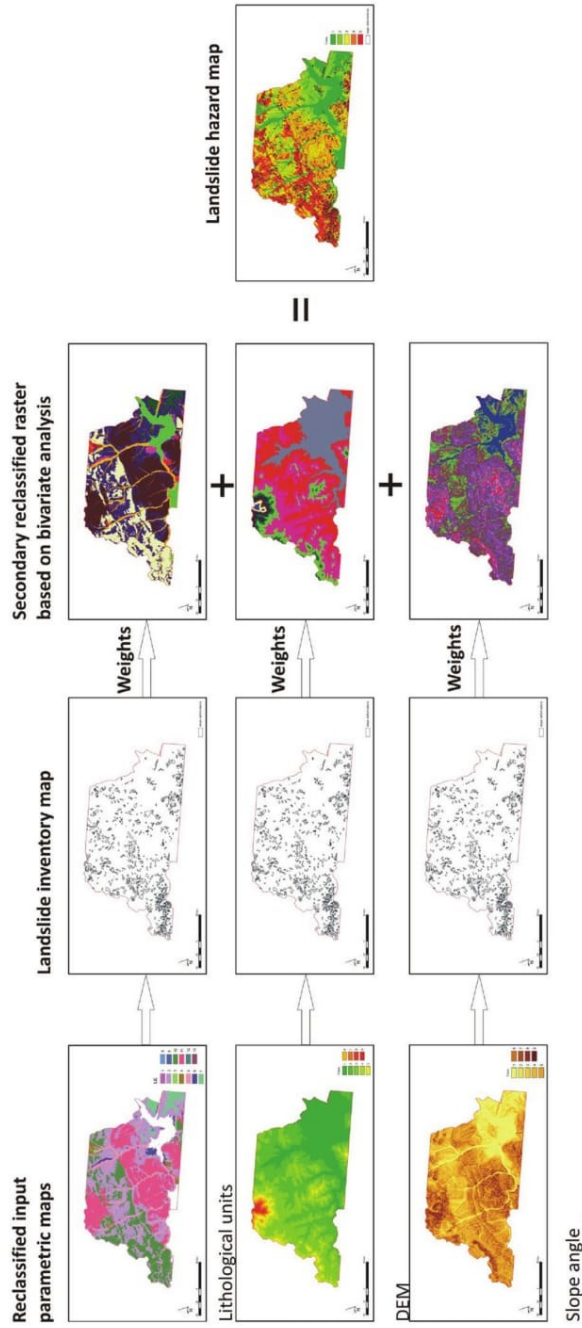
Multivariate statistical analysis is based on the mutual combination of all input parametric maps (lithology, slope, altitude, slope deformations) and a subsequent application of the information within areas, where no landslides have been registered (Figure 10.10). During this analysis the geohazard assessment does not include the weighting process.

In the case of the conditional analysis (Clerici, 2002) the outcome is a table containing the mutual combination of all input parametric maps, including all category combinations arising from the superposition of all the input maps. These combinations create new spatial units, the so-called unique conditional units (UCU), in the final map. For example, if there is the category 6 (10–15°) in the slope angle map, category 4 (slope sediments) in the lithology map and class 3 (spruce forest) in the land use map, the final unique conditional unit is the combination 6–4–3.

In the case of the multivariate analysis, no secondary reclassification and parameter weighting is needed. The final combinations containing landslides (value 1, true in the landslide map) are ordered based on the calculated occurrence density – the ratio of the landslide UCU cell number to the total area (the descending result gives the least favourable combinations for landsliding). The shell script in GIS GRASS may be used to classify all the combinations into the relevant class number (3 or 5) that expresses the degree of landslide susceptibility or hazard (Clerici, 2002; Bednarik *et al.* 2005).

10.6.2.2.2 Logistic regression analysis

Logistic regression models are used to predict a dependent variable Y that has a discrete distribution (it gains values from 0 to 1) and has a non-linear relationship to the predictor X. It estimates the probability of a specific event, while using the



AQ7 Figure 10.9 Principle of the bivariate statistical analysis determining the parameter's weight.

356 Environmental Hazards Methodologies for Risk Assessment

input factors related to the presence or absence of the event. The input factors are also processed in the form of parametric maps in GIS and as such they enter the process of statistical evaluation using the map algebra. Making use of the logistic regression for modelling the landslide hazard or susceptibility there are mutual combinations of all input parameters influencing the slope stability, the predictor X in this case, and their subsequent comparison with the landslide registration map, the dependent variable Y in this case. The logistic function equation is as below:

$$f(y) = \frac{e^y}{e^y + 1} = \frac{1}{1 + e^{-y}} \quad (10.3)$$

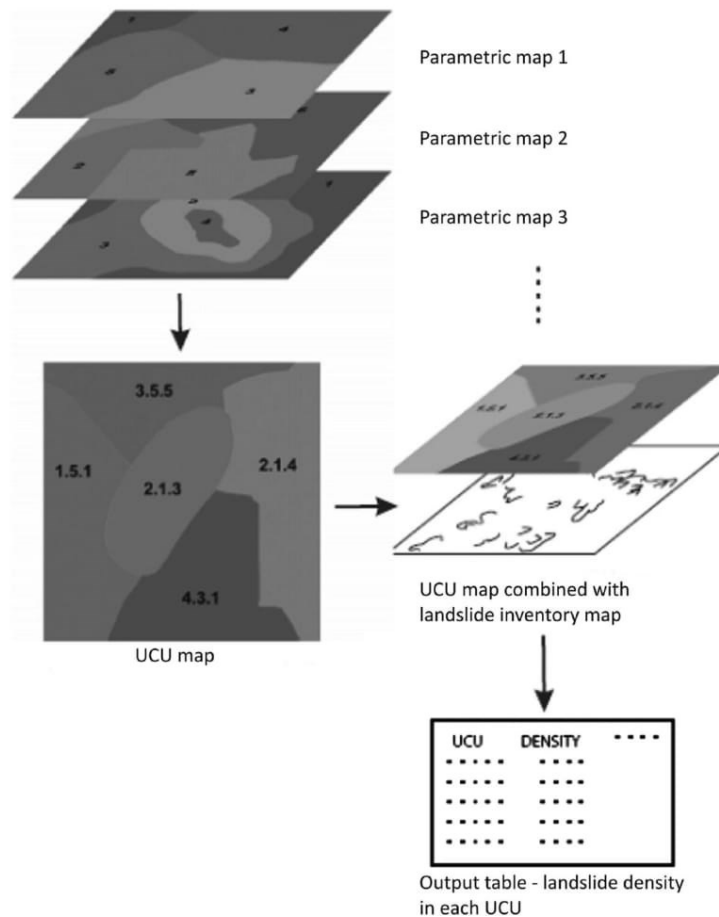


Figure 10.10 Principle of the multivariate statistical analysis (according to Pauditš, 2006).

where y is the input and $f(y)$ is the output. The variable y is affected by a certain set of independent variables, while $f(y)$ represents the probability of the given result arising from the set of variables. The variable y expresses the rate of the overall contribution of all independent variables used in the model. With regard to the amount of the independent variables $p(x_1, x_2, x_3, \dots, x_p)$, the vector $X = (x_1, x_2, x_3, \dots, x_p)$ is defined. The conditional probability that a landsliding event occurs is represented by the equation $P(y = 1/X)$. The course of the logistic function of the multiple models in logistic regression is defined as follows:

$$y = \beta_0 + \beta_1 x_1 + \beta_2 x_2 + \beta_3 x_3 + \dots + \beta_k x_k, \quad (10.4)$$

where β_0 is the constant in the equation and $\beta_1, \beta_2, \dots, \beta_k$ are the coefficients of the variables x_1, x_2, \dots, x_k , respectively. The probability $P(y = 1/X)$ may be expressed as:

$$P(y = 1/X) = \frac{1}{1 + e^{-(\beta_0 + \beta_1 x_1 + \beta_2 x_2 + \dots + \beta_k x_k)}} \quad (10.5)$$

10.6.2.2.3 Deterministic approach

Landslide hazard assessment by deterministic analyses requires a relatively high precision and variability of input parameters. For that reason, the application of the method in most cases has been limited to the small areas on a large scale with homogeneous geomorphologic and geological conditions. This method is not appropriate for small and medium scale given the lack of detailed input data, mainly geological, geotechnical and hydrogeological data (groundwater table level data). Required data have been determined in the field or the laboratory. However, the processing of input data, for example the spatial variability of data, sampling error or material properties, could induce the many limitations of the method.

The use of GIS tools for the deterministic approach allows the simulation of multiple scenarios, based on the hypothesis of the variability trigger factors and compilation of relatively reliable landslide hazard maps.

Deterministic models are based on physical laws of conservation of mass, energy or momentum (Terlien *et al.* 1995). The only one model that calculates the stability of the slope of each unit cell in GIS environment is separately infinite slope stability model. Using this geotechnical model, it is necessary to make some simplifications (Jelínek & Wagner, 2007):

- (1) availability of detailed and sufficiency geotechnical, hydrogeological and morphological input data must be available;
- (2) the method should be applied on small areas in a large scale, in consequence the absence of detailed physical and mechanical soil properties of large areas;
- (3) the method is suitable mostly for assessment of shallow landslides;

- (4) considering that the landslide material has been sliding along the planar slip-plane area parallel to the surface and soil layers merge into a single layer;
- (5) the simple infinite slope stability model is used;
- (6) assumption of quasi-homogeneous geological and geomorphologic conditions.

Assessing the landslide hazard of the selected area by deterministic method, is expressed as a factor of safety (FS), calculating for all the slopes and final classes of landslide hazard; divided by the degree of Factor of safety. Degree of FS is given by the ratio of the sum of the passive forces and active forces. When the final value of FS is less 1.0 then the stability conditions are not stable and mass movement may occur. The following formula may be used to calculate value of FS (according to Bruden & Prior, 1979, in van Westen, 1993):

$$FS = \frac{c_{ef} + (\gamma - m\gamma_w)z \cos^2 \beta \tan \varphi_{ef}}{\gamma z \sin \beta \cos \beta} \quad (10.6)$$

where:

c_{ef} – the effective cohesion [kPa];

φ_{ef} – the effective angle of shearing resistance [°];

γ – the unit weight of soil [$\text{kN} \cdot \text{m}^{-3}$];

γ_w – the unit weight of water [$\text{kN} \cdot \text{m}^{-3}$];

β – the slope angle [°];

z – the depth of slip surface below the terrain [m];

m – hw/z – the ratio of the height of groundwater table level above the slip surface hw [m] and the slip surface depth z [m].

An example of landslide hazard map based on deterministic approach is showed on Figure 10.11 (Kralovičová *et al.* 2014). As a study area landslide prone territory in Slovakia – the western boundary of Nitrianska pahorkatina Upland, part between the towns of Hlohovec and Sered' is assessed.

10.6.2.2.4 Fuzzy logic

Fuzzy logic is a branch of mathematics derived from fuzzy set theory. It is a quite young discipline, less than fifty years of history. Basic operation and mathematical principles of fuzzy logic are described in many articles; basics are in manuscript of Zadeh published in 1965 “Fuzzy sets”. Logical statements are expressed by function of membership, values are in the range from 0 to 1. In classical Boolean logic and predictive logic statements are valued as binary (dichotomic) 1 or 2; true or false; belongs or doesn't belong. Function of membership (FP) in fuzzy logic allows partial membership and associate membership to the set, so that it is extended to the whole interval $\langle 0; 1 \rangle$, including both border values. Fuzzy logic allows mathematically expressed concepts like “slightly,” “quite” or “a lot”. Therefore, it is preferable for a number of real decision-making tasks.

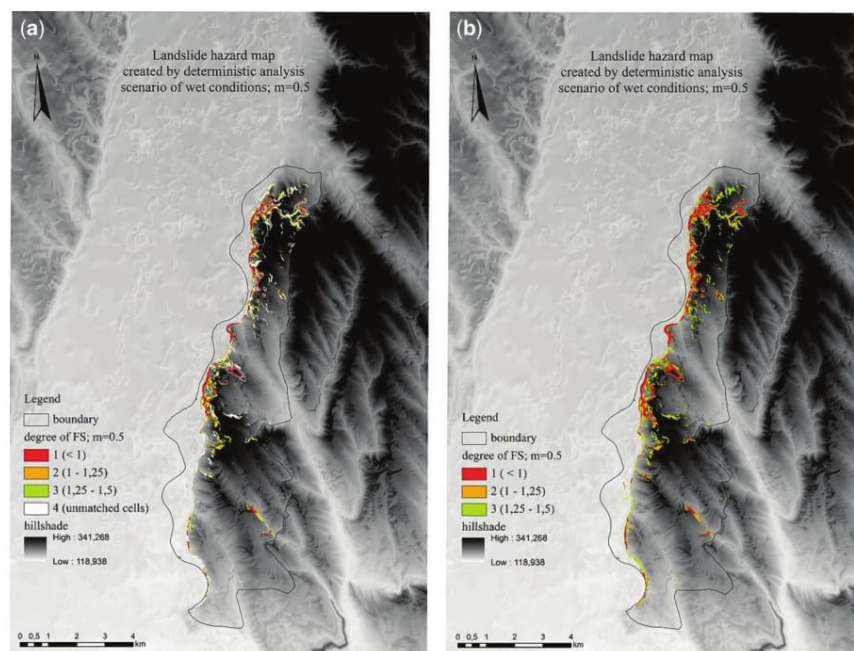


Figure 10.11 Landslide hazard maps for scenario of wet condition ($m = 0.5$) created by overlaying of partial hazard maps **(a)**, map only with the same degree of FS calculated in each partial hazard map, **(b)**, cells with FS value calculating less than 1.0 in each partial hazard map.

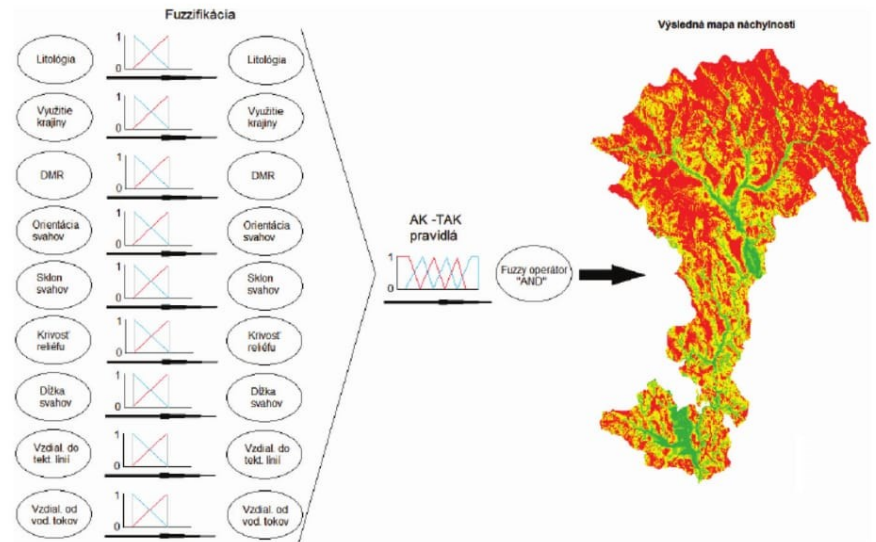
In a process of landslide hazard assessment, fuzzy logic defines the instability factors as members of a set reaching from 1, expressing the highest level of hazard or susceptibility, to 0 defining the lowest level of landslide hazard or susceptibility. The classes of individual parametric maps can be associated with fuzzy membership values based on expert opinion. Fuzzy represents membership widely defined, not strictly as probability.

Fuzzy logic has various operators – AND, OR, SUM, GAMMA etc., which allow to combine input parametric maps in several phases. Figure 10.12 shows an example of using fuzzy logic in landslide susceptibility assessment; study area here is a part of Flysch zone in northeast part of Slovakia.

10.6.2.2.5 Neural networks (NN)

Application of NN for interpretation data from remote sensing (RS) has been motivated by the ability to efficiently handle very large amounts of data from various sources. The rapid increase of NN applications in RS, mainly due to their

skills: working more accurately as, e.g. statistical classifiers, especially when the feature space and complex data sources have different statistical distribution works faster than other techniques.



AQ7

Figure 10.12 Landslide susceptibility map using fuzzy operator OR; an example from northeast part of Slovakia.

For landslide hazard assessment, multilayer forward neural network, the so-called Multilayer Perceptron (MLP) and the learning algorithm of back propagation error are used. MLP, as the name implies, consists of a series of layers, each consisting of a set of nodes (neurons). In the forward neural network, there are only forward connections between neurons, each neuron of one layer sends the signals to each neuron of the next layer, the connections to the previous layer or in one layer do not exist.

A neural network consists of a number of interconnected nodes. Each node is a simple processing element that responds to the weighted inputs it receives from other nodes. The arrangement of the nodes is called network architecture (Figure 10.13). The receiving node sums the weighted signals from all the nodes that it is connected to in the preceding layer (Pradhan & Lee, 2009). Neural network gets its ability to transform input data into output during the learning process. Learning is a fundamental and essential characteristic of neural networks. As already mentioned, the most used learning algorithm for multi-layered NN is a method of back propagation error (back propagation training algorithm). Figure 10.14 shows an example of application NN approach in landslide hazard

assessment; study area here is a central north part of Slovakia – Žilina region (Tornyai *et al.* 2016).

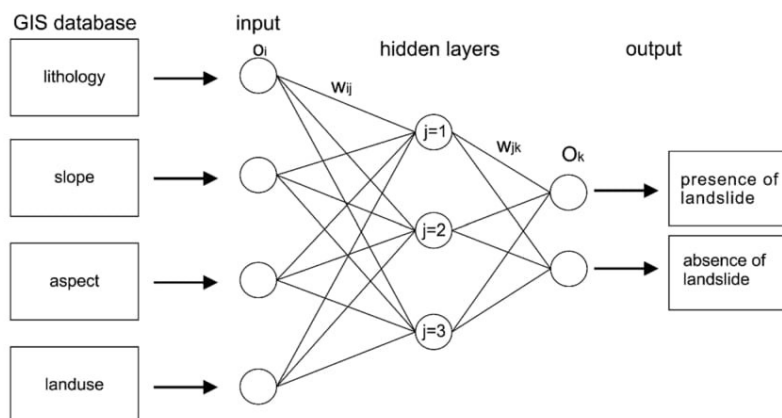
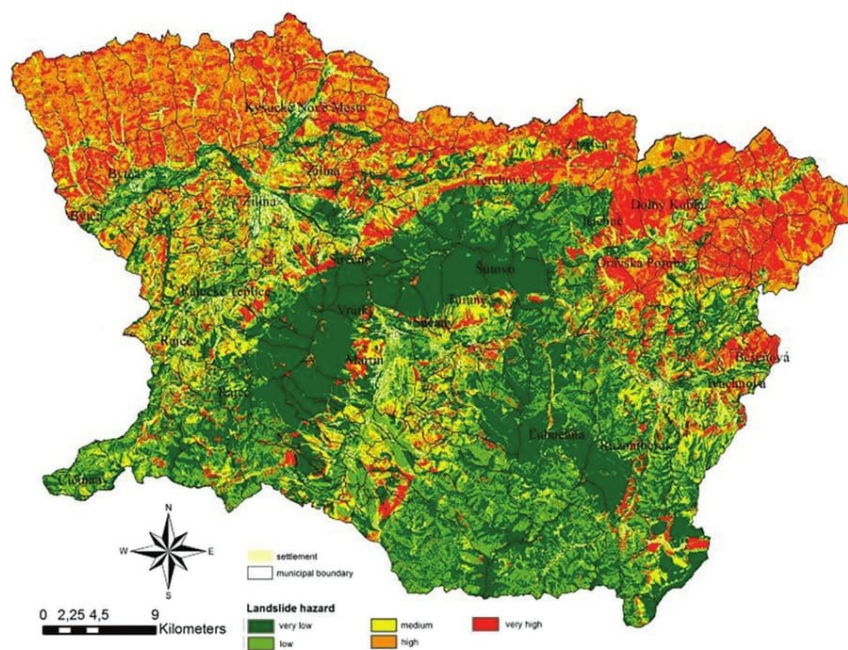


Figure 10.13 Basic architecture of neural network.



AQ7

Figure 10.14 Landslide hazard map created using NN approach.

10.6.3 Landslide risk assessment

It is important to assess the risk especially in urbanised zones or areas included in land use plans for socio-economic, technological and other purposes. Fundamental element in landslide risk assessment is evaluation of vulnerability with respect to the elements at risk. Among the elements at risk, there are primarily the population, buildings, economic activities, public services, infrastructure, etc.

10.6.3.1 Vulnerability assessment

The vulnerability assessment of the individual elements at risk is an indispensable part of landslide risk assessment and it helps to understand the interaction between the given landslide event and the affected elements at risk.

The elements at risk are most frequently defined from the current land use parametric map. The elements at risk are usually assessed based on the material vulnerability, while only potential direct losses caused by landslide hazard are taken into consideration. Indirect losses that may manifest in a certain time horizon after the given hazard activation, such as interrupted infrastructure and thus the interruption of the economic activities, e.g. due to a fallen road, generally are not included in the regional studies.

Having identified the elements of risk, the further vital and logical step is the financial evaluation that serves as the background for the calculation of vulnerability. The financial evaluation is usually processed in official prices as the market price for the individual elements at risk changes in dependence on the specific market demand.

Vulnerability is a simple product of the spatial distribution of the element at risk and the relevant price. It, thus, expresses the extent of the potential damage that occurs in a case of activation of a predicted landslide hazard.

The procedure of the material vulnerability calculation may be as follows:

- (1) classification of the evaluated elements at risk, e.g. in accordance with municipality cadastre maps, represented by a code;
- (2) delimitation of the risk element spatial distribution according to the level of landslide hazard map;
- (3) calculation of vulnerability as a product of the given risk element price and its spatial distribution within selected landslide hazard levels.

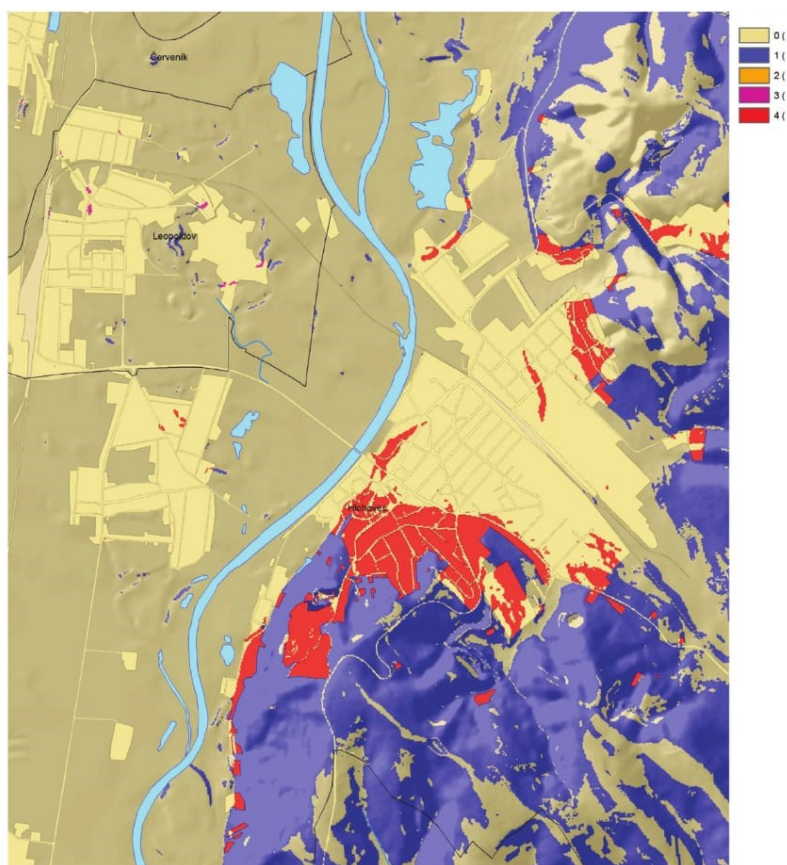
10.6.3.2 Landslide risk map

The landslide risk map shows the expected financial losses caused by slope deformations and makes use the results of prediction and analyses based on the landslide hazard assessment. Landslide risk presents simple multiplication of hazard and vulnerability assessment. The map of landslide risk is made using the following equation:

$$r = h * v \quad (10.7)$$

where: r – is the landslide risk value (e.g. expressed in Euros per pixel – 10×10 m), h – is the landslide hazard level, v – is the vulnerability of the elements at risk (per pixels).

The example used herein is the landslide risk map for the wider surroundings of the town of Hlohovec in Slovakia. The result is the “Euro – pixel” map mirroring the landslide risk in the model area (Figure 10.15). The landslide risk values are divided into 5 categories:



AQ7

Figure 10.15 Landslide risk map – an example from Hlohovec city (southwest Slovakia).

- category 0 – represents the zero value of the landslide risk per pixel,
- category 1 – Eur 30 to 100/pixel,
- category 2 – Eur 1 300/pixel,
- category 3 – Eur 2 000/pixel,
- category 4 – Eur 3 000/pixel.

The category 0 concerns areas that are not exposed to landslide hazard. The elements of vulnerability have been defined for such areas, but have zero landslide risk values. The category 1 covers the landslide risk value for arable land and forests in the model area. The elements of risk in the category 1 are in the 4th and 5th landslide hazard degree based on the hazard prediction map. The categories 2, 3 and 4 represent the landslide risk within the built-up areas (thus the high values arising from the material vulnerability values for the built-up areas). Similarly, they are exposed to the 4th and 5th landslide hazard degree, which arise from the above mentioned landslide hazard prediction map.

In the first place, such prepared maps of risk scenarios could serve as bases for the optimisation of the land use planning in towns and municipalities and further development of the individual cadastres in the model area.

10.6.3.3 Verification of the prediction maps

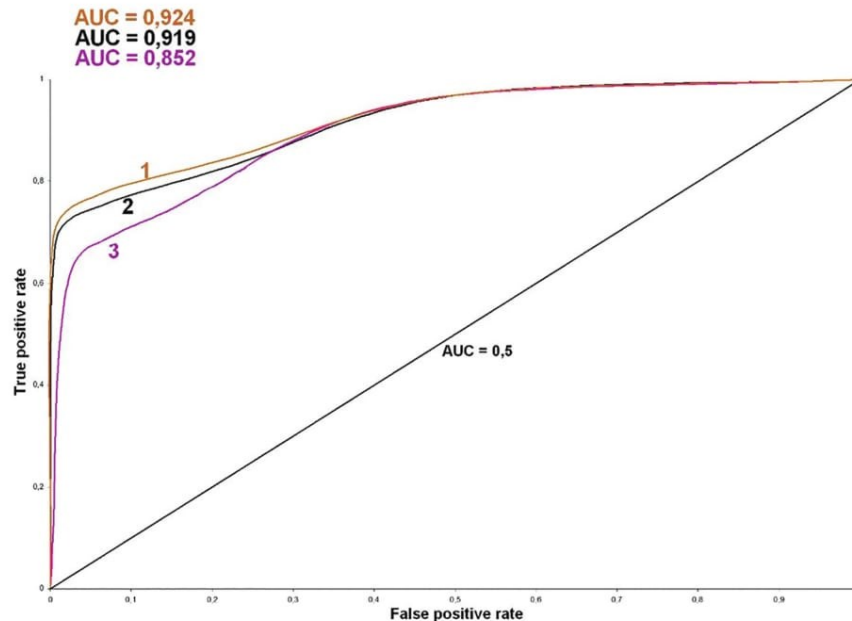
Having compiled the prediction map, it is vital to evaluate its informative value, this means to verify the map. The most important criterion for the evaluation of the prediction map quality is preparing the success model that considers the relationship between the prediction and the registered slope deformation map. In general, the success model compares the landslide density in the map of the registered slope deformations (presence or absence of the slope deformations, binary raster 1/0) with levels of landslide hazard.

The base element is construction of contingency table that compares the registered and predicted landslides, the combination of true and false, positive and negative classifications of landslides using random choice of an even number of pixels from both rasters. The contingency table analyses the relationship between two or more categorical variables. It was first used by Karl Pearson in 1904. The contingency table has that many rows and columns as is the number of categories in the prediction.

The literature discusses numerous techniques of prediction map verification. The most used are mostly the procedures using the methods of statistical success rates and ROC (Receiver Operating Characteristic) curves.

Correctness, accuracy or preciseness of the model is often evaluated using the ROC curves (ROC – Receiver Operating Characteristic). The ROC analysis was developed during the Second World War to evaluate the success rate of radar receivers to detect targets. The size of the area under curve (AUC) defines the overall quality of the prediction model; the larger the area, the more successful model. The maximum area of the chart is 1 (ideal model); the area for a model with 50% success rate has $AUC = 0.5$ (trivial model). It means that the closer the area's size to 1, the more precise the model is. The ROC curve is constructed according to the contingency tables and their number corresponds to the number of the cut-off – threshold values. Subsequently, the true and false positive values (TP and FP) are calculated for each contingency value. Those values then define the shape of the ROC curve. The closer the ROC curve to the upper left corner, the higher the

quality of the evaluated model is, and, thus, the higher AUC. Figure 10.16 shows the ROC curves to verify the model area in already mentioned Žilina region calculated using the bivariate and multivariate statistical analyses and neural networks. The size of the AUC varies from 0.852 to 0.924; together with the steepness of the curve itself, points to the success of the prediction models.



AQ7

Figure 10.16 ROC curves: (1) artificial neural network, (2) multivariate statistical analysis, (3) bivariate statistical analysis.

10.7 SNOW AVALANCHE MODELLING

10.7.1 Geoinformation technologies integration into the snow and avalanche research

Avalanches are regular effects of the mountain environment. This spontaneous gravitational shift of snow down a mountain slope is a natural mountain phenomenon, which often endangers natural sources, settlements, infrastructure and unfortunately very often also human lives. Therefore, the effort to understand all the processes connected with the instability of a snow cover and the related effort to minimize the negative consequences of avalanches is natural. It seems to be very important to predict an avalanche danger and to recognize the conditions leading to its increase. However, snow is one of the most variable natural materials for mathematical description. For that reason, an avalanche dynamics modelling

requires the use of complex, physically based numerical modelling tools and modern efficient computer technology. It is the development of computer and geoinformation technologies (GIT) that stand behind the great progress in the field of mass movements modelling.

The confirmation of this is the development of various modelling tools specialized exactly on the simulation and prediction of mass movement (snow) in a complex terrain. RAMMS and AVAL 1D, (developed by WSL Institute for Snow and Avalanche Research SLF), SAMOS-AT (developed by Austrian Service for Torrent and Avalanche Control), ELBA+ (developed at the University of Natural Resources and Applied Life Sciences in Vienna) belong among the most complex modelling tools nowadays. A considerable research in the avalanche dynamics in Europe was realized also in SATSIE project (Avalanche Studies and Model Validation in Europe), which is supported by the European Commission (MN2L and D2FRAM models). An accurate prediction of runout distances, flow velocities and impact pressures (Figure 10.17) in general three-dimensional terrain is the driving motivation for the development of dynamical mass movement models (Christen, 2013).

Avalanche dynamics modelling is in close connection with hydrological modelling, which deals with the formation and attributes of a snow cover (Figure 10.18).

It is possible to connect these two fields of modelling on the level of inputs and outputs with the help of GIS. Snow precipitation defines the distribution and attributes of a snow cover. These are the important factors, which define the regional distribution of potential avalanche release areas. However, snow avalanches can significantly affect back the hydrological terms of a specific area. The accumulation of avalanche deposit at the bottom of valleys can affect the process of snow melting. Depending on the conditions, snow melting can be accelerated or decelerated. There is a time shift of maximum water flow in the waterways fed from these valleys. At avalanches, a substantial mass of snow descends from higher to lower altitudes. Therefore, snow comes into warmer environment (in the consequence of the temperature gradient). Furthermore, an avalanche deposit can comprise different foreign materials and dirt that are gradually accumulated on the surface of a drift. The darker surface can absorb a bigger amount of sun radiation, what accelerates the melting process. The effect of this is that the maximum water flow comes earlier. When the snow in an avalanche drift is too dense, its melting can be significantly decelerated. The effective area of an avalanche drift is much smaller than the surface of the snow, which would not be released by the avalanche. These are the factors, which slow down the melting process and delay the maximum water flow.

10.7.2 Physically based numerical tools for avalanche dynamics modelling

Nowadays, the physically based numerical tools are the most widespread group of tools and they represent the most complex tool for quantitative analysis of a studied system. They are much less encumbered with the simplifying assumptions used in

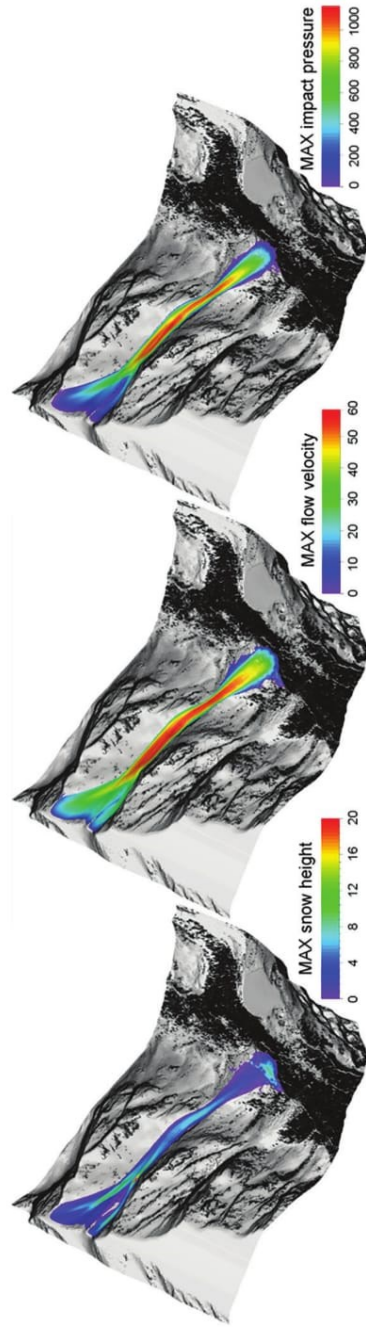


Figure 10.17 Avalanche dynamics modelling allows to predict maximal snow height, flow velocity and impact pressure of the avalanches.

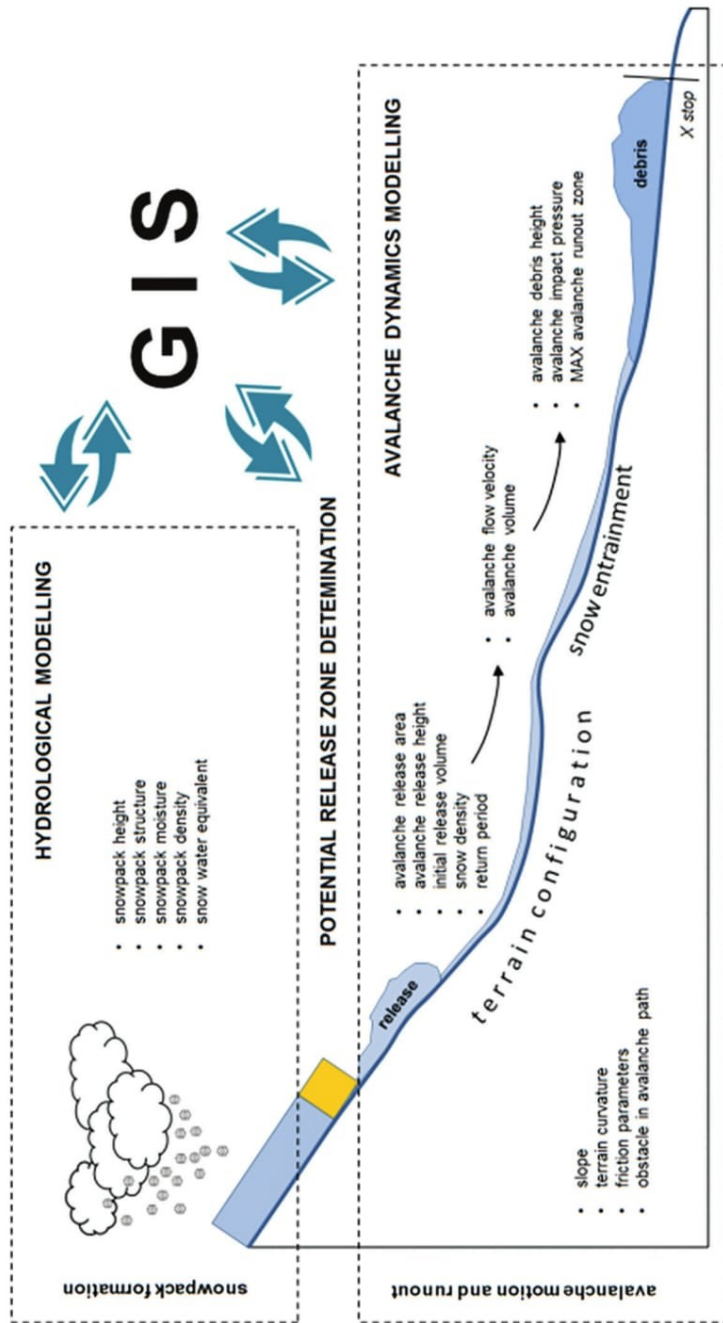


Figure 10.18 Avalanche dynamics modelling is in a close connection with hydrological modelling.

AQ7

analytical tools. Therefore, they are more appropriate for solving more complicated problems in more difficult conditions (Unucka, 2001). The main aim of avalanche dynamics studies is the answer to the question: in what way, how fast and how far does an avalanche move and what destructive potential is this movement connected with. The potential of dynamic numerical models is significant especially for the identification of potential avalanche runout distances. This identification is crucial for the evaluation of an avalanche danger. Furthermore, the avalanche impact pressure can be estimated by avalanche dynamics modelling (Figure 10.19) that brings a completely new dimension to the evaluation of an avalanche danger.

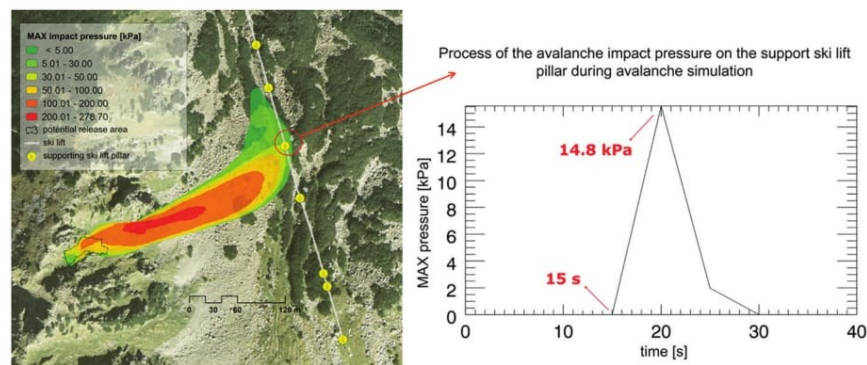
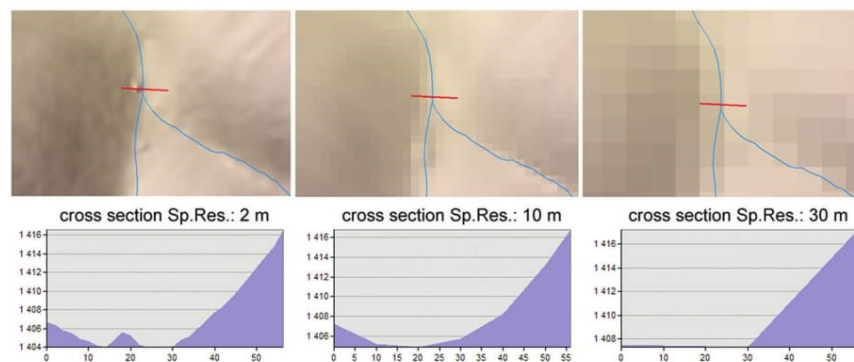


Figure 10.19 Avalanche impact pressure estimation brings a new dimension to the evaluation of an avalanche danger.

The definition of a possible avalanche path, the demarcation of potential avalanche runout distances and the estimation of avalanche destructive force represent an important basis for spatial planning and for projecting and dimensioning of avalanche protecting structures (Figure 10.19). Avalanche dynamics calculations are used to predict an extreme avalanche event and to delineate the different hazard zones (Gruber *et al.* 1998).

The determination of avalanche runout distances by numerical models is the process, which requires a lot of input data of high quality. The most important is the quality and accuracy of digital elevation model (DEM). The best results are achieved with DEM derived from LIDAR scanning. Another important group of input data are the parameters of avalanche release area (delimitation of release area, release height, snow density). These parameters underly the size, the volume and the type of an avalanche flow, which is consequently influenced by a terrain surface roughness, snow entrainment, the shape of an avalanche path, the presence of forests and other obstacles in an avalanche path. Also the selected spatial resolution of individual input layers is considerably important for the outcome of modelling. It is obvious, that the accuracy of DEM is significantly decreasing according to the lowering of spatial resolution (increasing pixel size). It is necessary

to define the spatial resolution with regard to a terrain character, so that all terrain features, which can significantly influence an avalanche flow, are included (Figure 10.20). This is also the principal problem, which restricts the usage of these tools at the modelling of small avalanches.



AQ7

Figure 10.20 Important terrain element with avalanche flow influence was not included into DEM with spatial resolution more than 2.

10.7.3 Model calibration and verification

The biggest danger of modelling is the possibility to easily generate the outputs that have little in common with reality. A model is always similar to the hypothesis, on which it is based, and to the data, which are input into it. However, every model works on a certain level of reliability and it is necessary to verify and test the acquired prognosis. A model calibration and the verification of results must be an inseparable part of each modelling. In the case of avalanche dynamics modelling, a calibration refers especially to the adjustment of terrain friction coefficients. According to these coefficients, an avalanche flow accelerates or decelerates. However, the avalanches in individual mountain areas have a very specific progress, due to a different combination of local, meteorological, geomorphological and climatic conditions. Therefore, it is not always possible to use the calibration coefficients relevant for one area also for runout distances modelling in another area. In the process of calibration, the selected calibration coefficients are set according to user's experience and detail knowledge of the local conditions in an examined area. The only possibility to set these parameters is to study the behaviour of a real system in the past with the intention to gather the information about initial conditions and about the reaction of the system to these conditions. An effort to set calibration coefficients in such a way that the range of a simulated avalanche agrees with the maximum range of a past avalanche is very frequent at avalanche runout distances. Such a method is known as a back-calculation (Figure 10.21).

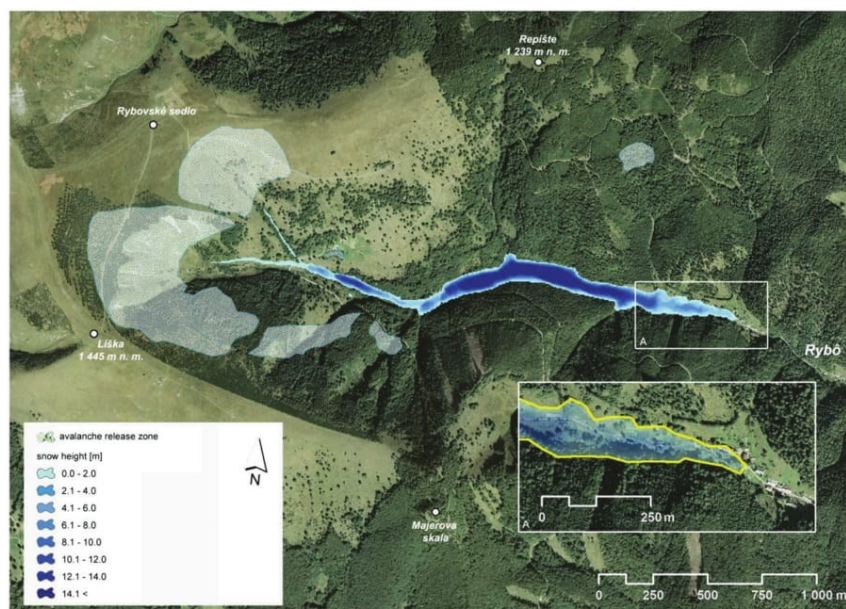


Figure 10.21 Back calculation and reconstruction of the avalanche in settlement Rybô, February 6, 1924.

The verification is used in order to evaluate the fact, whether a model simulates the behaviour of a real phenomenon in an acceptable rate. Every result of modelling should be complemented with the information about achieved simulation accuracy. There are several statistical methods that can be used for verification. The verification of the avalanche front line localization, but also the verification of the whole shape of an avalanche path is relevant for the modelling of avalanche runout distances. Also the verification of the snow height in a drift is important for a back-calculation. The places, in which the check figures are measured in a terrain, should be chosen with regard to local terrain features and a drift character. Only when a model is properly calibrated and its results are verified accurately enough, it can be used for the simulation of various cases.

10.7.4 Avalanche danger zoning

It is required to carefully examine and evaluate an avalanche danger when planning any human activities in avalanche prone areas (construction of buildings, roads, railways, ski-lifts, ski slopes, power lines and others). This includes a precise estimation of avalanche runout distances, impact pressure and return periods of the highest possible number of potential avalanches. The mistakes in these estimations

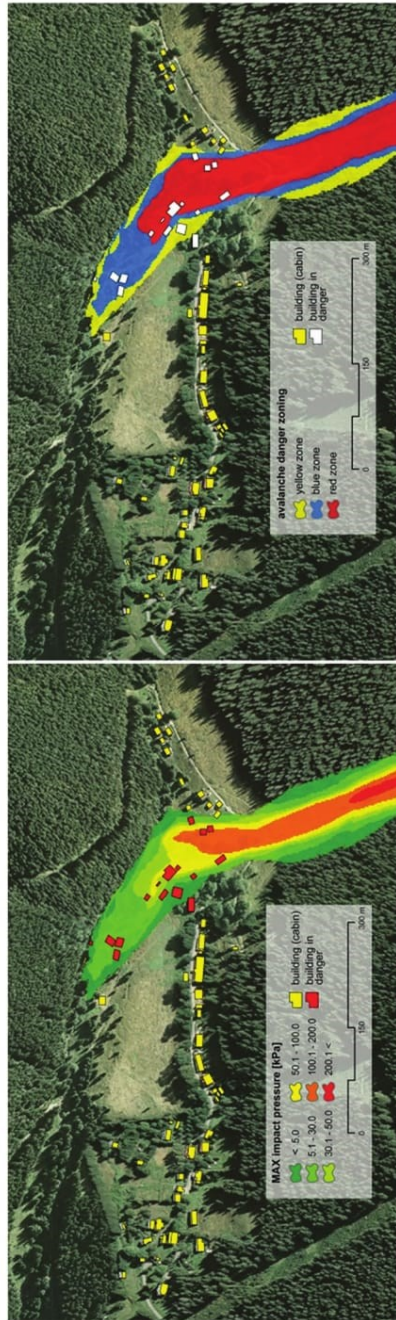


Figure 10.22 Avalanche danger zones according to maximal impact pressure reached by avalanche, settlement Magurka in Low Tatras, Slovakia.

can lead to great material damages and to losses of human lives. Also a too conservative evaluation of an avalanche danger can lead to unpractical restrictions, which inhibit the development of the region. This evaluation should be periodically examined, minimally once in 10 years (McLung & Schaerer, 2006).

The division of an area into different zones, according to their potential avalanche hazard, was established for the first time in Switzerland in 1961. The definition of individual avalanche danger zones was legislatively set and this Swiss model was established also in Austria, Italy, France, the USA and Canada. In accordance to this definition there are four zones (Figure 10.22) of potential danger (McLung & Schaerer, 2006):

- *Red Zone = High Hazard:* No new structures and buildings are permitted in this zone. Existing buildings must be protected either by control structures or reinforcement, and evacuation plans must be in place.
- *Blue Zone = Moderate Hazard:* New residences may be permitted in this zone, but they must be protected. No lift terminals, lodges, schools, or buildings that attract large crowds of people are allowed.
- *Yellow Zone = Low Hazard:* In this zone, structural measures against powder avalanches may be recommended.
- *White Zone = No Hazard:* No restrictions apply to development. No avalanches are reasonably expected to reach this zone.

10.8 SUMMARY AND CONCLUSIONS

The mass movements occur when the shearing stress acting on rock masses exceeds the shear strength of the material. The susceptibility of slope to failure is determined by a combined effect of pre-conditions (geology) and factors like slope angle and moisture content. There are various triggering factors, which generate sudden failures, such as intense heavy precipitation, natural (seismicity) or artificial (explosives, traffic) vibration, steepening of slopes (by undercutting), deforestation. The mass movements are distinguished based on various criteria, where the most commonly used is their rate. The slowest mass movement is creep. More rapid movements are termed landslides and they can be further subdivided based on the involvement of rock or soil in sliding, on the shape of shear plane, etc. Flows are even more rapid movements and they are again subdivided upon the character of the load. Fall is the quickest mass movement occurring on the very steep or overhang slopes. GIS assessment is effective tool in the hazard assessment processing. Prior to undertaking any area surveys, it is essential that the system is established for identifying and describing hazards and the infrastructure at risk. Once the assessment has been completed, hazard ranking can be carried out and the inevitable remedial measures can be designed.

The use of innovative geoinformation technologies opens a new perspectives for mapping and appraisal of natural hazards also in the field of avalanche prevention.

Their main aim is to evaluate an avalanche hazard with regard to the planning of human activities in mountains. The number, the importance and also the accuracy of avalanche dynamics modelling tools are developing in accordance to the development of computer technology. Such models, connected with a precise terrain research and study, represent a great contribution to the appraisal of an avalanche hazard in mountains.

REFERENCES

- Alean J. C. (1985). Ice avalanches: some empirical information about their formation and reach. *Journal of Glaciology*, **31**(109), 324–333.
- Aleotti P. and Chowdhury R. (1999). Landslide hazard assessment: summary review and new perspectives. *Bulletin of Engineering Geology and Environment*, **58**(1), 21–44.
- Bednarik M., Clerici A., Tellini C. and Vescovi P. Using GIS GRASS in evaluation of landslide susceptibility in Termina valley in the Northern Apennines (Italy). In: Proceedings of the Conference on Engineering Geology: Forum for Young Engineering Geologists, M. Moser (ed.), April 6th–9th 2005, DGGT Erlangen-Nürnberg, Friedrich – Alexander – University of Erlangen- Nürnberg, pp. 19–24.
- Bednarik M., Magulová B., Matys M. and Marschalko M. (2010). Landslide susceptibility assessment of the Kral'ovany–Liptovský Mikuláš railway case study. *Physics and Chemistry of the Earth*, **35**(3–5), Elsevier Ltd., ISSN 1474-7065.
- Christen M., Bartelt P. and Kowalski J. (2008). Calculation of dense snow avalanches in three-dimensional terrain with the numerical simulation programme RAMMS. In: International Snow Science Workshop 2008, Whistler, BC, Canada.
- Clerici A. (2002) A GRASS GIS based shell script for landslide susceptibility zonation by the conditional analysis method. In: Proceedings of the Open Source GIS GRASS Users Conference, M. Ciolli and P. Zatelli (eds), Trento, Italy.
- Constantin, M., Bednarik, M., Jurchescu, M. C. and Vlaicu, M. The landslide susceptibility assessment using the bivariate statistical analysis and the index of entropy in the Sibiciu Basin (Romania). *Environmental Earth Sciences*, DOI 10.1007/s12665-010-0724-y, Published online: 05 September 2010.
- Cruden D. M. and Varnes D. J. (1996). Landslide types and processes. In: Landslides: Investigation and Mitigation, Special Report 247, National Academy Press, Washington, DC, pp. 26–75. ISBN 0-309-06151-2.
- Gruber U., Bartelt P. and Haefner H. (1998). Avalanche hazard mapping using numerical Voellmy-fluid models. In: 25 Years of Snow and Avalanche Research (NGI), International Symposium Held in Voss May 1998, Norges Geotekniske Institutt, pp. 117–121.
- Jelínek R. and Wagner P. (2007). Landslide hazard zonation by deterministic analysis (Veľká Čausa landslide area, Slovakia). *Landslides*, **4**(4), 339–350, ISSN 1612-510X.
- Kääb A., Paul F. and Huggel C. (2003). Glacier monitoring from ASTER imagery: accuracy and applications. In: Proceedings EARSeL Workshop, Observing our Cryosphere from Space, March 11–13, Bern, pp. 43–53.
- Kern M. A., Bartelt P. and Sovilla B. (2010). Velocity profile inversion in dense avalanche flow. *Annals of Glaciology*, **51**, 27–31.
- Kralovičová L., Bednarik M., Trangoš I. and Jelínek R. (2014). Landslide hazard assessment using deterministic analysis – a case study from the Chmiňany landslide. *Slovak Geological Magazine*, **14**(1), 41–63, ISSN 1335-096X.

- Leroi E. (1996). Risk maps at different scales: objectives, tools and developments. In: Landslides, K. Senneset (ed.), Balkema, Rotterdam, pp. 35–51, 2014.
- Margreth S. and Funk M. (1999). Hazard mapping for ice and combined snow/ice avalanches: two case studies from the Swiss and Italian Alps. *Cold Regions Science and Technology*, **30**(1–3), 159–173.
- McLung D. and Schaerer P. (2006) *The Avalanche Handbook*, 3rd edn. The Mountaineers Books, Seattle, USA.
- Pauditš P. (2006). Landslide Susceptibility Assessment Using Statistical Methods within GIS. *Geol. Práce, Spr. 112, ŠGÚDŠ, Bratislava*, pp. 41–58: (In Slovak).
- Plafker G. and Ericksen F. E. (1978). Nevados Huascaran avalanches, Peru. In: *Rockslides and Avalanches, Natural Phenomena*, B. Voight (ed.), Elsevier, Amsterdam, pp. 277–314.
- Pradhan B. and Lee S. (2009). Landslide risk analysis using artificial neural network model focussing on different training sites. *International Journal of Physical Sciences*, **4**(1), 001–015, ISSN 1992 - 1950 © 2009 Academic Journals.
- Salzmann N., Kääh A., Huggel C., Allgöwer B. and Haeberli W. (2004). Assessment of the hazard potential of ice avalanches using remote sensing and GIS-modelling. *Norwegian Journal of Geography*, **58**, 74–84.
- Schweizer J., Jamieson B. and Schneebeili M. (2003). Snow avalanche formation. *Reviews of Geophysics*, **41**.
- Terlien M. T. J., Van Ash T. W. J. and Van Westen C. J. (1995). Deterministic modeling in GIS – based landslide hazard assessment. In: *Geographical Information Systems in Assessing Natural Hazard*, Kluwer Academic, Dordrecht, pp. 55–77, ISBN 0-7923-3502-3.
- Tornyai R., Bednarik M. and Havlín A. (2016) Application of neural network to assess landslide hazard and comparison with bivariate and multivariate statistical analyses. Submitted Manuscript to Journal AGEOS.
- Tremper B. (2001). *Staying Alive in Avalanche Terrain*, 1st edn. The Mountaineers Books, Seattle, WA.
- Unucka J. (2010). *Možnosti propojení GIS a environmentálních modelů pro potřeby krizového řízení a ochrany přírody* (GIS and Environmental Models Connectivity for the Needs of Crisis Management and Nature Protection). Habilitation thesis, VŠB – Technical University of Ostrava, Czech Republic.
- Van Westen C. J. (1993). GISSIZ – Training Package for Geographic Information Systems in Slope Instability Zonation. Part 1: Theory. Project on Geo-Information for Environmentally Sound Management of Natural Resources (ITC Publication Nb. 15). UNESCO – International Institute for Aerospace Survey and Earth Sciences (ITC). ISBN 90-6164-078-4.
- Varnes D.J. (1978). Slope movement types and processes. In: *Landslides: Analysis and Control*. Transportation Research Board. Special Report 29, National Research Council, Washington, D C, pp. 170–197.
- Varnes D. J. (1984). *Landslide Hazard Zonation – a Review of Principles and Practise*. UNESCO, Paris, p. 63.